



**UNIVERSITÀ DEGLI STUDI DI PALERMO**

Dottorato in Ingegneria dell'Innovazione Tecnologica  
Dipartimento dell'Innovazione Industriale e Digitale  
ING-IND/27

**Evaluating the Utilization of Innovative Electrochemical  
Methodologies for the Real Wastewater Treatment**

**LA DOTTORESSA**

**Ing. Pengfei Ma**

**IL COORDINATORE**

**Prof. Ing. Salvatore Gaglio**

**IL TUTOR**

**Prof. Ing. Onofrio Scialdone**

**IL CO TUTOR**

**Prof. Ing. Alessandro Galia**

**CICLO XXXIII**

**2017-2020**

物来顺应，未来不迎，当时不杂，既过不恋

——曾国藩

## Nomenclature and symbols

AEM	anion exchange membrane
AO	anodic oxidation
AO7	acid orange 7
AOP	advanced oxidation process
BDD	boron-doped diamond
CE	current efficient
CEM	cation exchange membrane
COD	chemical oxygen demand
$D_m$	diffusion coefficients
$\sigma$	diffusion layer thickness
DSA	dimensionally stable anode
DSA-Cl <sub>2</sub>	DSA used for chlorine evolution
DSA-O <sub>2</sub>	DSA used for promoting the OER
$E_{cell}$	potential between the anode and cathode
EAOP	electrochemical advanced oxidation process
EC	energy consumption
EF	electro-Fenton
F	Faraday constant
$K_m$	mass-transport coefficient
$i$	current intensity
$j$	current density
$j_{lim}$	limiting current density
$i_{app}$	applied current density
IEO	indirect electro-oxidation

M	anode surface
MO	metal oxide electrode
OCV	open circuit potential
P	power density
R	the universal gas constant
$R_{\text{ext}}$	external load resistance
$R_p$	reaction rate
SCE	saturated calomel electrode
T	the absolute temperature
TOC	total organic carbon
V	solution volume
$\alpha$	the average permselectivity of the membrane pair
z	the electrochemical valence

# CONTENTS

<b>NOMENCLATURE AND SYMBOLS .....</b>	<b>I</b>
<b>INTRODUCTION .....</b>	<b>1</b>
<b>CHAPTER 1. STATE OF ART ON ADVANCES TECHNOLOGIES ELECTROCHEMICAL WASTEWATER TREATMENT .....</b>	<b>5</b>
<b>1.1 Introduction .....</b>	<b>5</b>
<b>1.2 Anodic oxidation by HO• .....</b>	<b>6</b>
1.2.1 Effect of anode material .....	7
1.2.2 Effect of supporting electrolyte and conductivity .....	8
1.2.3 Effect of current density .....	9
<b>1.3 Indirect electro-oxidation with active chlorine .....</b>	<b>10</b>
1.3.1 The effect of anode materials and pH.....	10
1.3.2 Effect of supporting electrolyte (chloride ion content) .....	13
<b>1.4 Electro-Fenton .....</b>	<b>14</b>
1.4.1 Electrode materials .....	15
1.4.2 The effect of pH.....	16
1.4.3 The effect of catalyst .....	16
1.4.4 The effect of current density.....	16
1.4.5 The effect of electrolyte.....	17
1.4.6 Reactor design .....	17
<b>1.5 Reference .....</b>	<b>18</b>
<b>CHAPTER 2. STATE OF ART ON MICROFLUIDIC REACTOR WASTEWATER TREATMENT TECHNOLOGY.....</b>	<b>27</b>
<b>2.1 Introduction .....</b>	<b>27</b>
<b>2.2 Application of microfluidic reactor in electrochemical technology .....</b>	<b>27</b>
<b>2.3 Application of microfluidic reactor in electrochemical wastewater treatment technology.....</b>	<b>35</b>
2.3.1 Abatement of 1,1,2,2-tetrachloroethane in micro reactors .....	36
2.3.2 Abatement of chloroacetic acid in micro reactors .....	37
2.3.3 Abatement of acid orange 7 in micro reactors.....	38

<b>2.4 Reference .....</b>	<b>40</b>
----------------------------	-----------

## **CHAPTER 3. STATE OF ART ON REVERSE ELECTRODIALYSIS**

<b>TECHNOLOGY OF THE WASTEWATER TREATMENT.....</b>	<b>43</b>
--	-----------

<b>3.1 Introduction .....</b>	<b>43</b>
-------------------------------	-----------

<b>3.2 Principle of reverse electrodialysis system .....</b>	<b>45</b>
--	-----------

<b>3.3 The effect of operative conditions on the power generation in RED process ...</b>	<b>46</b>
--	-----------

3.3.1 The effect of investigated redox processes.....	46
---	----

3.3.2 The effect of cell number of membranes.....	47
---	----

3.3.3 Effect of HC and LC solution flow rate .....	48
--	----

<b>3.4 Coupled processes of electric energy generation and wastewater treatment in RED system .....</b>	<b>49</b>
---	-----------

3.4.1 Energy generation and abatement of Cr(VI) in RED process .....	50
--	----

3.4.2 Energy generation and abatement of Acid Orange 7 in RED process.....	52
--	----

<b>3.5 Reference .....</b>	<b>53</b>
----------------------------	-----------

## **CHAPTER 4. TREATMENT OF WASTEWATER CONTAINING PHENOL BY DIFFERENT ELECTROCHEMICAL PROCESSES WITH CONVENTIONAL REACTORS .....**

<b>4.1 Introduction .....</b>	<b>59</b>
-------------------------------	-----------

<b>4.2 Experimental.....</b>	<b>59</b>
------------------------------	-----------

4.2.1 Materials and reactor .....	59
-----------------------------------	----

4.2.2 Methods .....	61
---------------------	----

4.2.3 Analysis .....	62
----------------------	----

<b>4.3 Results and discussion .....</b>	<b>64</b>
---	-----------

4.3.1 IOAC with Ti/RuO <sub>2</sub> anode .....	64
---	----

4.3.2 EO with BDD anode.....	68
------------------------------	----

4.3.3 Energy efficiency analysis.....	71
---------------------------------------	----

4.3.4 Electro-Fenton process .....	75
------------------------------------	----

4.3.5 Effect of the ratio between the anode and the cathode surfaces and of other operative parameters on H <sub>2</sub> O <sub>2</sub> electro-generation .....	79
--	----

<b>4.4 Summary .....</b>	<b>90</b>
--------------------------	-----------

<b>4.5 Reference .....</b>	<b>92</b>
----------------------------	-----------

<b>CHAPTER 5. ELECTROCHEMICAL TREATMENT OF LOW CONDUCTIVITY REAL WASTEWATER WITH MICROFLUIDIC REACTORS .....</b>	<b>95</b>
<b>5.1 Introduction .....</b>	<b>95</b>
<b>5.2 Experimental.....</b>	<b>96</b>
5.2.1 Experimental materials and reactor .....	96
5.2.2 Methods .....	97
5.2.3 Analysis .....	98
<b>5.3 Results and discussion .....</b>	<b>98</b>
5.3.1 Electrolyses performed in conventional cell in the absence of supporting electrolyte .....	98
5.3.2 Electrolyses performed in conventional cell in the presence of supporting electrolyte .....	101
5.3.3 Electrolyses performed in micro cells in the absence of supporting electrolyte .....	106
5.3.4 Technical and economical comparison between adopted routes.....	109
<b>5.4 Summary .....</b>	<b>115</b>
<b>5.5 References.....</b>	<b>116</b>
<b>CHAPTER 6. DEVELOPMENT OF A PROCESS WITHOUT ENERGY INPUTS USING A REVERSE ELECTRODIALYSIS STACK AND THE SALINITY GRADIENT OF WASTEWATERS .....</b>	<b>119</b>
<b>6.1 Introduction .....</b>	<b>119</b>
<b>6.2 Experimental.....</b>	<b>120</b>
6.2.1 Experimental materials and reactor .....	120
6.2.2 Methods .....	123
6.2.3 Analysis .....	125
<b>6.3 Results and discussion .....</b>	<b>126</b>
6.3.1 Treatment of two wastewaters using their salinity gradient to drive the process .....	126
6.3.2 Effect of external resistance .....	130
6.3.3 Optimization of the process.....	132
6.3.4 Effect of the salinity ratio .....	135
6.3.5 Energy consumption assessment with 1 membrane system .....	139

<b>6.4 Summary .....</b>	<b>141</b>
<b>6.5 References.....</b>	<b>142</b>
<b>CHAPTER 7. FIRST UTILIZATION OF ASSISTED REVERSE ELECTRODIALYSIS FOR CO<sub>2</sub> ELECTROCHEMICAL CONVERSION AND TREATMENT OF WASTEWATER .....</b>	<b>143</b>
<b>7.1 Introduction .....</b>	<b>143</b>
<b>7.2 Experimental.....</b>	<b>144</b>
7.2.1 Experimental materials and reactor .....	144
7.2.2 Methods .....	145
7.2.3 Analysis .....	147
<b>7.3 Results and discussion .....</b>	<b>147</b>
7.3.1 Anodic treatment of synthetic wastewater.....	147
7.3.2 Cathodic conversion of carbon dioxide to formic acid.....	156
<b>7.4 Summary .....</b>	<b>161</b>
<b>7.5 References.....</b>	<b>162</b>
<b>CHAPTER 8. CONCLUSIONS AND INNOVATIONS .....</b>	<b>165</b>
<b>ACKNOWLEDGEMENTS .....</b>	<b>167</b>
<b>PUBLICATIONS AND MEETINGS.....</b>	<b>168</b>
<b>APPENDIX A: THE ACTIVITY COEFFICIENT OF THE NA<sub>2</sub>CO<sub>3</sub> SOLUTION .....</b>	<b>170</b>
<b>APPENDIX B: CONDUCTIVITY OF DIFFERENT NA<sub>2</sub>CO<sub>3</sub> CONCENTRATION SOLUTION .....</b>	<b>171</b>



## Introduction

In the last years, many efforts have been devoted to the development of electrochemical processes for the effective treatment of wastewater contaminated by organic pollutants resistant to conventional biological processes and/or toxic for microorganisms. It was shown that some electrochemical approaches, including the direct anodic oxidation at suitable anodes such as boron doped diamond (BDD) and/or the oxidation by electro-generated active chlorine and/or electro-Fenton (EF) using suitable operating conditions and cells, can allow to treat effectively a very large number of organic pollutants. Electrochemical processes present several advantages with respect to other advanced oxidation processes such as: very mild operative conditions, no transport or storage of oxidants, limited operative and capital costs, wide versatility and very high removal of various kinds of pollutants.

As a result of all these considerations, a plethora of studies were dedicated to the evaluation of various electrochemical approaches and to the selections of proper operating conditions and cells. However, most of the investigations were performed using synthetic wastewater. Hence, it is now mandatory to study the problems connected to the passage from synthetic wastewater to the real ones. Furthermore, such processes present various problems such as the necessity to use significant amounts of electric energy and very high cell potentials needed to treat wastewater with low conductivity. In this thesis, various solutions were proposed and studied to face these problems, the following studies were performed.

- (1) Electrochemical degradation of phenol containing wastewater with high and low conductivity. The abatement of organic in synthetic wastewater with high and low NaCl content was performed by various routes, in order to evaluate the effect of the NaCl concentration on the process.
- (2) Electrochemical treatment of real wastewater with low conductivity. The problem of wastewater with low conductivity was investigated in detail, using a real wastewater

containing organics and characterized by quite low conductivity, coming from the separation of oil and water phases performed from one company devoted to the treatment of wastewater. Two different cells were used: a conventional undivided batch cell operated both in the absence and in the presence of a supporting electrolyte, and a micro cell, with the main aim to evaluate if real wastewater with low conductivity can be properly treated by electro-chemical oxidation at BDD anode and to select the more promising cell and route.

- (3) Study on electro-Fenton process. Large attention was devoted to the key stage of the cathodic conversion of oxygen to  $H_2O_2$  focusing on the effect of various parameters (such as the nature and the area of the anode, the ratio between the cathode and anode surface, the current density and the mixing rate) that can affect also the anodic oxidation of  $H_2O_2$  in undivided cells.
- (4) Treatment of synthetic wastewaters without energy inputs using the salinity gradient of wastewaters and a reverse electrodialysis stack. A RED process for the treatment of synthetic wastewaters contaminated by organics, without energy inputs, using the salinity gradient of different synthetic wastewaters, was studied for the first time. Two very simple wastewater matrices, containing only formic acid as a model organic compound and NaCl, were used in order to provide a first proof of the proposed concept, with the main aim of evaluating if it is possible to use the salinity gradients of these synthetic wastewaters to remove their TOC.
- (5) Assisted reverse electrodialysis for  $CO_2$  electrochemical conversion and treatment of wastewater. The utilization of A-RED was proposed for the first time for two very different purposes: (i) the treatment of synthetic wastewater contaminated by organics; (ii) the conversion of carbon dioxide to high added value products. These processes are chosen as particularly promising examples, since for both an improvement of economics is necessary for the passage on an applicative scale, which could potentially be achieved using salinity gradients available in industrial plants.

**Highlights:**

- (1) This study provides a new and simple route to improve the production of  $\text{H}_2\text{O}_2$ . Differently from the current literature, this route involves a high  $A_{\text{cathode}}/A_{\text{anode}}$  ratio, avoiding the usage of expensive cells design and electrodes.
- (2) An electrochemical microfluidic reactor is used to treat low conductivity real wastewater without additional electrolyte. The usage of this kind of reactor results in both a high pollutant removal efficiency and low energy consumption. This provides a pathway for the application of the electrochemical treatment process of low-salt wastewater in industrial scale.
- (3) Both the degradation of organic pollutants and the production of chemicals are performed using reverse electrodialysis, RED, without or with a low supplied external electricity, Assisted-RED. In RED and A-RED, electric energy is provided by salinity gradients of two water streams with different salt content.



## **Chapter 1. State of art on advances technologies electrochemical wastewater treatment**

### **1.1 Introduction**

In the past three decades, intensive studies on the application of advanced oxidation processes (AOPs) for wastewater treatment have been carried out [1-4]. Compared with conventional treatment technologies, AOPs could achieve higher removal rates for organic pollutants, especially for the refractory substances. Using AOPs for organic pollutants removal in some cases presents several challenges, including: (a) incomplete mineralization of the pollutants. (b) the production of toxic intermediates (c) high cost of processes. In order to overcome those drawbacks, in the last years, many efforts have been devoted to the development of electrochemical processes for the effective treatment of wastewater contaminated by organic pollutants resistant to conventional biological processes and/or toxic for microorganisms. Fig.1-1 reports some electrochemical approaches, including the direct/indirect anodic oxidation at suitable anodes and/or electro-Fenton (EF) at suitable operating conditions and reactors. Furthermore, their attractiveness is enhanced by three other relevant factors:

- the possibility to use both cathodic and anodic processes to enhance the effectiveness of the treatment;
- the possibility to couple the wastewater treatment performed in one compartment of the cell with another process carried out in the other compartment, such as, for example, the carbon dioxide conversion to useful chemicals or fuels, thus improving dramatically the economics;
- the possibility to use the amount of intermittent electric energy generated by renewable sources in excess with respect to the needs of the grid.

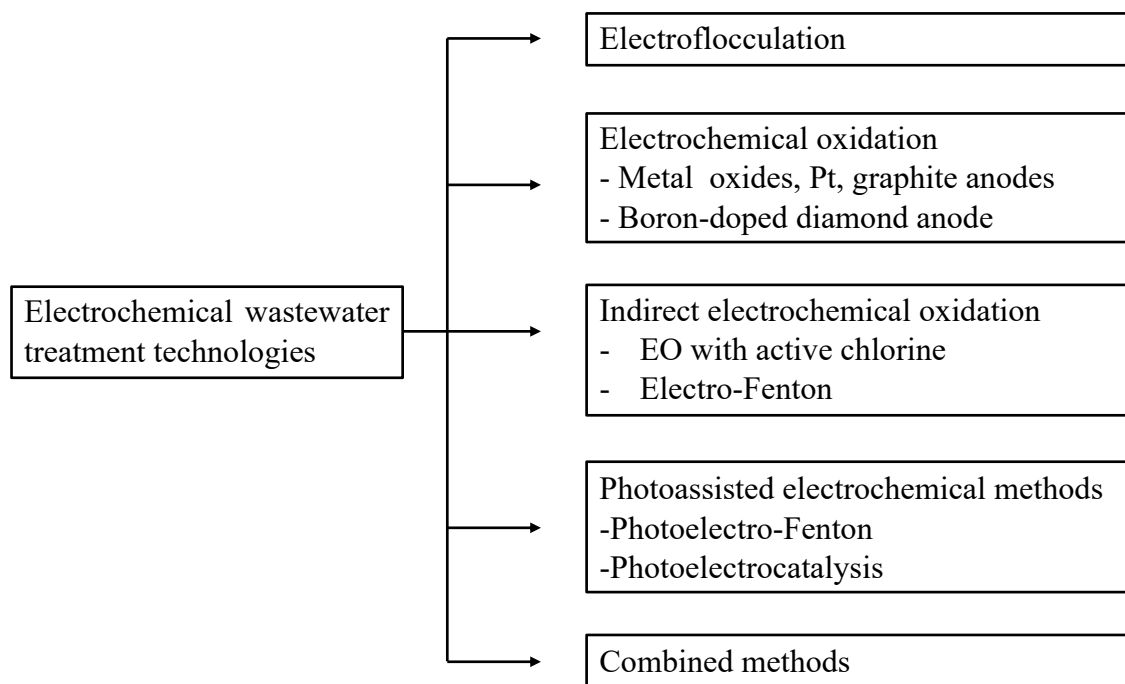


Fig.1-1 Electrochemical wastewater treatment technologies [5]

However, in spite of the advantages mentioned above, there are still many factors limiting their application on an industrial scale. For example, the short life of some electrode materials, the low current efficiency obtained under certain reaction conditions, the high energy consumption, etc. In addition, the effect of various operative parameters was not fully understood in many cases [6-8].

## 1.2 Anodic oxidation by HO•

As stated by several experts, the HO• electro-generation consists by physisorption HO• and chemisorption HO• [9-12]. In the case of physical adsorption, HO• is weakly linked to the anode surface and the nonselective oxidation of organics was often observed, which may cause complete combustion to CO<sub>2</sub>. The chemisorbed HO• is easily transformed into a higher state oxide or superoxide MO, and in most of cases only partial oxidation of organics is achieved; the refractory aromatic organics can be however selectively transformed into biodegradable compounds like carboxylic acids.

Nevertheless, the efficiency of decontamination (poor, partial, or total) by both processes is affected by several conditions (electrode materials, pH, pollutant, conductivity of the solution, current density, etc.), as discussed in the next sections.

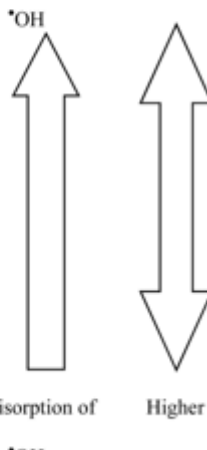
### **1.2.1 Effect of anode material**

The efficiency of the EO process is highly dependent on the nature of the anode material. A high number of anodes have been tested for the treatment of dyes including metal oxides, carbonaceous materials, Pt and PbO<sub>2</sub>, boron-doped diamond (BDD). Table 1-1 presents the oxygen evolution potential of several most commonly used anode materials in the EO process. RuO<sub>2</sub>, IrO<sub>2</sub>, Pt and graphite electrodes are typical examples of active anodes (that gave chemisorption of hydroxyl radicals), exhibiting potential for O<sub>2</sub> evolution lower than 1.8 V/SHE, whereas PbO<sub>2</sub>, Ti/SnO<sub>2</sub>-Sb<sub>2</sub>O<sub>5</sub>, BDD can be considered as non-active electrodes (i.e., they give physical adsorption of hydroxyl radicals), presenting oxygen evolution potentials from 1.8 to 2.6 V/SHE [13,14]. Due to its high anodic stability and wide potential window, BDD is considered to be an effective material for the direct combustion of organics in wastewater.

Panizza et al. [15] reported the effect of different anode materials on the degradation of 2-naphthol. In the same electrolysis conditions, the organic pollutants were totally removed in 6 h and 24 h by BDD and PbO<sub>2</sub> anode, respectively, while, just 10% removed by using DSA/Ti–Ru–Sn anode in 24 h. Martínez-Huitle et al. [16] conducted the similar electrochemical degradation studies on chloranilic acid. The COD removal rate reached 100% in 6.4 h by BDD anodes, 80% in 11 h by PbO<sub>2</sub> anodes, while only 50% after 15 h by DSA/IrO<sub>2</sub> anodes.

Table 1-1 Classification of anode materials based on their oxidation power and potential for O<sub>2</sub> evolution in acidic media [13]

anode type	composition	electrocatalytic ability for the OER	oxidation potential (V)	overpotential for OER (V) <sup>b</sup>	adsorption enthalpy of M- <sup>*</sup> OH	oxidation power of anode
Active	RuO <sub>2</sub> – TiO <sub>2</sub>	Good	1.4-1.7	0.18	Chemisorption of	Lower
	(DSA <sup>®</sup> - Cl <sub>2</sub> )				<sup>*</sup> OH	
	IrO <sub>2</sub> – Ta <sub>2</sub> O <sub>5</sub>	Good	1.5-1.8	0.25		
	(DSA <sup>®</sup> - O <sub>2</sub> )					
	Ti/Pt	Good	1.7-1.9	0.30		
	Carbon and Graphite	Good	1.7			
Non-active	Ti/PbO <sub>2</sub>	Poor	1.8-2.0	0.50		
	Ti/SnO <sub>2</sub> -Sb <sub>2</sub> O <sub>5</sub>	Poor	1.9-2.2	0.70		
	p-Si/BDD	Poor	2.2-2.6	1.3	Physisorption of	Higher



### 1.2.2 Effect of supporting electrolyte and conductivity

The performances of electro-chemical treatment are expected to strongly depend on the conductivity of the wastewater. Typically, most lab-scale studies reported in the literature use synthetic solutions of a given pollutant (or a mixture of pollutants) and large concentrations of salts are added as supporting electrolyte to increase the conductivity, thus reaching concentrations much higher than those found in real effluents [6,17,18]. Usually, NaCl or Na<sub>2</sub>SO<sub>4</sub> are routinely added [19]. It is worth highlighting that when chlorides are used, the Cl-mediated oxidation will be favored. For example, Rabaaoui et al. [20] reported the addition of equal amounts of Na<sub>2</sub>SO<sub>4</sub>, KCl, NaClO<sub>4</sub>, NaCl, as electrolytes on the treatment of the o-nitrophenol solution with BDD anodes. It was shown that the best organic removal rate was obtained when the electrolyte was Na<sub>2</sub>SO<sub>4</sub>. Thiam et al. [21] reported the direct electrochemical degradation studies on Allura Red AC dye wastewater by BDD electrodes with the aid of ultraviolet radiation; they found that similar TOC abatements were obtained in the presence of different concentrations of



$\text{Na}_2\text{SO}_4$ . In contrast, González et al. [22] found that the highest removal efficiency of organic was obtained with  $70 \text{ g L}^{-1}$   $\text{Na}_2\text{SO}_4$  in the degradation of the antibiotic trimethoprim wastewater by BDD anode.

The treatment of real wastewater is much more complex. As stated, studies with synthetic wastewater are far from the real scenario in which the concentrations of pollutants and salts are fully determined by the industrial process in which they are produced. Furthermore, many domestic and industrial wastewater present quite low conductivity. In spite of this, in most of cases wastewater with high conductivity were selected [23,24]. In few cases real wastewater with low conductivity were used [25-28]; in some occasions, the researchers solved the problem of the low conductivity, by the addition of a supporting electrolyte such as  $\text{Na}_2\text{SO}_4$ . However, from an applicative point of view, the addition of chemicals to the solution leads to a strong increase of the operating costs and to a more difficult authorization procedure since it can cause the formation of secondary pollutants. As a further example, Tsantaki et al. [29] studied the electrochemical treatment of a textile wastewater adding perchloric acid ( $\text{HClO}_4$ ) as supporting electrolyte to increase effluent conductivity and decrease the electrical consumption, a critical approach in view of both the cost and the toxicity of  $\text{ClO}_4^-$ .

### 1.2.3 Effect of current density

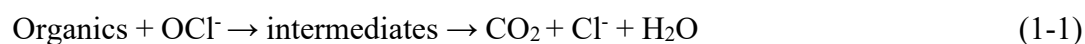
In the process of electrochemical oxidation at the anode surface, the electro-generation of oxidants can be controlled by adjusting the current density directly [19,30]. Normally, when the electrolysis reaction is running at a low current density, the anodic oxidation reaction is not controlled by the mass transfer of pollutants to the anode surface, and the current efficiency and the removal rate of pollutants will increase with the increase of current density; on the contrary, when the electrolysis reaction is operated under high current density, the oxidation at the anode surface is likely to be controlled by mass transfer, and the increase of the current density is coupled with the increase of the oxygen evolution, resulting in lower current efficiency and pollutant removal rate; the electrolysis

reaction is under mixed kinetic control when the current density is at an intermediate value [13].

Furthermore, there are also other several operation variables that affects EO process, including pH, temperature, the nature and concentration of the organic pollutant. The effect of pH and temperature have been investigated in many papers, with different findings depending on the target pollutants, supporting electrolytes and the anode materials. In general, many studies reported that the removal efficiency of organic pollutants by EO tends to increase in the lower pH range and higher temperature.

### **1.3 Indirect electro-oxidation with active chlorine**

Aqueous solutions of organic pollutants can be decontaminated by indirect oxidation with electro-generated active chlorine (IOAC), where anodic oxidation of chloride ions leads to the formation of free chlorine, hypochlorous acid and/or hypochlorite, which can oxidize the organics near to the anode or/and in the bulk of the solution (Eq.1-1) [31-36].



In the IOAC process, the main factors that affect the yield of active chlorine and the degradation of organics are: anode material, pH, current and potential, fluid dynamics, chloride ion concentration, organic pollutant concentration, reaction temperature, etc.

#### **1.3.1 The effect of anode materials and pH**

The anode material plays a decisive role in these processes. Likewise, the instantaneous current efficiency for the formation of active chlorine strongly depends on the nature of the anode, and it is influenced by the competition between the formation of active chlorine and parasitic reactions such as (1) the production of hydroxyl radicals, which directly oxidize and degrade the organic pollutants; (2) oxygen evolution reaction, reducing the

efficiency of active chlorine generation; (3) the electrochemical reaction to generate chlorate and the reduction of the generated oxidants at the cathode[37-39].

According to some researchers' work, chloride oxidation is enhanced at low pH (see Fig. 1-2) [40] and porous anodes can exhibit in the porous structure substantially lower pH than in the bulk of the solution. Thus, the OER at the anode causes the acidification of the aqueous medium, leading to a gradient of pH between the anode surface and the bulk solution. For porous anodes, a very low pH is maintained in the porous structure of the anode nearly independent of the bulk pH, allowing the oxidation of chlorides to active chlorine even in nonacidic solutions [41]. In this context, it is important to remember that metal oxide anodes often present a porous-like structure, thus favoring chlorine evolution at nonacidic pH.

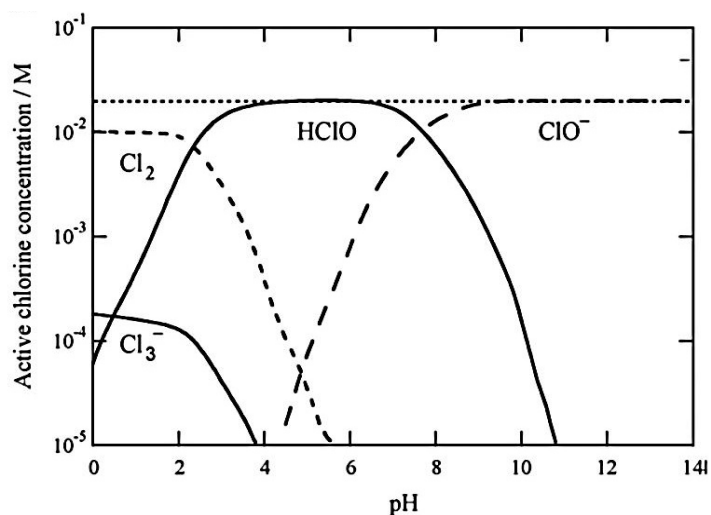


Fig. 1-2 Speciation diagram for the chlorine vs pH [40].

As shown in Fig. 1-3, Kraft et al. [42] summarized the free chlorine production efficiency on the chloride concentration for two DSA made with active coatings of IrO<sub>2</sub> or IrO<sub>2</sub>/ RuO<sub>2</sub>, Pt, and BDD. It can be seen that both DSA outperform the other two anodes. Metal oxide anodes are usually preferred to graphite, Pt and BDD for a higher ICEAC. In particular, among metal oxides, active anodes (such as Ir- and Ru-based electrodes) often yield higher ICEAC than nonactive ones (such SnO<sub>2</sub> and PbO<sub>2</sub>).

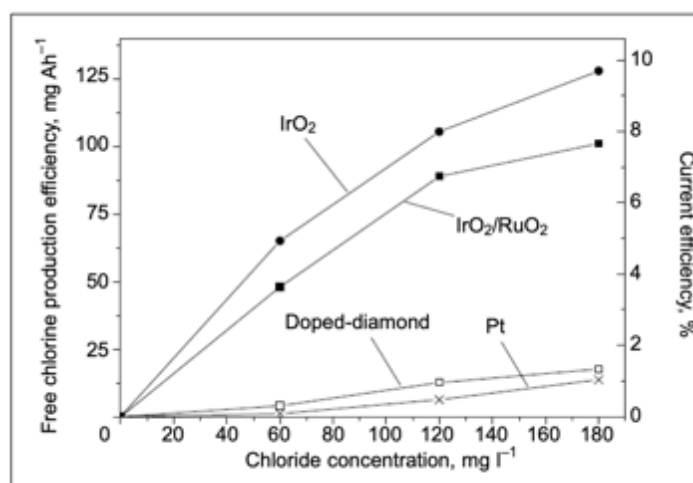


Fig. 1-3 Dependence of the electrochemical free chlorine production efficiency on the chloride content of the electrolysed water under standard conditions using four different anode materials (iridium oxide, mixed iridium/ruthenium oxides, platinum, doped-diamond) [42].

Scialdone and co-workers [43] reported that when the electrolysis reaction is carried out under the charge transfer control, the current efficiency increases with the increase of the current density while Neodo and Choi et al. [44] reported that when the electrolysis reaction is under mass transport control, the current efficiency in the electrochemical production of active chlorine will decrease with the increase of current density. On overall, when organics are mainly oxidized by active chlorine and the oxidation of chloride is not limited by mass transport, the mineralization of organics is likely to increase upon enhancing the current density and, for many systems, decreasing the flow or the mixing rate. Conversely, if the oxidation of organics occurs by active chlorine whose formation is mass transport controlled, the current efficiency for the mineralization of organics should decrease upon enhancement of the current densities and decrease of the flow or the mixing rate.

### 1.3.2 Effect of supporting electrolyte (chloride ion content)

Chloride ions are often present in liquid effluents and natural water, thus making inevitable the appearance of active chlorine during the wastewater treatment. Commonly, the degradation efficiency of organic pollutants increases with the increasing of the chloride ions concentration, since the increase of active chlorine produced during the IOAC process. For example, Grgur et al. [36] found that methomyl cannot undergo degradation reactions on the surface of active DSA (Ti/RuO<sub>2</sub>) anodes without the participation of chloride ions. When a certain amount of NaCl was added, a good removal effect was obtained. Zhou et al. [45] used the same anode to treat methyl orange containing wastewater; the decolorization and degradation of methyl orange were improved by adding a small amount of NaCl. However, the researchers found the opposite conclusion with the inactive anode. Costa and co-workers [46] showed that the addition of NaCl to a phosphate buffer solution of acid black 210 dye at BDD gave a decrease in the abatement of TOC in a large range of pH. Scialdone and co-workers [47,48] showed that the addition of NaCl resulted in a lower COD abatement in the EO process of acid orange 7 or chloroacetic acid wastewater using BDD.

From the above discussion, it can be seen that the degradation of organic pollutants by indirect electrochemical oxidation of active chlorine is more complicated, and different reaction conditions show different removal effects. During the reaction, parasitic reactions such as chlorate and perchlorate will greatly reduce the amount of active chlorine produced. In addition, it is difficult to degrade some types of refractory organic pollutants, and most large organic molecules pollutants can be only converted into the small one, which cannot be degraded completely. These factors have greatly affected the application of indirect electrochemical oxidation of active chlorine in real wastewater treatment projects.

### 1.4 Electro-Fenton

As shown in Fig.1-4, in the EF process, H<sub>2</sub>O<sub>2</sub>, generated through the reduction of dissolved oxygen on the surface of the cathode (Eq.1-2), reacts with Fe<sup>2+</sup> to generate the HO• radicals in the solution (Eq. 1-3). The polarized cathode allows the continuous in situ electro-generation of H<sub>2</sub>O<sub>2</sub> and the regeneration of Fe(II) (Eq. 1-4), thus avoiding the use of high quantities of H<sub>2</sub>O<sub>2</sub> and Fe(II) salt and increasing the effectiveness of the process [49-53].



These formed •OH react with organics, leading to their oxidation / mineralization (Eq.1-5).

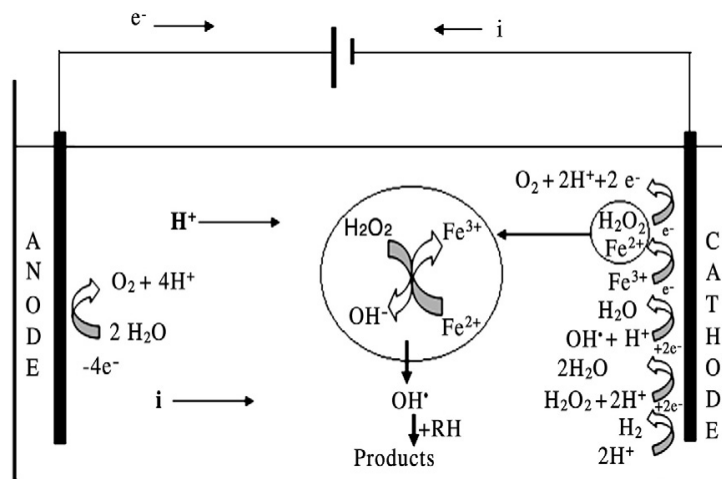


Fig. 1-4 Schematic diagram of the main mechanism of the electric Fenton reaction process [54].

Compared with the traditional chemical Fenton process, electro-Fenton shows various advantages such as: (i) on-site production of  $\text{H}_2\text{O}_2$  effectively avoids risks occurring during transportation, storage or usage; (ii) the continuous regeneration reaction of  $\text{Fe}^{2+}$  on the cathode surface; (iii) an increased degradation of organic pollutants, (iv) the production of iron-containing sludge is greatly reduced and (v) lower operating cost. In order to improve the electric Fenton process in the wastewater treatment, various reaction conditions were analyzed and furthermore optimized such as pH, current density, catalyst content, pollutant types, cathode materials, dissolved oxygen and reactor design [55-58].

#### **1.4.1 Electrode materials**

Due to the low solubility of oxygen in aqueous solutions, the production of hydrogen peroxide is greatly restricted. In order to improve the performances of the process, many works were devoted in the last years to the study of various kinds of cathodes such as graphite [59,60], hierarchically porous carbon [61], carbon cloth [62], carbon sponge [63], reticulated vitreous carbon [64] or carbon felt [65,66]. The utilization of cathodes fabricated by the combination of different carbon powders and polytetrafluoroethylene (PTFE) [67,68] or by the deposition of carbon and PTFE mixtures on carbonaceous supports [69-71] often allowed to increase the working current density with respect to unmodified materials and, therefore, the rate of production of hydrogen peroxide. In particular, gas diffusion electrodes (GDE) [72] allowed the generation of quite high concentrations of hydrogen peroxide [73-76]. However, the utilization of such electrodes enhances the complexity and the cost of the cell, thus making more difficult the development of the process on an applicative scenario. Hence, carbon-felt was often chosen as cathode for EF process, for its high specific surface that favors the fast generation of both components of the Fenton's reagent ( $\text{H}_2\text{O}_2$  and  $\text{Fe}^{2+}$ ), enhancing the generation of  $\text{HO}\cdot$  from Fenton's reaction.

### 1.4.2 The effect of pH

pH is a very important factor in EF process. Indeed, both too high and too low pH are not beneficial to the progress of the electro-Fenton reaction. When the pH is high, iron-containing sludge is produced [77]. Furthermore, higher pH will accelerate the decomposition of  $\text{H}_2\text{O}_2$  to oxygen and water. When the pH is too low, a large amount of iron ions will exist in the form of complex  $[\text{Fe}(\text{H}_2\text{O})_6]^{2+}$ , which reacts slowly with hydrogen peroxide, decreasing the generation of  $\text{HO}\cdot$  [78]. After a lot of researches, it has been proved that the optimal pH should be controlled at about 3 [79].

### 1.4.3 The effect of catalyst

Pimentel et al. [80] reported the effect of different catalysts on the conversion of  $\text{H}_2\text{O}_2$  to  $\text{HO}\cdot$ ; iron, cobalt, manganese and copper were adopted, respectively. It was demonstrated that  $\text{Fe}^{2+}$  is particularly effective for the electro-Fenton system. Usually, the degradation efficiency of organic pollutants by the EF process increases with the increase of  $\text{Fe}^{2+}$  input. However, in the study of Sankara et al. [81], it is pointed out that within a certain range, excessively increasing the concentration of  $\text{Fe}^{2+}$  has little effect on the removal efficiency of organic. At the same time, excessive  $\text{Fe}^{2+}$  will increase the iron salt content in the water, thereby increasing the total dissolved solid content in the discharged water, resulting in the secondary pollution.

### 1.4.4 The effect of current density

The use of high currents density causes an increase in the production of hydrogen peroxide which causes an increase in the amount of  $\text{HO}\cdot$ , so that the degradation process will be increased [81]. In addition, the use of high current density also causes an increase in regeneration of ions, resulting the increase of the efficiency in the Fenton process [82].



However, Nidheesh et al. [54] pointed out that when the applied current density exceeds a certain value, the competing parasitic reactions include oxygen evolution reaction on the anode surface and the hydrogen evolution reaction on the cathode surface lead to the drop of the organic degradation efficiency in wastewater.

#### **1.4.5 The effect of electrolyte**

Adding electrolyte to the electrolysis system helps to increase the conductivity of the solution. In EF system,  $\text{Na}_2\text{SO}_4$  is commonly used as electrolyte. Zhou et al. [51] pointed out, for the degradation of methyl orange by the electro-Fenton method, that the degradation efficiency of pollutants is improved as the addition of  $\text{Na}_2\text{SO}_4$  in the solution increases, since the production of hydrogen peroxide is accelerated. Daneshvar et al. [83] reported out that when the content of  $\text{Na}_2\text{SO}_4$  was increased from 0.05 to 0.1 M, there was no change in the cumulative amount of hydrogen peroxide in the reaction. Ghoneim et al. [84] reported the effect of equal amounts of  $\text{Na}_2\text{SO}_4$ ,  $\text{NaCl}$ ,  $\text{KCl}$  as electrolytes on the EF system and found that  $\text{Na}_2\text{SO}_4$  has the best degradation effect on sunset yellow in wastewater.

#### **1.4.6 Reactor design**

Various authors have shown that the performances of the process can be strongly improved using proper reactors that enhance the mass transfer of oxygen to the cathodes such as pressurized [85,86], micro [87] or venturi ones or cells equipped with rotating cathodes [88]. The cathodic generation of  $\text{H}_2\text{O}_2$  can be achieved in both divided and undivided cells. The utilization of divided cells allows to prevent the anodic oxidation of hydrogen peroxide but requires both higher investment and operating costs, due, respectively, to the cost of the membrane and to the higher cell potentials. Hence, undivided cells are often preferred, especially in the frame of electro-Fenton process, in order to reduce the overall costs of the process. However, in this case the performances

of the process are expected to depend not only by the parameters that influence the cathodic process but also by the parameters that affect the anodic routes.

### 1.5 Reference

- [1] Rueda-Márquez J J, Sillanpää M, Pocostales P, et al. Post-treatment of biologically treated wastewater containing organic contaminants using a sequence of H<sub>2</sub>O<sub>2</sub> based advanced oxidation processes: Photolysis and catalytic wet oxidation. *Water Research*, 2015, 71: 85–96.
- [2] Chávez A M, Gimeno O, Rey A, et al. Treatment of highly polluted industrial wastewater by means of sequential aerobic biological oxidation-ozone based AOPs. *Chemical Engineering Journal*, 2019, 361: 89–98.
- [3] Ganiyu S O, Zhou M, Martínez-Huitle C A, et al. Heterogeneous electro-Fenton and photoelectro-Fenton processes: A critical review of fundamental principles and application for water/wastewater treatment. *Applied catalysis B: Environmental*, 2018, 235: 103–129.
- [4] Wang N, Zheng T, Zhang G, et al. A review on Fenton-like processes for organic wastewater treatment. *Journal of Environmental Chemical Engineering*, 2016, 4 (1): 762–787.
- [5] Sirés I, Brillas E, Oturan M A, et al. Electrochemical advanced oxidation processes: Today and tomorrow. A review. *Environmental Science and Pollution Research*, 2014, 21 (14): 8336–8367.
- [6] Moreira F C, Boaventura R A R, Brillas E, et al. Electrochemical advanced oxidation processes: A review on their application to synthetic and real wastewaters. *Applied Catalysis B: Environmental*, 2017, 202: 217–261.
- [7] Mandal P, Dubey B K, Gupta A K. Review on landfill leachate treatment by electrochemical oxidation: Drawbacks, challenges and future scope. *Waste Management*, 2017, 69: 250–273.
- [8] Brillas E. Electro-fenton, UVA photoelectro-Fenton and solar photoelectro-Fenton treatments of organics in waters using a boron-doped diamond anode: A review. *Journal of the Mexican Chemical Society*, 2014, 58 (3): 239–255.

- [9] Comninellis C. Electrocatalysis in the electrochemical conversion / combustion of organic pollutants. *Electrochimica Acta*, 1994, 39 (1): 1857–1862.
- [10] Martínez-Huitle C A, Andrade L S. Electrocatalysis in wastewater treatment: recent mechanism advances. *Quimica Nova*, 2011, 34 (5): 850–857.
- [11] Marselli B, Gomez G J, Michaud P A, et al. Electrogeneration of hydroxyl radicals on boron-doped diamond electrodes. *Journal of the Electrochemical Society*, 2003, 150 (3): D79.
- [12] Zhu X, Tong M, Shi S, et al. Essential explanation of the strong mineralization performance of boron-doped diamond electrodes. *Environmental Science and Technology*, 2008, 42 (13): 4914–4920.
- [13] Martínez-Huitle C A, Rodrigo M A, Sirés I, et al. Single and coupled electrochemical processes and reactors for the abatement of organic Water Pollutants: A critical Review. *Chemical reviews*, 2015, 115 (24): 13362–13407.
- [14] Panizza M, Cerisola G, Direct and mediated anodic oxidation of organic pollutants, *Chemical reviews*, 2009, 109: 6541–6569.
- [15] Panizza M, Cerisola G. Influence of anode material on the electrochemical oxidation of 2-naphthol: Part 2. Bulk electrolysis experiments. *Electrochimica Acta*, 2004, 49 (19): 3221–3226.
- [16] Martínez-Huitle C A, Quiroz M A, Comninellis C, et al. Electrochemical incineration of chloranilic acid using Ti/IrO<sub>2</sub>, Pb/PbO<sub>2</sub> and Si/BDD electrodes. *Electrochimica Acta*, 2004, 50 (4): 949–956.
- [17] He Y , Lin H, Guo Z, et al. Recent developments and advances in boron-doped diamond electrodes for electrochemical oxidation of organic pollutants. *Separation and Purification Technology*, 2019, 212: 802–821.
- [18] Martínez-huitle C A, Ferro S. Electrochemical oxidation of organic pollutants for the wastewater treatment: direct and indirect processes. *Chemical Society Reviews*, 2006, 35: 1324–1340.
- [19] Khandegar V, Saroha A K. Electrocoagulation for the treatment of textile industry effluent. A review. *Journal of Environmental Management*, 2013, 128: 949–963.
- [20] Rabaaoui N, EI M, Saad K, et al. Anodic oxidation of o-nitrophenol on BDD electrode : Variable effects and mechanisms of degradation. *Journal of Hazardous Materials*, 2013, 250–251: 447–453.

- [21] Thiam A, Sirés I, Garrido J A, et al. Decolorization and mineralization of Allura Red AC aqueous solutions by electrochemical advanced oxidation processes. *Journal of Hazardous Materials*, 2015, 290: 34–42.
- [22] Thiam A, Sirés I, Garrido J A, et al. Effect of anions on electrochemical degradation of azo dye Carmoisine ( Acid Red 14 ) using a BDD anode and air-diffusion cathode. *Separation and Purification Technology*, 2015, 140: 43–52.
- [23] Amishi Popat, P.V. Nidheesh, T.S. Anantha Singh, et al. Mixed industrial wastewater treatment by combined electrochemical advanced oxidation and biological processes. *Chemosphere*, 2019, 237: 124419.
- [24] Wang C T, Chou W L, Chung M H, et al. COD removal from real dyeing wastewater by electro-Fenton technology using an activated carbon fiber cathode. *Desalination*, 2010, 253: 129–134.
- [25] Phalakornkule C, Polgumhang S, Tongdaung W, et al. Electrocoagulation of blue reactive, red disperse and mixed dyes, and application in treating textile effluent, *Journal of Environmental Management*, 2010, 91: 918–926.
- [26] da Silva A J C, dos Santos E V, de Oliveira Morais C C, et al. Electrochemical treatment of fresh, brine and saline produced water generated by petrochemical industry using Ti/IrO<sub>2</sub>-Ta<sub>2</sub>O<sub>5</sub> and BDD in flow reactor. *Chemical Engineering Journal*, 2013, 233: 47–55.
- [27] Martínez-Huitle C A, dos Santos E V, de Araújo D M, et al. Applicability of diamond electrode/anode to the electrochemical treatment of a real textile effluent, *Journal of Electroanalytical Chemistry*, 2012, 674: 103–107.
- [28] Aquino J M, Rocha-Filho R C, Ruotolo L A M, et al. Electrochemical degradation of a real textile wastewater using  $\beta$ -PbO<sub>2</sub> and DSA® anodes. *Chemical Engineering Journal*, 2014, 251: 138–145.
- [29] González T, Domínguez J R, Palo P, et al. Development and optimization of the BDD-electrochemical oxidation of the antibiotic trimethoprim in aqueous solution. *Desalination*, 2011, 280 (1–3): 197–202.
- [30] Angela A, Urtiaga A, Ortiz I. Contributions of electrochemical oxidation to wastewater treatment: Fundamentals and review of applications. *Journal of Chemical Technology and Biotechnology*, 2009, 84 (12): 1747–1755.

- [31] Yang C, Lee C, Wen T . Hypochlorite generation on Ru-Pt binary oxide for treatment of dye wastewater. *Journal of Applied Electrochemistry*, 2000, 30: 1043–1051.
- [32] Comminellis C, Nerini A. Anodic oxidation of phenol in the presence of NaCl for wastewater treatment. *Journal of Applied Electrochemistry*, 1995, 25 (1): 23–28.
- [33] Rajkumar D, Kim J G. Oxidation of various reactive dyes with in situ electro-generated active chlorine for textile dyeing industry wastewater treatment. *Journal of Hazardous Materials*, 2006, 136 (2): 203–212.
- [34] Bonfatti F, Ferro S, Lavezzo F, et al. Electrochemical incineration of glucose as a model organic substrate. II. Role of active chlorine mediation. *Journal of the Electrochemical Society*, 2000, 147 (2): 592.
- [35] Martínez-Huitle C A, Ferro S, De Battisti A. Electrochemical incineration in the presence of halides. *Electrochemical and Solid-State Letters*, 2005, 8 (11): D35.
- [36] Grgur B N, Mijin D Ž. A kinetics study of the methomyl electrochemical degradation in the chloride containing solutions. *Applied Catalysis B: Environmental*, 2014, 147: 429–438.
- [37] Scialdone O, Galia A, Randazzo S. Electrochemical treatment of aqueous solutions containing one or many organic pollutants at boron doped diamond anodes. Theoretical modeling and experimental data. *Chemical Engineering Journal*, 2012, 183: 124–134.
- [38] Neodo S, Rosestolato D, Ferro S, et al. On the electrolysis of dilute chloride solutions: Influence of the electrode material on faradaic efficiency for active chlorine, chlorate and perchlorate. *Electrochimica Acta*, 2012, 80: 282–291.
- [39] Gretton A, Doucet A, Herbrich R, et al. Support vector regression for black-box system identification. *Proceedings of the 11th IEEE Signal Processing Workshop On Statistical Signal Processing*, 2008: 341–344.
- [40] Martínez-Huitle C A, Brillas E. Decontamination of wastewaters containing synthetic organic dyes by electrochemical methods: A general review. *Applied Catalysis B: Environmental*, 2009, 87 (3–4): 105–145.
- [41] Trasatti S. Progress in the understanding of the mechanism of chlorine evolution at oxide electrodes. *Electrochimica Acta*, 1987, 32: 369–382.
- [42] Kraft, A. Electrochemical Water Disinfection: a Short Review. *Electrodes Using Platinum Group Metal Oxides. Platinum Metals Review*, 2008, 52: 177–185.

- [43] Scialdone O, Galia A, Guarisco C, et al. Electrochemical incineration of oxalic acid at boron doped diamond anodes: Role of operative parameters. *Electrochimica Acta*, 2008, 53 (5): 2095–2108.
- [44] Choi J, Shim S, Yoon J. Design and operating parameters affecting an electrochlorination system. *Journal of Industrial and Engineering Chemistry*, 2013, 19 (1): 215–219.
- [45] Zhou M, Särkkä H, Sillanpää M. A comparative experimental study on methyl orange degradation by electrochemical oxidation on BDD and MMO electrodes. *Separation and Purification Technology*, 2011, 78 (3): 290–297.
- [46] Costa C R, Montilla F, Morallón E, et al. Electrochemical oxidation of acid black 210 dye on the boron-doped diamond electrode in the presence of phosphate ions: Effect of current density, pH, and chloride ions. *Electrochimica Acta*, 2009, 54 (27): 7048–7055.
- [47] Scialdone O, Galia A, Sabatino S. Abatement of Acid Orange 7 in macro and micro reactors. Effect of the electrocatalytic route. *Applied Catalysis B: Environmental*, 2014, 148–149: 473–483.
- [48] Scialdone O, Corrado E, Galia A, et al. Electrochemical processes in macro and microfluidic cells for the abatement of chloroacetic acid from water. *Electrochimica Acta*, 2014, 132: 15–24.
- [49] Özcan A, Oturan M A, Oturan N, et al. Removal of Acid Orange 7 from water by electrochemically generated Fenton's reagent. *Journal of Hazardous Materials*, 2009, 163 (2–3): 1213–1220.
- [50] Ltaïef A H, Sabatino S, Proietto F, et al. Electrochemical treatment of aqueous solutions of organic pollutants by electro-Fenton with natural heterogeneous catalysts under pressure using Ti/IrO<sub>2</sub>-Ta<sub>2</sub>O<sub>5</sub> or BDD anodes. *Chemosphere*, 2018, 202: 111–118.
- [51] Zhou M, Yu Q, Lei L, et al. Electro-Fenton method for the removal of methyl red in an efficient electrochemical system. *Separation and Purification Technology*, 2007, 57 (2): 380–387.
- [52] Zhang B, Sun J, Wang Q, et al. Electro-Fenton oxidation of coking wastewater: optimization using the combination of central composite design and convex optimization method. *Environmental Technology (United Kingdom)*, 2017, 38 (19): 2456–2464.

- [53] El-Ghenymy A, Oturan N, Oturan M A, et al. Comparative electro-Fenton and UVA photoelectro-Fenton degradation of the antibiotic sulfanilamide using a stirred BDD/air-diffusion tank reactor. *Chemical Engineering Journal*, 2013, 234: 115–123.
- [54] Nidheesh P V, Gandhimathi R. Trends in electro-Fenton process for water and wastewater treatment: An overview. *Desalination*, 2012, 299: 1–15.
- [55] Garrido A, Mari R. Catalytic behavior of the  $\text{Fe}^{3+} / \text{Fe}^{2+}$  system in the electro-Fenton degradation of the antimicrobial chlorophene. *Applied Catalysis B: Environmental*, 2007, 72: 382–394.
- [56] Babuponnusami A, Muthukumar K. Removal of phenol by heterogenous photo electro Fenton-like process using nano-zero valent iron. *Separation and Purification Technology*, 2012, 98: 130–135.
- [57] Sultana S, Choudhury M R, Bakr A R, et al. Effectiveness of electro-oxidation and electro-Fenton processes in removal of organic matter from high-strength brewery wastewater. *Journal of Applied Electrochemistry*, 2018, 48 (5): 519–528.
- [58] Zhou M, Oturan M A, Sirés I. *Electro-Fenton process*. Singapore: Springer Nature. 2018: 205-239.
- [59] Cui L, Ding P, Zhou M, et al. Energy efficiency improvement on in situ generating  $\text{H}_2\text{O}_2$  in a double-compartment ceramic membrane flow reactor using cerium oxide modified graphite felt cathode. *Chemical Engineering Journal*, 2017, 330: 1316–1325.
- [60] Yang W, Zhou M, Liang L. Highly efficient in-situ metal-free electrochemical advanced oxidation process using graphite felt modified with N-doped graphene. *Chemical Engineering Journal*, 2018, 338: 700–708.
- [61] Liu Y, Quan X, Fan X, et al. High-yield electrosynthesis of hydrogen peroxide from oxygen reduction by hierarchically porous carbon. *Angewandte Chemie*, 2015, 127: 6941–6945.
- [62] García-Rodríguez O, Bañuelos J A, Rico-Zavala A, et al. Electrocatalytic activity of three carbon materials for the in-situ production of hydrogen peroxide and its application to the electro-fenton heterogeneous process. *International Journal of Chemical Reactor Engineering*, 2016, 14: 843–850.
- [63] Özcan A, Şahin Y, Savaş Koparal A, et al. Carbon sponge as a new cathode material for the electro-Fenton process: comparison with carbon felt cathode and

- application to degradation of synthetic dye basic blue 3 in aqueous medium. *Journal of Electroanalytical Chemistry*, 2008, 616: 71–78.
- [64] Gyenge E L, Oloman C W. Electrosynthesis of hydrogen peroxide in acidic solutions by mediated oxygen reduction in a three-phase (aqueous/organic/gaseous) system Part I: emulsion structure, electrode kinetics and batch electrolysis. *Journal of Applied Electrochemistry*, 2003, 33: 655–663.
- [65] Yu F, Zhou M, Zhou L, et al. A novel electro-Fenton process with H<sub>2</sub>O<sub>2</sub> generation in a rotating disk reactor for organic pollutant degradation, *Environmental Science & Technology Letters*, 2014, 1: 320–324.
- [66] Miao J, Zhu H, Tang Y, et al. Graphite felt electrochemically modified in H<sub>2</sub>SO<sub>4</sub> solution used as a cathode to produce H<sub>2</sub>O<sub>2</sub> for preoxidation of drinking water. *Chemical Engineering Journal*, 2014, 250: 312–318.
- [67] Sheng Y, Zhao Y, Wang X, et al. Electrogeneration of H<sub>2</sub>O<sub>2</sub> on a composite acetylene black–PTFE cathode consisting of a sheet active core and a dampproof coating. *Electrochimica Acta*, 2014, 133: 414–421.
- [68] Luo H, Li C, Wu C, et al. In situ electrosynthesis of hydrogen peroxide with an improved gas diffusion cathode by rolling carbon black and PTFE. *RSC Advances*, 2015, 5: 65227–65235.
- [69] Yu F, Zhou M, Yu X. Cost-effective electro-Fenton using modified graphite felt that dramatically enhanced on H<sub>2</sub>O<sub>2</sub> electro-generation without external aeration. *Electrochimica Acta*, 2015, 163: 182–189.
- [70] Ren G, Zhou M, Liu M, et al. A novel vertical-flow electro-Fenton reactor for organic wastewater treatment, *Chemical Engineering Journal*, 2016, 298: 55–67.
- [71] Xu A, Han W, Li J, et al. Electrogeneration of hydrogen peroxide using Ti/IrO<sub>2</sub>–Ta<sub>2</sub>O<sub>5</sub> anode in dual tubular membranes Electro-Fenton reactor for the degradation of tricyclazole without aeration. *Chemical Engineering Journal*, 2016, 295: 152–159.
- [72] Thiam A, Sirés I, Garrido J A, et al. Effect of anions on electrochemical degradation of azo dye Carmoisine (Acid Red 14) using a BDD anode and air-diffusion cathode. *Separation and Purification Technology*, 2015, 140: 43–52.
- [73] Ma L, Zhou M, Ren G, et al. A highly energy-efficient flow-through electro-Fenton process for organic pollutants degradation. *Electrochimica Acta*, 2016, 200: 222–230.



- [74] Brillas E, Martínez-Huitle C A. *Synthetic Diamond Films: Preparation, Electrochemistry, Characterization and Applications*, Wiley, 2011.
- [75] Giomo M, Buso A, Fier P, et al. A small-scale pilot plant using an oxygen-reducing gas-diffusion electrode for hydrogen peroxide electro-synthesis. *Electrochimica Acta*, 2008, 54: 808–815.
- [76] Luo H, Li C, Wu C, et al. Electrochemical degradation of phenol by in situ electro-generated and electro-activated hydrogen peroxide using an improved gas diffusion cathode. *Electrochimica Acta*, 2015, 186: 486–493.
- [77] Mollah M Y A, Schennach R, Parga J R, et al. Electrocoagulation (EC)- Science and applications. *Journal of Hazardous Materials*, 2001, 84 (1): 29–41.
- [78] De Laat J, Gallard H. Catalytic decomposition of hydrogen peroxide by Fe(III) in homogeneous aqueous solution: Mechanism and kinetic modeling. *Environmental Science and Technology*, 1999, 33 (16): 2726–2732.
- [79] Ramirez J H, Duarte F M, Martins F G, et al. Modelling of the synthetic dye Orange II degradation using Fenton's reagent: From batch to continuous reactor operation. *Chemical Engineering Journal*, 2009, 148 (2–3): 394–404.
- [80] Pimentel M, Oturan N, Dezotti M, et al. Phenol degradation by advanced electrochemical oxidation process electro-Fenton using a carbon felt cathode. *Applied Catalysis B: Environmental*, 2008, 83 (1–2): 140–149.
- [81] Sankara Narayanan T S N, Magesh G, Rajendran N. Degradation of o-chlorophenol from aqueous solution by electro-fenton process. *Fresenius Environmental Bulletin*, 2003, 12 (7): 776–780.
- [82] Zhang H, Fei C, Zhang D, et al. Degradation of 4-nitrophenol in aqueous medium by electro-Fenton method. *Journal of Hazardous Materials*, 2007, 145 (1–2): 227–232.
- [83] Daneshvar N, Aber S, Vatanpour V, et al. Electro-Fenton treatment of dye solution containing Orange II: Influence of operational parameters. *Journal of Electroanalytical Chemistry*, 2008, 615 (2): 165–174.
- [84] Ghoneim M M, El-Desoky H S, Zidan N M. Electro-Fenton oxidation of Sunset Yellow FCF azo-dye in aqueous solutions. *Desalination*, 2011, 274 (1–3): 22–30.
- [85] Scialdone O, Galia A, Gattuso C, et al. Effect of air pressure on the electro-generation of H<sub>2</sub>O<sub>2</sub> and the abatement of organic pollutants in water by electro-Fenton process. *Electrochimica Acta*, 2015, 182: 775–780.

- [86] Pérez J F, Galia A, Rodrigo M A, et al. Effect of pressure on the electrochemical generation of hydrogen peroxide in undivided cells on carbon felt electrodes. *Electrochimica Acta*, 2017, 248: 169–177.
- [87] Scialdone O, Galia A, Sabatino S. Electro-generation of H<sub>2</sub>O<sub>2</sub> and abatement of organic pollutant in water by an electro-Fenton process in a microfluidic reactor. *Electrochemistry Communications*, 2013, 26 (1): 45–47.
- [88] Yu F, Zhou M, Zhou L, et al. A novel electro-Fenton process with H<sub>2</sub>O<sub>2</sub> generation in a rotating disk reactor for organic pollutant degradation. *Environmental Science and Technology Letters*, 2014, 1 (7): 320–324.

---

## **Chapter 2. State of art on microfluidic reactor wastewater treatment technology**

### **2.1 Introduction**

Microfluidic reactors are defined as reactors that have microstructures for chemical reactions with typical dimensions from 10 to 500  $\mu\text{m}$ . A large number of studies have shown that chemical reactions in microfluidic devices enhance the heat and kinetics transfer process, and improve the selectivity and safety in the reaction process. The main features of microfluidic reactors are [1-4]:

- high mixing efficiency and short reaction time;
- high heat-transfer ability;
- small reactant volumes and controllable residence time;
- high surface-to-volume ratios.

In particular, the microfluidic reactor has a very high relative specific surface area. The specific surface area of the microstructure reactor is about 10000-50000  $\text{m}^2\cdot\text{m}^{-3}$ , while the specific surface area of the traditional reactor is generally only 100  $\text{m}^2\cdot\text{m}^{-3}$ , and in rare cases it can reach 1000  $\text{m}^2\cdot\text{m}^{-3}$ . Therefore, the catalytic efficiency can be improved since the catalysts can be fixed on the inner surfaces of microfluidic reactors.

### **2.2 Application of microfluidic reactor in electrochemical technology**

Daisuke Horii et al. [5-9] have confirmed that a microfluidic reactor with a distance of tens of microns between the cathode and the anode can be successfully used in the treatment of wastewater contaminated by organic pollutants and in electrochemical synthesis. The use of electrochemical microreactors has other very important advantages,

such as it can be used under low voltage and low electrolyte conditions (without additional electrolyte).

Compared with traditional reactors that is usually operated under batch conditions, the microfluidic reactor can be operated under continuous mode due to its extremely small inter-electrode distance and high conversions achieved in a single passage. In continuous operation mode, two or more reactors with different current densities or electrode materials can be connected in series to maximize the current efficiency and minimize the reaction time. According to the material of the reactor and different technical parameters, the microfluidic reactor can be divided into different types.

Attour and co-workers [10] proposed a microfluidic reactor containing, as shown in Fig. 2-1, polyetheretherketone used as the reactor shell, stainless steel as the anode, and glassy carbon as the cathode. Among them, polyether ether ketone has excellent chemical and mechanical stability and good processability. The anode is composed of ten  $1 \times 1 \text{ cm}^2$  cells, separated from each other by a 1 mm wide insulator. The surface of the anode is first coated with a layer of 50  $\mu\text{m}$  thick PTFE coating. The back of the glassy carbon chip of the anode is covered with a gold soil layer to provide good electrical conductivity and minimize contact resistance. The distance between the plates is 100  $\mu\text{m}$ , forming a  $1 \times 0.01 \text{ cm}^2$  cross-sectional channel. The electrolytic cell uses a programmable CNC (computer numerical control) machine to grind the PEEK shell and the stainless steel plate. In order to obtain a more precise shape and avoid unnecessary breakage, the glass carbon plate is cut by a laser method.

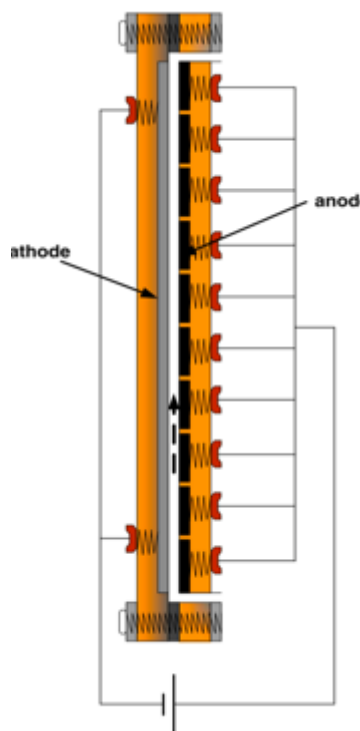


Fig. 2-1 Schematic view of the thin-gap cell.

Pletcher's [11] group proposed the system reported in Fig. 2-2B. The reactor consists of rectangular electrode plates ( $53 \times 40 \times 2$  mm), the anode is carbon-filled polyvinylidene fluoride, the cathode is stainless steel, and the plates are  $500 \mu\text{m}$  thick "snake-shaped" perfluoro rubber. The surface of the stainless-steel electrode plate is processed with a groove with a depth of  $250 \mu\text{m}$ , as shown in Fig. 2-2C, to allow the serpentine gasket to be inserted into it. An outlet and an inlet are installed at both ends of the reactor. This design provides an electrolysis path length of  $700 \text{ mm}$ , a depth of  $200 \mu\text{m}$ , and a width of  $1.5 \text{ mm}$ . The volume of a single electrolytic solution is  $0.21 \text{ cm}^3$ , and the electrode area involved in the reaction is  $1050 \text{ mm}^2$ .

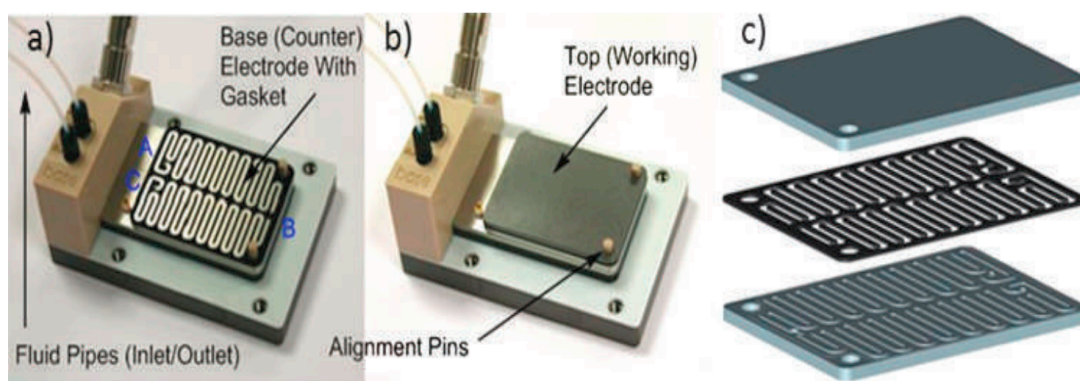


Fig. 2-2. Photographs of the microflow cell and components. (a) Electrolysis cell showing recessed electrode and gasket. (b) Electrolysis cell with top electrode. (c) Graphic showing arrangement of recessed electrode, gasket, and top electrode.

The flow cell used by Mayank and co-workers [12] is made of two-layer poly (PMMA) by CNC milling with 0.5, 1, 3, and 6 mm carbide drill bits (Fig. 2-3). The external dimensions of the flow cell are 35 mm  $\times$  30 mm  $\times$  4 mm. The top layer has 29 mm long, 10 mm wide and 1 mm deep grooves to accommodate the DropSens SPE electrodes. This layer also has spiral channels for transporting liquid on the surface of the working electrode. The diameter of the spiral is 3.8 mm, the width and depth of the channel is 0.6 mm and 140  $\mu$ m depth, respectively. The total length and internal volume are 19.45 mm and 3.30  $\mu$ L, respectively. There are 2 holes (1 mm in diameter) at both inlet and outlet. The two plates also have holes with a diameter of 6.2mm and a depth of 3.5mm to accommodate the NdFeB magnets (diameter 6mm, height 3mm) used to clamp the plate and electrode together.

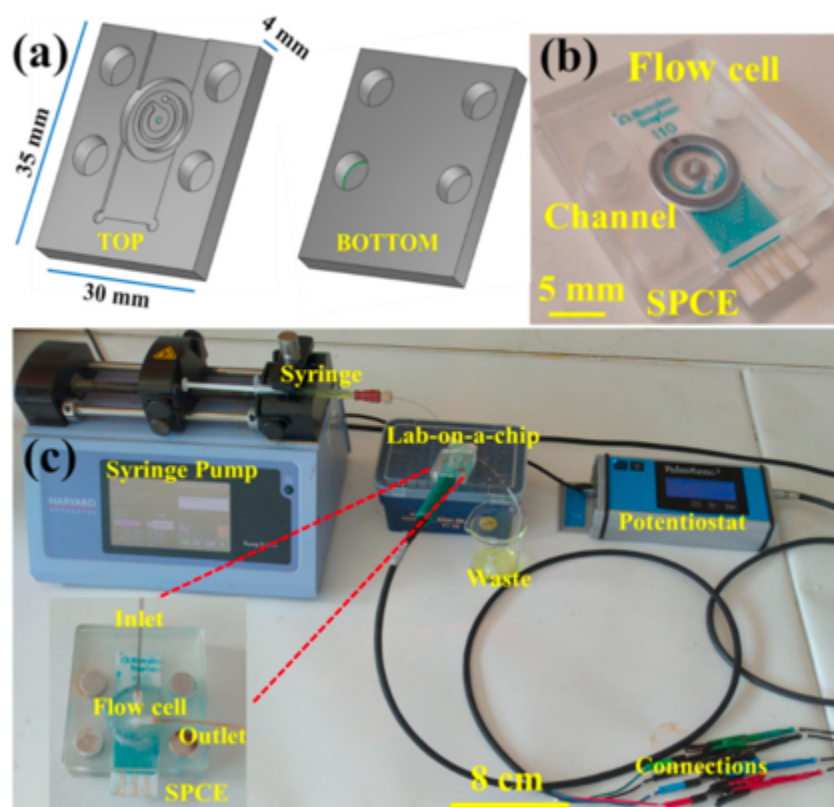


Fig 2-3. (a, b) Details of the microfluidic flow cell design. (c) Photograph of the experimental setup showing the syringe pump and collection vessel for fluid movement through the microfluidic flow cell with integrated SPCE electrode connected to a small potentiostat for recording of electrochemical measurements.

Kuleshova et al. [13] proposed a circular electrochemical microfluidic reactor shown in Fig. 2-4. The device consists of two flat circular electrodes with a diameter of 100 mm, separated by a microchannel with a width of 1 mm and a total length of 600 mm. The anode is made of 5 mm thick conductive carbon/polyvinylidene fluoride, the cathode is 3 mm thick stainless steel, and the electrode spacing is 500  $\mu\text{m}$ . In order to keep the reactor tight and prevent electrolyte leakage, the upper and lower round aluminum housings are connected by 10 edge bolts and a center bolt. The bolts are placed in a tubular polymer gasket with a 6 mm outer diameter so that it's insulated with the electrodes, the stress and deformation in the channel are minimized when the bolts are tightened, and finally the fluid inlet and outlet are connected on two aluminum connectors.

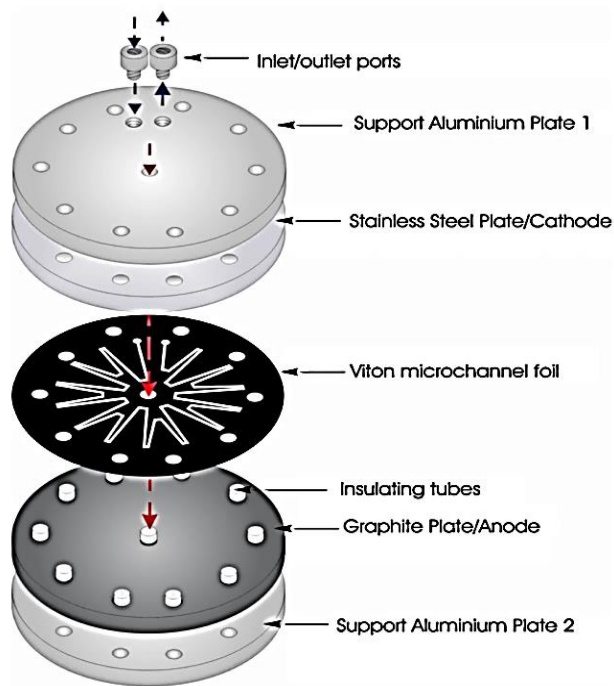


Fig. 2-4 Schematic illustration of the microflow reactor showing the essential components of the electrolysis cell.

In Mousset's research [14], the cell was designed in order to allow the visual inspection of the internal reactor (Fig. 2-5). It's manufactured by poly (methyl methacrylate) (PMMA) which is chemically and thermally resistant to the applied conditions. The graphite felt was embedded in the cathode chamber as a cathode, and the felt was connected to the graphite rod to avoid leakage which also ensured that no contact between the cathode and the anode occurs at the extremely short distance between the electrodes. The gap between the electrodes was changed by polytetrafluoroethylene (PTFE) gaskets of different thicknesses. The geometric surface area of the cathode and anode was  $50 \text{ cm}^2$ .



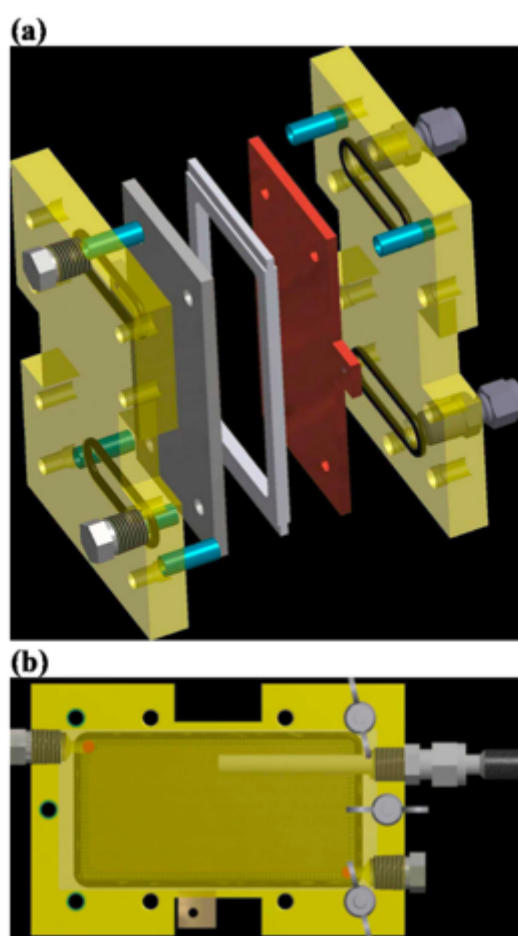


Fig. 2-5 Scheme of the microfluidic electrochemical reactor developed in the laboratory. a) Exploded view of the complete cell and b) view of the graphite felt cathode compartment.

Rodrigo's group [15] proposed a new microfluidic reactor (see Fig. 2-6) which allows the use of high flow rates and multi-pass configurations. The electrochemical cell is made of polycarbonate sheet, which is optically-transparent and chemically-resistant. The inter-electrode spacer is a plastic film (300  $\mu\text{m}$ ), and an aluminum thin foil (50  $\mu\text{m}$  each) was used to make the current collector, creating a electrode-gap of 400  $\mu\text{m}$ . The cross section of the fluid is 33 cm. 3D-mesh Diachem® diamond and stainless steel were used as anode and cathode, respectively.

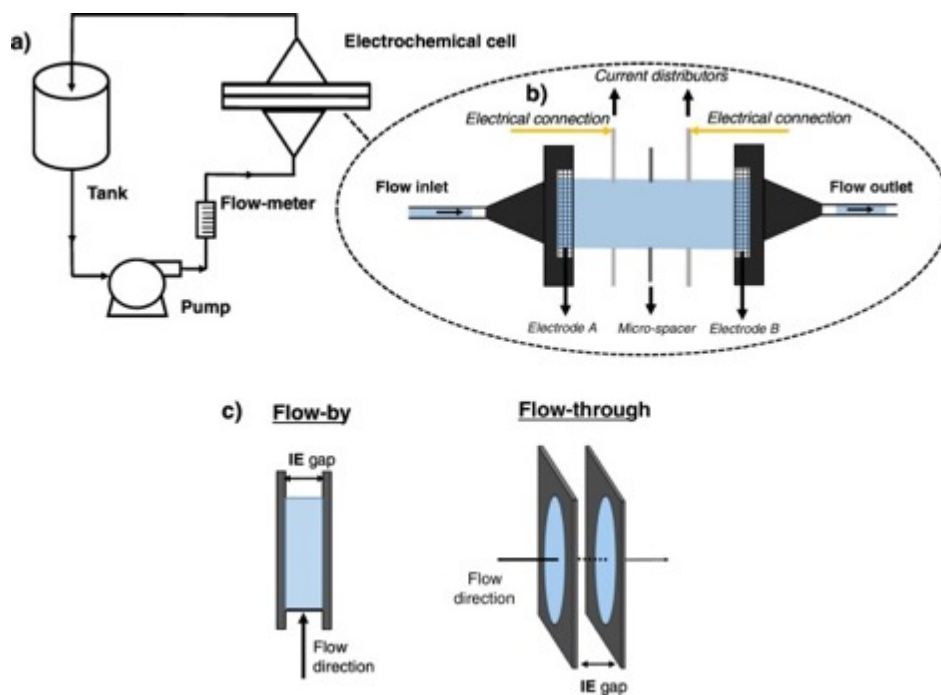


Fig. 2-6 (a) Flow diagram, (b) electrochemical cell (c) comparison of flow-by and flow-through configurations.

In Scialdone's group, a kind of electrochemical microreactor was designed [16] which is constituted by (as shown in Fig. 2-7): two steel plates provided with two holes, to impart mechanical stability to the cell; two plates of teflon equally provided with holes one for inlet and one for the outlet of the fluid; two neoprene gaskets, each of which is interposed between the plate of Teflon containment and the electrode, which ensure the sealing and prevent any loss of solution from the cell; two electrodes consisting of two flat plates with the same dimensions; one or more spacers (made of PTFE by Bohlender GmbH) which allow to define the working area.

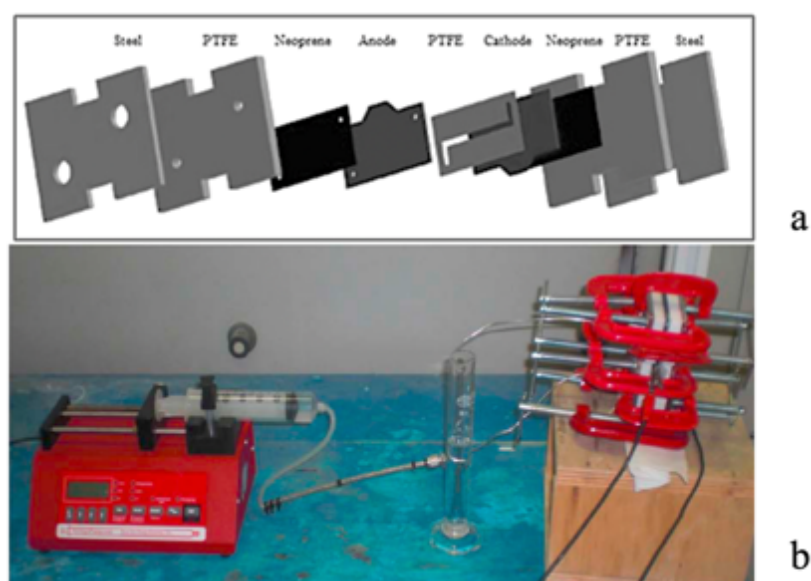


Fig. 2-7. (a) Scheme of the micro-reactor (b) micro reactor system with pump, and tubing.

### 2.3 Application of microfluidic reactor in electrochemical wastewater treatment technology

Compared with conventional electrochemical reaction devices, the use of electrochemical microfluidic reactors can greatly improve the removal efficiency of organic pollutants in wastewater. On the one hand, the extremely small distance between the electrodes lead to smaller ohmic drops between the two electrode plates during the reaction, so the organic pollutants in the wastewater can be electrochemically degraded under low voltage or low conductivity (no additional electrolyte is required); on the other hand, the mass transfer process of the organic pollutant to the surface of the electrode is enhanced during the reaction process. In contrast, for conventional electrochemical reactors, when the conductivity of the solution is poor, in order to obtain a reasonable and effective cell voltage, a certain amount of electrolyte (such as NaCl, Na<sub>2</sub>SO<sub>4</sub>) is usually added to the reaction system, resulting in high operating costs. Scialdone' group conducted a series of studies on the degradation of organics such as 1,1,2,2-tetrachloroethane, chloroacetic acid and acid orange 7, using a microfluidic reactor.

### 2.3.1 Abatement of 1,1,2,2-tetrachloroethane in micro reactors

The experiments were performed in a microfluid reactor assembled with different distances (50, 75  $\mu\text{m}$ ) between anode and cathode. As shown in Fig. 2-8, an increase of both the abatement and the current efficiency was obtained by operating with lower distances between the electrodes. Furthermore, very high abatements were achieved in one single passage of the solution inside the cell using low flow rates [17].

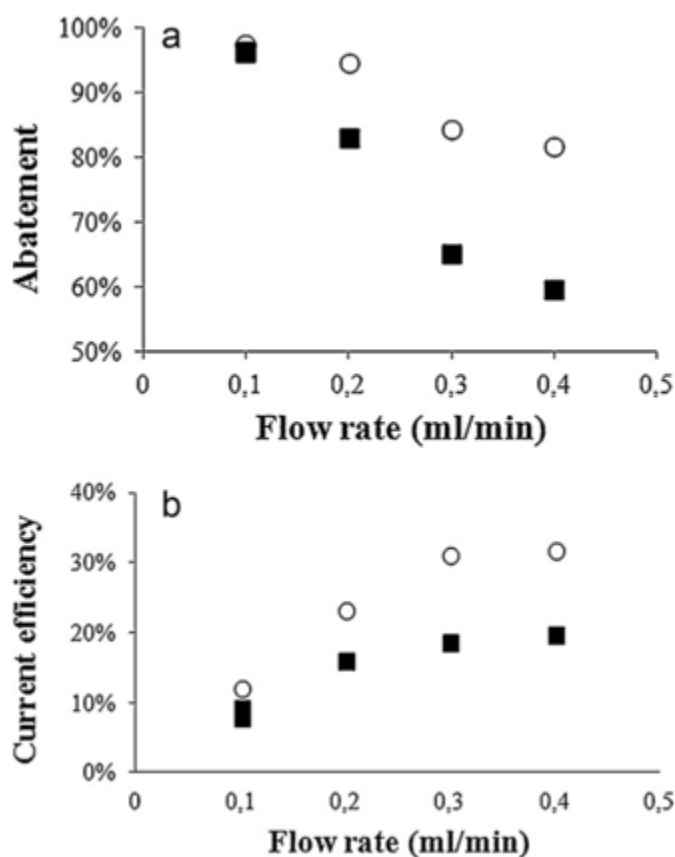


Fig. 2-8. Effect of the nominal distance between the electrodes (50 (O) and 75  $\mu\text{m}$  (■)) on the abatement (a) and the current efficiency (b) of the oxidation process of 1,1,2,2-tetrachloroethane performed at a BDD anode in a micro reactor at different flow rates. Current density: 3 mAcm<sup>-2</sup>. Initial concentration of 1,1,2,2-tetrachloroethane 0.9 mM. Cathode: nickel.

### 2.3.2 Abatement of chloroacetic acid in micro reactors

The electrochemical abatement of chloroacetic acid was performed both in macro and microfluidic cells, using different electrochemical approaches, including anodic oxidation at BDD, electro-Fenton (EF) and a coupled approach. As shown in Fig. 2-9, in the degradation of CAA using EF process, a higher abatement of CAA was obtained in microreactor than in macro one. As shown in Fig. 2-10, the coupled process led to significantly faster abatements compared to single treatments performed with EF (DSA/graphite) and EO (BDD/steel) micro cells [18].

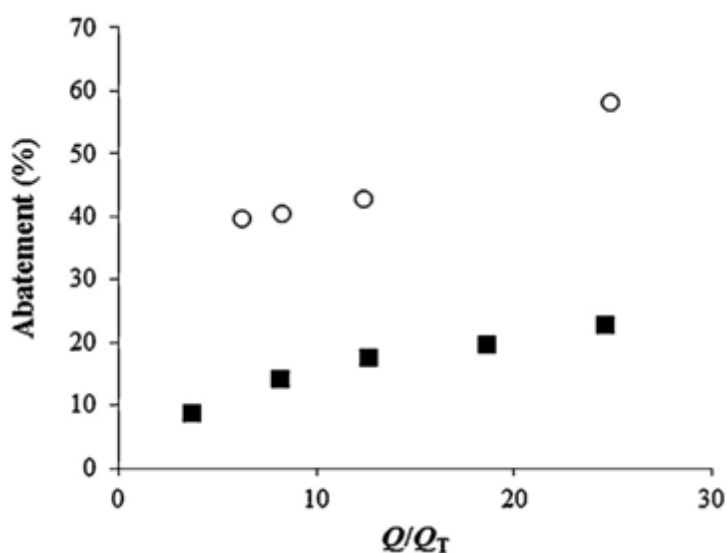


Fig. 2-9. Abatement of CAA using a compact graphite cathode in (■) macro and (○) microreactor vs. dimensionless charge  $Q/Q_T$  (ratio between charge passed and theoretical charge). The electrolyses of solutions of 5 mM CAA with 0.5 mM  $Fe_2SO_4$  were performed at pH  $\sim$  3 and 8  $mA\ cm^{-2}$ . The experiments in the microfluidic cell were carried out at  $0.1\ mL\ min^{-1}$  with an interelectrode gap of  $100\ \mu m$ . Anode:  $Ti/IrO_2-Ta_2O_5$ . Electrode surface:  $5\ cm^2$ .

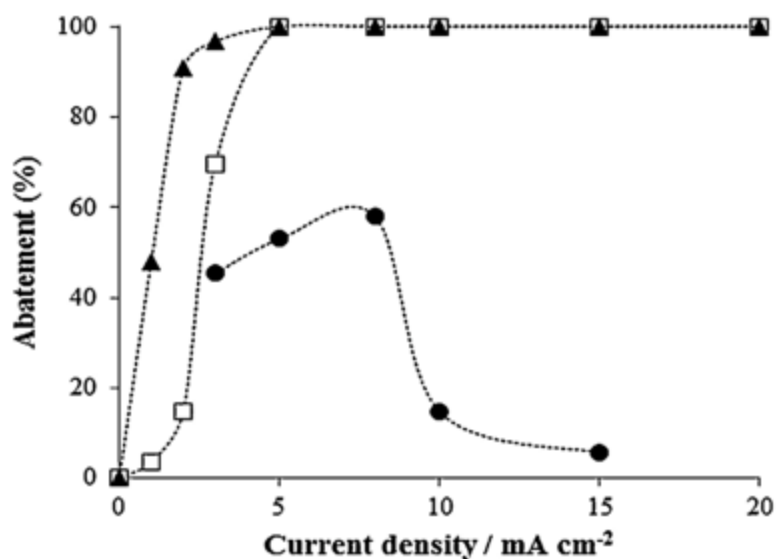


Fig. 2-10 Abatement of CAA by (□) electro-oxidation with BDD (with a stainless-steel cathode), (●) reduction at compact graphite cathode (with Ti/IrO<sub>2</sub>-Ta<sub>2</sub>O<sub>5</sub> as anode) and (▲) coupled process (BDD anode and graphite cathode).

### 2.3.3 Abatement of acid orange 7 in micro reactors

In the case of the treatment of solutions of acid orange 7 by anodic oxidation process, higher COD abatements were obtained, as shown in Fig. 2-11, in the microcell. On the other hand, in the case of the oxidation achieved by electro-generated active chlorine a similar TOC abatement was obtained in the macro and in the micro reactors, which indicates that this indirect electrochemical oxidation process is not limited by mass transfer kinetics [19].

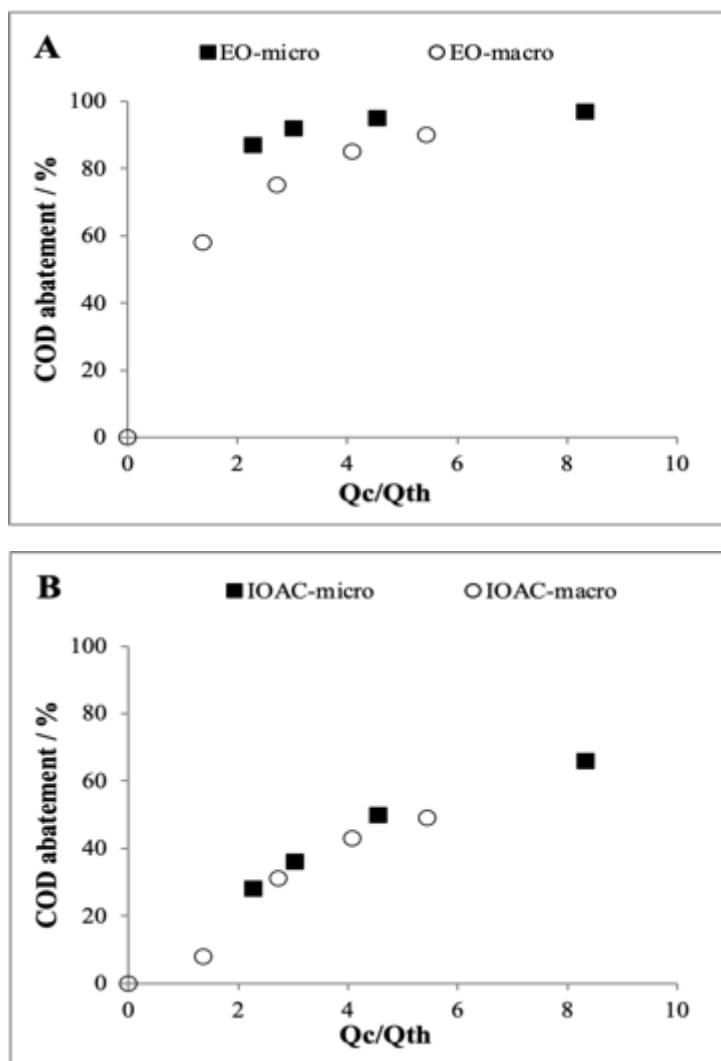


Fig. 2-11. Trend of abatement of COD vs.  $Q_c/Q_{th}$  for the electrochemical oxidation of AO7 by direct oxidation at BDD ( $\blacksquare$ ), electrogenerated active chlorine at  $\text{Ti}/\text{IrO}_2\text{-Ta}_2\text{O}_5$  with 17 mM of NaCl ( $\circ$ ) in the micro reactor at  $100 \text{ A m}^{-2}$ . Cathode: Nickel. Nominal distance between the electrodes in the micro reactor  $50 \mu\text{m}$ . Flow rate in the micro reactor: 0.1–0.4 mL/min.

However, all the researches were performed using synthetic wastewater; hence, a further investigation focused on the utilization of real wastewater is necessary to better evaluate the potentialities of microcell.

## 2.4 Reference

- [1] Yao X, Zhang Y, Du L, et al. Review of the applications of microreactors. *Renewable and Sustainable Energy Reviews*, 2015, 47: 519–539.
- [2] Jähnisch K, Hessel V, Löwe H, et al. Chemistry in microstructured reactors. *Angewandte Chemie*, 2004, 43(4): 406-446.
- [3] Wang J, Liu W, Wang J, et al. Microfluidic device: A miniaturized platform for chemical reactions. *Chinese Journal of Chemistry*, 2013, 31 (3): 304–316.
- [4] Samargia J, Sher M, Pino J S, et al. Quantitative analysis of sperm rheotaxis using a microfluidic device. *Microfluidics and Nanofluidics*, 2018, 22 (9): 1–11.
- [5] Horii D, Atobe M, Fuchigami T, et al. Self-supported paired electrosynthesis of 2,5-dimethoxy-2,5-dihydrofuran using a thin layer flow cell without intentionally added supporting electrolyte. *Electrochemistry Communications*, 2005, 7 (1): 35–39.
- [6] Kuleshova J, Hill-Cousins J T, Birkin P R, et al. The methoxylation of N-formylpyrrolidine in a microfluidic electrolysis cell for routine synthesis. *Electrochimica Acta*, 2012, 69: 197–202.
- [7] Jolley K E, Pickering S, Pletcher D, et al. The influence of non-ionic surfactants on electrosynthesis in extended channel, narrow gap electrolysis cells. *Electrochemistry Communications*, 2019, 100: 6–10.
- [8] Green R A, Brown R C D, Pletcher D, et al. An extended channel length microflow electrolysis cell for convenient laboratory synthesis. *Electrochemistry Communications*, 2016, 73: 63–66.
- [9] He P, Watts P, Marken F, et al. Scaling out of electrolyte free electrosynthesis in a micro-gap flow cell. *Lab on a Chip*, 2007, 7 (1): 141–143.
- [10] Attour A, Rode S, Ziogas A, et al. A thin-gap cell for selective oxidation of 4-methylanisole to 4-methoxy-benzaldehyde-dimethylacetal. *Journal of Applied Electrochemistry*, 2008, 38 (3): 339–347.
- [11] Kuleshova J, Hill-Cousins J T, Birkin P R, et al. The methoxylation of N-formylpyrrolidine in a microfluidic electrolysis cell for routine synthesis. *Electrochimica Acta*, 2012, 69: 197–202.
- [12] Mayank Garg , Martin Gedsted Christensen , Alexander Iles, et al. Microfluidic-Based Electrochemical Immunosensing of Ferritin. *Biosensors*, 2020, 10: 1-13.



- 
- [13] Kuleshova J, Hill-cousins J T, Birkin P R, et al. A simple and inexpensive microfluidic electrolysis cell. *Electrochimica Acta*, 2011, 56 (11): 4322–4326.
- [14] Emmanuel Mousset, Marta Puce, Marie-Noëlle Pons. Advanced Electro-Oxidation with Boron-Doped Diamond for Acetaminophen Removal from Real Wastewater in a Microfluidic Reactor: Kinetics and Mass-Transfer Studies. *ChemElectroChem* 2019, 6: 2908–2916.
- [15] Pérez J F, Llanos J, Sáez C, et al. Development of an innovative approach for low-impact wastewater treatment: A microfluidic flow-through electrochemical reactor. *Chemical Engineering Journal*, 2018, 351: 766–772.
- [16] Sabatino S, Galia A, Scialdone O. Electrochemical abatement of organic pollutants in continuous-reaction systems through the assembly of microfluidic cells in series. *ChemElectroChem*, 2016, 3 (1): 83–90.
- [17] Scialdone O, Galia A, Guarisco C, et al. Abatement of 1,1,2,2-tetrachloroethane in water by reduction at silver cathode and oxidation at boron doped diamond anode in micro reactors. *Chemical Engineering Journal*, 2012, 189–190: 229–236.
- [18] Scialdone O, Galia A, Sabatino S, et al. Electrochemical conversion of dichloroacetic acid to chloroacetic acid in a microfluidic stack and in a series of microfluidic reactors. *ChemElectroChem*, 2015, 2 (5): 684–690.
- [19] Scialdone O, Galia A, Sabatino S. Abatement of Acid Orange 7 in macro and micro reactors. Effect of the electrocatalytic route. *Applied Catalysis B: Environmental*, 2014, 148–149: 473–483.



---

## **Chapter 3. State of art on reverse electro dialysis technology of the wastewater treatment**

### **3.1 Introduction**

In the last two decades, a large effort was carried out to increase the utilization of renewable energies. In 2017, 13.5% of the world total primary energy supply was produced from renewable energy sources, which includes the exploitation of hydro, solar, wind, biofuels, waste and geothermal resources [1]. In addition, several researchers are trying to exploit other forms of renewable energy including salinity gradient energy (SGE). SGE is available when two solutions with different salinity levels are mixed together. As an example, when rivers discharge into the sea, they release about 1.7 MJ per m<sup>3</sup> of river water [2]. Salinity gradients are widely available both in nature (estuaries or coastal areas, mixing of seawater and brackish water) [3] and in industrial plants (as an example, wastewater with different salinities) [4,5] or they can be obtained using thermolytic solutions [6] regenerated with waste heat (> 40 °C) [7,8]. Reverse electro dialysis (RED) is a process for direct electricity production from salinity-gradient energy, based on the use of many pairs of anion and cation exchange membranes situated between two electrodes and on the utilization of proper redox processes (as shown in Fig.3-1) [9-11]. Many membrane pairs are needed for the utilization of salinity gradients to produce electricity, resulting in high investment costs for RED systems devoted to the production of electric energy. In this context, in order to improve the economic figures of the overall RED process, several works investigated the effect of the main operative parameters on the process, including load resistance, residence time, feed flow rate, stack design, etc..

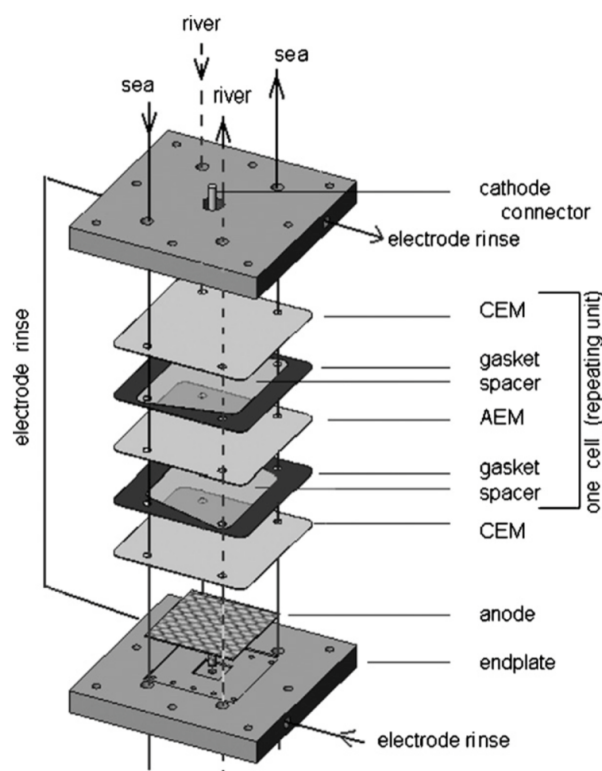


Fig. 3-1 Main components of the stack, showing a block of ion exchange membranes situated between the electrodes, the electrodes, flow path of the high and low concentrated solutions (HC and LC respectively) and of electrolyte solution [9].

As an alternative, some authors have proposed to use salinity gradients to sustain redox processes for the synthesis of chemicals or the treatment of wastewater contaminated by recalcitrant organics adopting RED stacks assembled with relatively few membrane pairs and salinity gradients available in nature or in industrial plants [12-24], thus saving the electric energy necessary for conventional electrolysis processes. In particular, some groups have shown that it is possible to use river, seawater and/or brine solutions to treat various kinds of wastewater both in lab-scale devices [16,17] and in a pilot-plant scale [15], while others have shown that RED can be used for the generation of hydrogen using both natural salinity gradients and thermolytic solutions regenerated by waste heat [17-22]. In this frame, recently, it has been observed that the plants devoted to the treatment of industrial wastewater deal often with waters characterized by different salinity and the

relative salinity gradient can be potentially used to depurate part of these wastewaters by RED, allowing potentially a huge saving of energy [4].

### 3.2 Principle of reverse electro dialysis system

RED is based on the use of many pairs of anion and cation exchange membranes situated between two electrodes. The supply of two solutions with different salt concentration in the RED stack (a high concentration solution and a diluted one, named in the following  $HC_{stack}$  and  $LC_{stack}$ , respectively) gives rise to a potential difference between the electrodes that can be used to produce electric energy and to drive redox processes at the electrodes that can be potentially used for many purposes [25-28]. The working principle of RED is shown in Fig. 3-2.

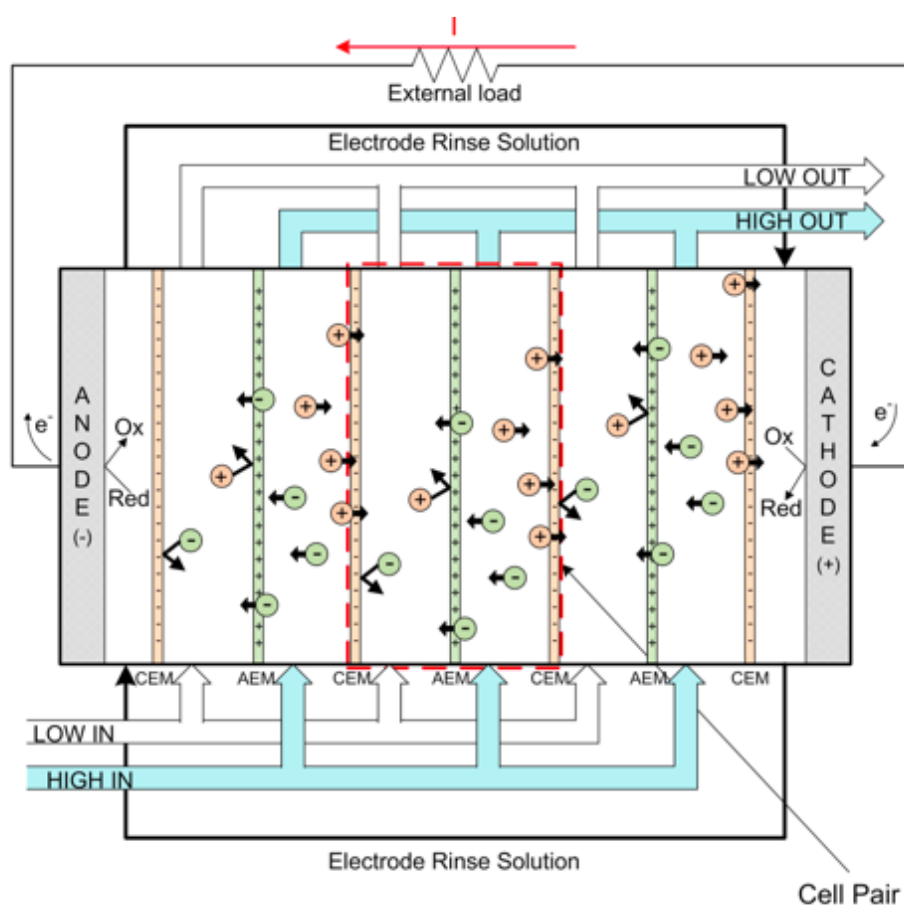


Fig. 3-2 Schematic representation of the RED process [28].

In particular, the electromotive force for a stack assembly of N membrane pairs fed with water solutions of NaCl can be estimated by Eq. 3-1 [27].

$$E = 2N\alpha \frac{RT}{zF} \ln \left( \frac{\alpha_c}{\alpha_d} \right) \quad (3-1)$$

where R is the gas constant, T the absolute temperature, p is the average permselectivity of the membrane pair, F the Faraday constant and  $a_c$  and  $a_d$  the solute activities in concentrated and diluted solutions, respectively.

In the reverse electrodialysis process, in order to convert the electric potential into electric energy, the reactor needs to contain: i) ion exchange membranes (cationic and anionic), which must have high selective permeability, good mechanical properties and high chemical and thermal stability and relatively low costs; ii) gaskets; iii) an electrode system, composed of electrodes and electrode solution, containing suitable redox pairs for electrochemical reaction process.

### **3.3 The effect of operative conditions on the power generation in RED process**

#### **3.3.1 The effect of investigated redox processes**

As shown in Table 3-1, different kinds of electrode systems for RED were compared with the main aim to ensure high power density, safety, health and environment protection, technical feasibility and low costs. Among them, the widely investigated system water/NaCl gives rise to products such as gaseous chlorine, active chlorine, hydroxyl ions and hydrogen [29,30].

Table 3-1 Main characteristics of investigated redox processes [29,30]

Redox processes (V vs. SHE)	$\Delta V$ (V)	Stability of redox species and electrodes	Toxicity	maximum power(W)
$H_2O \rightarrow 2H^+ + 0.5O_2 + 2e^-$ (0.99 V at pH 2) $H_2O + e^- \rightarrow OH^- + 0.5H_2$ (-0.83 V at pH = 14)	2.4–2.5 <sup>a</sup>	Very high	No with suitable supporting electrolytes	0.07
$Cl^- \rightarrow 0.5Cl_2 + e^-$ (1.36 V) $H_2O + e^- \rightarrow 0.5H_2 + OH^-$ (-0.83 V at pH = 14)	2.25–2.35 <sup>a</sup>	Very high	Possible concerns for chlorine, active chlorine, chlorate and perchlorate potential formation. Very low in water solutions	0.11
$Fe^{3+} + e^- \rightarrow Fe^{2+}$ (E = 0.77 V)	0.4–0.6 <sup>b</sup>	Very high for pH < 3–4 and in absence of air		0.26
$[Fe(CN)_6]^{3-} + e^- \rightarrow [Fe(CN)_6]^{4-}$ (E = 0.356 V)	0.2–0.4 <sup>b</sup>	Very high in absence of air and light	Very low toxicity release of toxic gas after reaction with strong acids. Possible release of HCN under no proper operative conditions	0.31

<sup>a</sup> Computed by the sum of anode voltage on Ru at pH of 2, cathode voltage at Pt at pH 14 and ohmic drops in the anode and cathode compartments at 1 mA cm<sup>-2</sup> estimated on the basis of literature.

<sup>b</sup> Computed on the basis of electrolyses in undivided cells at 1 mA cm<sup>-2</sup> at graphite electrode for Fe(III)/Fe(II) and at Iridium based electrodes for  $[Fe(CN)_6]^{3-}/[Fe(CN)_6]^{4-}$ .

### 3.3.2 The effect of cell number of membranes

The Eq. 3-1 show that the number of membranes in the RED system is a very important factor affecting the energy production. As shown in Fig. 3-3, when the number of membrane pairs was increased from 10 to 40 and 50, a drastic increase of power density output occurred at higher values of current density and cell voltage [30].

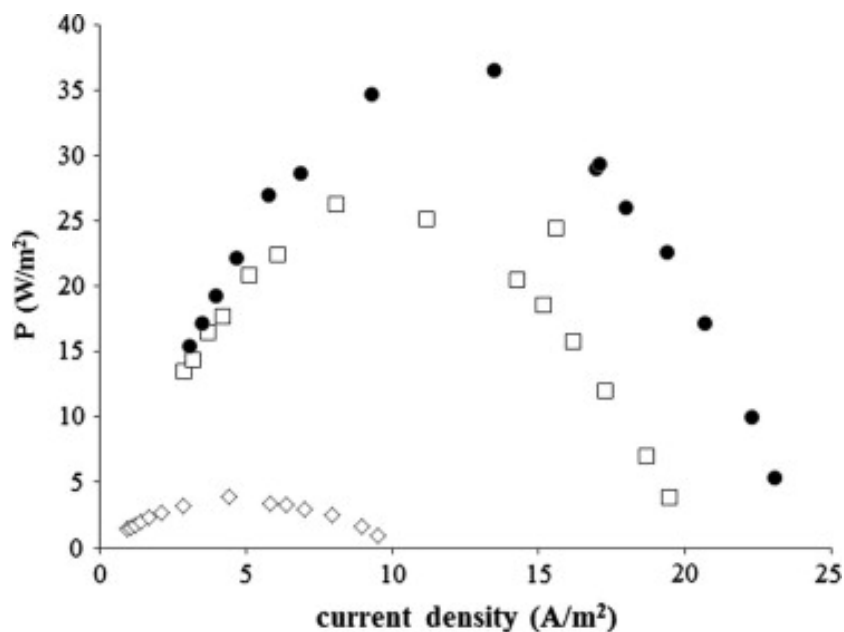


Fig. 3-3 Plot of power densities (computed as the ratio between the power and the geometric area of electrode) vs. current density recorded in a stack equipped with 10 (◇), 40 (□) and 50 (●) membrane pairs with an external resistance varied between 1 and 160 ohm with fixed HC (NaCl 0.5 M) and LC (NaCl 0.01 M) compositions [30].

### 3.3.3 Effect of HC and LC solution flow rate

Scialdone' group reported the utilization of a reverse electrodialysis process at the pilot plant scale. Experiments were performed using an electrode rinse solution containing 0.3 M FeCl<sub>2</sub>, 0.3 M FeCl<sub>3</sub> and 2.5 M Na<sub>2</sub>SO<sub>4</sub> as supporting electrolyte. As shown in Fig. 3-4, the flow rates of HC and LC solutions drastically affect the power output. A maximum power output of 158 W was obtained using feed flow rates of 32 L min<sup>-1</sup> (LC); 147.6 W was achieved for HC and LC flow rates of 23 L min<sup>-1</sup>, and 137.2 W for HC and LC flow rates of 16 L min<sup>-1</sup>. This result is mainly due to the lower residence time of solutions inside stack, leading to a larger concentration difference along the stack and to lower polarization effects at the solution/ membrane interfaces that bring to higher OCV [15].



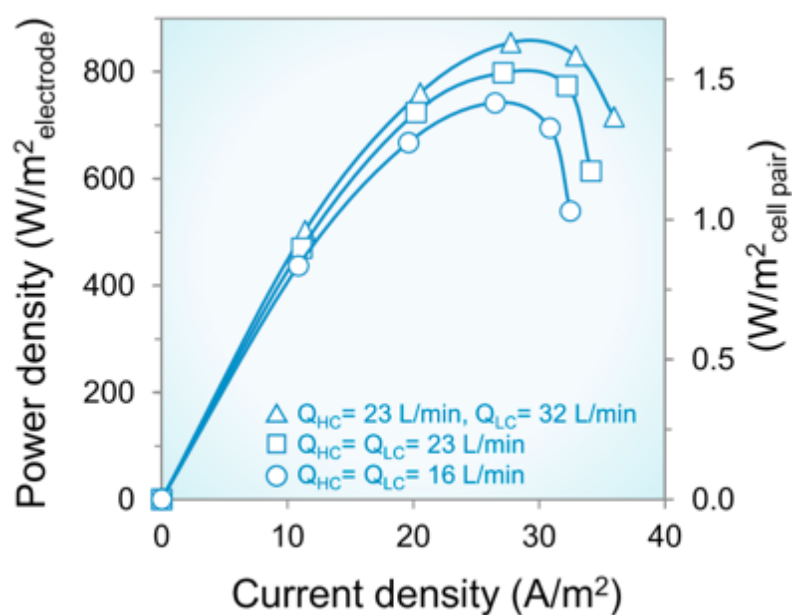


Fig. 3-4 Plot of power density vs current density in a stack equipped with 500 membrane pairs for  $\text{FeCl}_2/\text{FeCl}_3$  electrode solution with a flow rate of  $2 \text{ L min}^{-1}$  and varying HC and LC flow rates [15].

### 3.4 Coupled processes of electric energy generation and wastewater treatment in RED system

As described in the previous sections, in the last years it has been shown that various electrolysis processes, including direct anodic oxidation, cathodic reduction, oxidation by electro-generated active chlorine and electro-Fenton, can allow to treat effectively wastewater contaminated by various inorganic pollutants and a large number of organics resistant to conventional biological processes. However, to favor the utilization of these processes on an applicative scale, it would be particularly important to reduce the energetic costs necessary to sustain the electrolysis. In this frame, to avoid the necessity to supply electric energy, three different approaches were recently proposed:

- (i) the abatement of inorganic pollutants such as  $\text{Cr(VI)}$  or of organic pollutants can be achieved without energy inputs, by direct reduction at the cathode or electro-Fenton process in the cathodic compartment of a microbial fuel cell (MFC) using in the anolyte

water solutions containing biodegradable organics and suitable microorganisms [31-33]; however, MFCs present very long treatment times that make this solution poorly suitable on an applicative scale;

(ii) the electrochemical treatment of wastewater can be performed without energy inputs, but conversely generating electric energy, by reverse electrodialysis (RED), that convert salinity gradients into cell potentials, allowing to use anodic and cathodic compartments to remove organic and/or inorganic pollutants [34-37];

(iii) the treatment of wastewater can be achieved also by microbial reverse electrodialysis (MRD), that combines in the same stack a MFC and a RED, allowing to reduce the number of membranes necessary to drive the process [16].

Among these three routes, RED seems the most promising since it requires drastically lower treatment times with respect to MFC and a less complex system with respect to MRD.

#### **3.4.1 Energy generation and abatement of Cr(VI) in RED process**

Scialdone's group studied the treatment of synthetic solutions of the toxic heavy metal hexavalent chromium in a RED system containing a DSA anode and a carbon felt cathode. Cathodic solution contained Cr(VI) with an initial concentration of 2, 25 or 50 mg/L and 0.1 or 0.5 M Na<sub>2</sub>SO<sub>4</sub> as supporting electrolyte at a pH = 2. 5 M and 0.01 M concentration of NaCl was used in the HC and LC chambers, respectively, and 10 cell pairs of membranes were assembled in the stack [35]. The main reactions in the electrode chamber are shown in Fig. 3-4.

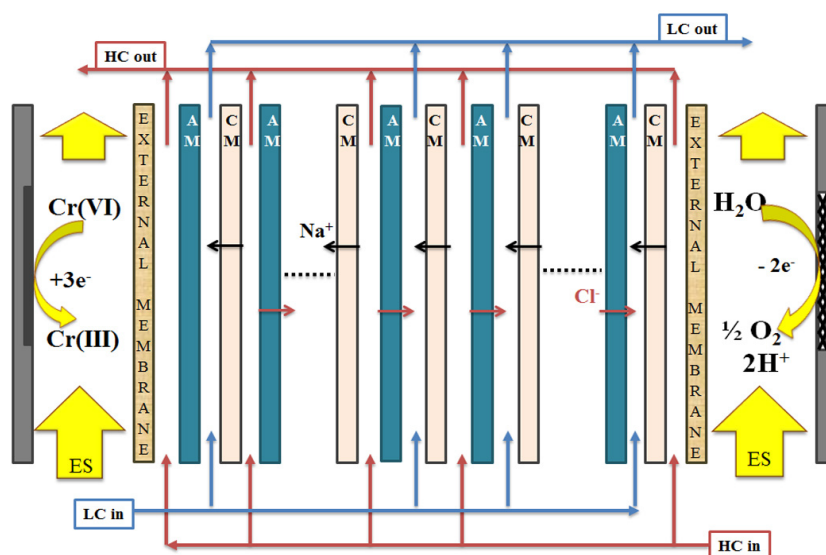


Fig. 3-4 Scheme of RED stack for the energy generation and the reduction of hexavalent chromium [35].

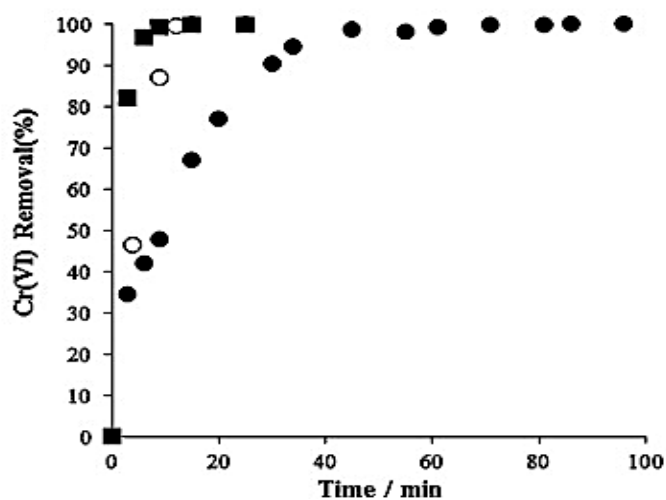


Fig. 3-5 The removal of Cr(VI) achieved in the cathodic compartment of a stack equipped with 10 (●), 40 (○) and 50 (■) cell pairs membrane fed with HC and LC solutions (5 M and 0.5 M NaCl, respectively) and with an initial concentration of 25 ppm of Cr(VI) in the cathodic compartment [35].

As shown in Fig.3-5, a high abatement of Cr(VI) was achieved by cathodic reduction at carbon electrodes with the simultaneous generation of electric current. Furthermore,

the addition of Cr(VI) to the cathodic solution gave an enhancement of the power output in the process of RED electric generation.

### 3.4.2 Energy generation and abatement of Acid Orange 7 in RED process

The utilization of a RED stack for the simultaneous generation of electric energy and the treatment of wastewaters contaminated by organic pollutants (Acid Orange 7) resistant to conventional biological processes was also evaluated [36]. The scheme of the process is shown in Fig. 3-6.

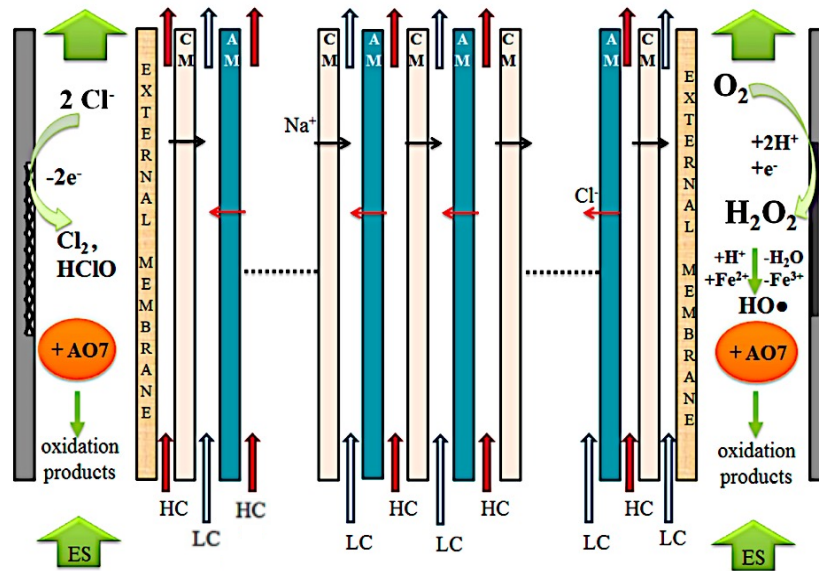


Fig. 3-6 Scheme of RED stack for the energy generation and abatement of acid orange 7 [36].

It is shown that the simultaneous generation of electric energy and the treatment of waters contaminated by Acid Orange 7 can be achieved by RED processes using salinity gradients. Both the utilization of electro-Fenton at the cathode and the oxidation by electrogenerated active chlorine at the anode were successfully used (see Table 3-2) with a good AO7 abatement.

Table 3-2 The removal of AO7 and the generation of electric energy

Entry	Concentration of NaCl in HC and LC (M)	Number of membrane pairs	Time <sup>a</sup> (h)	Abatement of color and TOC (%)	Cell potential (V)		Current density (A/m <sup>2</sup> )		Power density (W/m <sup>2</sup> )	
					Initial value	Final value	Initial value	Final value	Initial value	Final value
1 <sup>a</sup>	0.5–0.01	40	4	>99–55	0.7	0.2	20	4.3	13.5	0.9
2 <sup>a</sup>	5–0.01	40	4	100–58	1.6	1.0	30	22	48	22
3 <sup>a</sup>	5–0.01	60	2	>99–63	1.6	1.2	37.5	27	61	33
4 <sup>b</sup>	5–0.01	40	4.5	100–60 (cath.); 100–76 (anode)	1.3	1.0	36	22	45	22

Experiments performed in a stack equipped with carbon felt cathode (geometric area of 100 cm<sup>2</sup>) and Ti/Ru–Ir anode. Flow rate of electrodic solutions: 75 mL/min; flow rate of HC and LC solutions: 190 mL/min. Power density computed as the ratio between the power and the geometric area of the electrode. Two external anionic membranes from Selemion were used.

<sup>a</sup> Experiments performed with one hydraulic circuit connecting both cathodic and anodic compartments. The electrolytic solution contained AO7 (150 mg/L), NaCl or KCl (0.085 M), and 0.5 mM FeSO<sub>4</sub>·7H<sub>2</sub>O and H<sub>2</sub>SO<sub>4</sub> (pH 2).

<sup>b</sup> Two separated electrodic compartments were used. Anodic solution contained 150 mg/L of AO7, NaCl or KCl (0.085 M) and HCl (pH = 2). Cathodic solution AO7 (150 mg/L), Na<sub>2</sub>SO<sub>4</sub> (0.085 M), 0.5 mM FeSO<sub>4</sub>·7H<sub>2</sub>O and H<sub>2</sub>SO<sub>4</sub> (pH = 2).

However, the utilization of RED for the treatment of wastewater was studied up to now using as sources of salinity gradients only seawater and freshwater and brine and seawater/freshwater. However, this imposes a strong limitation to the exploitation of such method to the industrial sites that generate/treat the wastewater located in river estuaries or in salt ponds, where these salinity gradients are available. Hence, in order to extend the applicability of this appealing method, other sources of salinity gradients have to be found.

### 3.5 Reference

- [1] International energy agency, <https://www.iea.org/statistics/renewables/>.
- [2] Veerman J, Saakes M, Metz S J, et al. Reverse electrodialysis: evaluation of suitable electrode systems. *Journal of Applied Electrochemistry*, 2010, 40: 1461–1474.
- [3] Post J W, Hamelers H V M, Buisman C J N. Energy recovery from controlled mixing salt and fresh water with a reverse electrodialysis system. *Environmental Science and Technology*, 2008, 42: 5785–5790.
- [4] Ma P, Hao X, Galia A, et al. Electrochemical treatment of wastewaters with different salt content. Development of a process without energy inputs using a

- reverse electrodialysis stack and the salinity gradient of wastewaters. *Chemosphere*, 2020, 248:125994 .
- [5] Salvo J L D, Cosenza A, Tamburini A, et al. Long-run operation of a reverse electrodialysis system fed with wastewaters. *Journal of Environmental Sciences-China*, 2018, 217: 871–887 .
- [6] Cusick R D, Kim Y, Logan B E. Energy capture from thermolytic solutions in microbial reverse-electrodialysis cell. *Science*, 2012, 335: 1474–1477 .
- [7] McCutcheon J R, McGinnis R L, Elimelech M. A novel ammonia-carbon dioxide forward (direct) osmosis desalination process. *Desalination*, 2005, 174: 1–11.
- [8] Bevacqua M, Tamburini A, Papapetrou M, et al. Reverse electrodialysis with  $\text{NH}_4\text{HCO}_3$  -water systems for heat-to-power conversion. *Energy*, 2017, 137 : 1293–1307 .
- [9] Veerman J, Saakes M, Metz S J, et al. Reverse electrodialysis: Performance of a stack with 50 cells on the mixing of sea and river water. *Journal of Membrane Science*, 2009, 327 (1–2): 136–144.
- [10] Veerman J, Saakes M, Metz S J, et al. Reverse electrodialysis: A validated process model for design and optimization. *Chemical Engineering Journal*, 2011, 166 (1): 256–268.
- [11] Güler E, Nijmeijer K. Reverse electrodialysis for salinity gradient power generation: Challenges and future perspectives. *Journal of Membrane Science and Research*, 2018, 4 (3): 108–110.
- [12] Xu S, Leng Q, Wu X, et al. Experimental investigate on the joint degradation for acid Orange 7 by anode and cathode in RED reactor. *Acta Scientiae Circumstantiae*, 2019, 39: 2163–2171 .
- [13] Zhou Y, Zhao K, Hu C, et al. Electrochemical oxidation of ammonia accompanied with electricity generation based on reverse electrodialysis. *Electrochimica Acta*, 2018, 269: 128–135 .
- [14] Yen F, You S, Chang T. Performance of electrodialysis reversal and reverse osmosis for reclaiming wastewater from high-tech industrial parks in Taiwan: a pilot-scale study. *Journal of Environmental Management*, 2017, 187: 393–400 .
- [15] D’Angelo A, Tedesco M, Cipollina A, et al. Reverse electrodialysis performed at pilot plant scale: evaluation of redox processes and simultaneous generation of electric energy and treatment of wastewater. *Water Research*, 2017, 125: 123–131 .

- [16] D'Angelo A, Galia A, Scialdone O. Cathodic abatement of Cr(VI) in water by microbial reverse-electrodialysis cells. *Journal of Electroanalytical Chemistry*, 2015, 748: 40–46 .
- [17] Xu S, Xu Z, Wu X, et al. Study on the mechanism of organic wastewater oxidation degradation with reverse electrodialysis powered by concentration gradient energy of solutions. *Acta Scientiae Circumstantiae*, 2018, 38: 4642–4651 .
- [18] Higa M, Watanabe T, Yasukawa M, et al. Sustainable hydrogen production from seawater and sewage treated water using reverse electrodialysis technology. *Water Practice Technology*, 2019, 14: 645–651 .
- [19] Hatzell M C, Ivanov I, Cusick R D, et al. Comparison of hydrogen production and electrical power generation for energy capture in closed-loop ammonium bicarbonate reverse electrodialysis systems. *Physical Chemistry Chemical Physics*, 2014, 16: 1632–1638 .
- [20] Tufa R A, Rugiero E, D. Chanda , J. Hnát , W. van Baak , J. Veerman , E. Fontananova , G. Di Profio , E. Drioli , K. Bouzek , E. Curcio , Salinity gradient power-reverse electrodialysis and alkaline polymer electrolyte water electrolysis for hydrogen production, *Journal of Membrane Science*, 514 (2016) 155–164 .
- [21] Krakhella K W, Bock R, Burheim O S, et al. Heat to H<sub>2</sub>: using waste heat for hydrogen production through reverse electrodialysis. *Energies*, 2019, 12: 3428 .
- [22] Nazemi M, Zhang J , Hatzell M C. Harvesting natural salinity gradient energy for hydrogen production through reverse electrodialysis power generation. *Journal of Electrochemical Energy Conversion and Storage*, 2017, 14: 020702 .
- [23] Veerman J , Saakes M, Metz S J, et al. Reverse electrodialysis: a validated process model for design and optimization. *Chemistry and Engineering*, 2011, 166: 256–268 .
- [24] Tufa R A, Piallat T, Hnát J, et al. Salinity gradient power reverse electrodialysis: cation exchange membrane, design based on polypyrrole-chitosan composites for enhanced monovalent selectivity, *Chemistry and Engineering*, 2020, 380: 122461
- [25] Post J W, Hamelers H V M, Buisman C J N. Energy recovery from controlled mixing salt and fresh water with a reverse electrodialysis system. *Environmental Science and Technology*, 2008, 42 (15): 5785–5790.

- 
- [26] Cipollina A, Gurreri L, Ciofalo M, et al. CFD prediction of concentration polarization phenomena in spacer-filled channels for reverse electrodialysis. *Journal of Membrane Science*, 2014, 468: 133–148.
- [27] Weinstein J N, Leitz F B. Electric power from differences in salinity: the dialytic battery. *Science*, 1976, 191: 557–559.
- [28] Tedesco M, Mazzolaa P, Tamburini A, et al. Analysis and simulation of scale-up potentials in reverse electrodialysis. *Desalination and Water Treatment*, 2015, 55: 1-13.
- [29] Scialdone O, Albanese A, D'Angelo A, et al. Investigation of electrode material – Redox couple systems for reverse electrodialysis processes. Part I: Iron redox couples O. *Journal of Electroanalytical Chemistry*, 2012, 681: 66–75.
- [30] Scialdone O, Albanese A, D'Angelo A, et al. Investigation of electrode material - Redox couple systems for reverse electrodialysis processes. Part II: Experiments in a stack with 10-50 cell pairs. *Journal of Electroanalytical Chemistry*, 2013, 704: 1–9.
- [31] Huang LP, Logan R B E. Electricity generation and treatment of paper recycling wastewater using a microbial fuel cell. *Applied Microbiology Biotechnology*, 2008,80: 349.
- [32] Wang G, Huang L, Zhang Y. Cathodic reduction of hexavalent chromium [Cr(VI)] coupled with electricity generation in microbial fuel cells. *Biotechnology Letters*, 2008, 30: 1959–1966.
- [33] Riccobono G, Pastorella G, Vicari F, et al. Abatement of AO7 in a divided microbial fuel cells by sequential cathodic and anodic treatment powered by different microorganisms. *Journal of Electroanalytical Chemistry*, 2017, 799: 293–298.
- [34] Scialdone O, D'Angelo A, Pastorella G, et al. Electro chemical processes and apparatuses for the abatement of acid orange 7 in water. *Chemical Engineering Transactions*, 2014, 41: 31–36.
- [35] Scialdone O, D'Angelo A, De Lumè E, et al. Cathodic reduction of hexavalent chromium coupled with electricity generation achieved by reverse-electrodialysis processes using salinity gradients. *Electrochimica Acta*, 2014, 137: 258–265.



- [36] Scialdone O, D'Angelo A, Galia A. Energy generation and abatement of Acid Orange 7 in reverse electrodialysis cells using salinity gradients. *Journal of Electroanalytical Chemistry*, 2015, 738: 61–68.
- [37] Zhou Y, Zhao K, Hua C, et al. Electrochemical oxidation of ammonia accompanied with electricity generation based on reverse electrodialysis. *Electrochimica Acta*, 2018, 269: 128–135.



## Chapter 4. Treatment of wastewater containing phenol by different electrochemical processes with conventional reactors

### 4.1 Introduction

Phenolic compounds are important toxic pollutants in wastewater generated by pharmaceutical factories, oil refineries, coking plants and pulp and food processing industries [1-4]. In this chapter, the electrochemical treatment of wastewater containing phenol was studied. Direct anodic oxidation, oxidation by electro-generated active chlorine and electro-Fenton processes were used to treat phenol containing wastewater. The degradation effect and energy consumption of different processes were compared. The last part of the chapter was devoted to electro-Fenton process. Since this process depends on the amount of  $H_2O_2$  generated at the cathode, a specific study on the effect of operative parameters on the generation of hydrogen peroxide was carried out.

### 4.2 Experimental

#### 4.2.1 Materials and reactor

##### a) Reagents

Table 4-1. Main reagents

Reagents	Standards	Company
NaCl	Chemical	Janssen
Na <sub>2</sub> SO <sub>4</sub>	Chemical	Janssen
FeSO <sub>4</sub> ·7H <sub>2</sub> O	analytical	Fluka
C <sub>6</sub> H <sub>5</sub> OH (phenol)	analytical	Sigma Aldrich
O <sub>5</sub> STi·H <sub>2</sub> SO <sub>4</sub>	analytical	Fluka

## b) Reactor

The electrolytic reaction was carried out in a cylindrical glass cell (Fig.4-1A) in the presence of different chemical compounds (Table 4-1). The saturated calomel electrode (SCE) was used as the reference electrode. According to the selected process, different types of anodes and cathodes were used as reported in Table 4-2.

Table 4-2 Electrode materials

Name	Company
Ti/IrO <sub>2</sub> -Ta <sub>2</sub> O <sub>5</sub>	De Nora SpA
Ti/RuO <sub>2</sub> -IrO <sub>2</sub>	De Nora SpA
BDD	Condias
graphite	Carbone Lorraine
Ni	Carlo Erba
Carbon felt	Electosynthesis Co.
compressed air	Rivoira

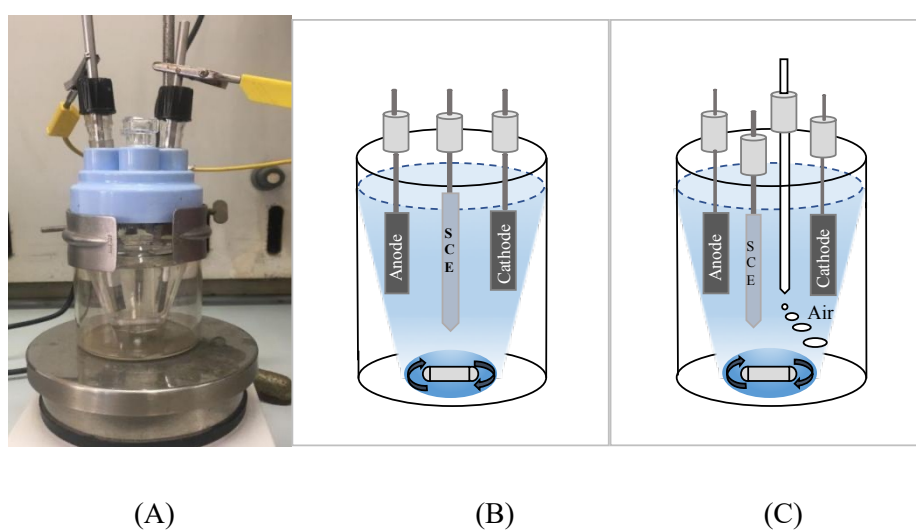


Fig. 4-1 Photo of undivided electrolysis cell adopted and simple draw of the system.

## 4.2.2 Methods

Electrolyses were performed in batch mode in a cylindrical undivided tank glass cell (Fig. 4-1) containing 50 mL of solution, under relatively vigorous stirring performed by a magnetic stirrer (the speed of most experiments was controlled at 600 rpm). The inter-electrode gap was about 2 cm. The initial phenol concentration was 100 mg L<sup>-1</sup>. The electrolyses were driven by an Amel 2053 potentiostat/galvanostat operated in galvanostatic or potentiostatic mode. According to the selected process, different types of anodes and cathodes were used. The total organic carbon (TOC) was analyzed by a TOC analyzer Shimadzu VCSN ASI TOC-5000 A. To evaluate the formic acid concentration, Agilent HP 1100 HPLC fitted out with Rezex ROA-Organic Acid H+ (8%) column at 55°C and coupled with a UV detector (420 nm) was used. The specific operative conditions are described below for the different electrochemical methods tested.

### **a) Oxidation by electro-generated active chlorine (IOAC) with DSA-Ti/RuO<sub>2</sub> anode:**

DSA-Cl<sub>2</sub> (Ti/RuO<sub>2</sub>) and DSA-O<sub>2</sub> (Ti/IrO<sub>2</sub>-Ta<sub>2</sub>O<sub>5</sub>) were used as working electrode (anode) and Ni as cathode. The area of electrode was 3 cm<sup>2</sup> and the rotating speed was 600 rpm (see Fig. 4-1B). 50 mg L<sup>-1</sup> and 100 g L<sup>-1</sup> of NaCl was used as electrolyte respectively. The reaction lasted for 6 h and the concentrations of phenol and the TOC were determined every hour.

### **b) Direct Anodic oxidation (AO) with BDD:**

BDD was used as working electrode (anode). Other conditions are the same as the process of IOAC.

### **c) Electro Fenton (EF):**

Carbon felt (4 mm thick) was used as working electrode (cathode) while DSA-O<sub>2</sub> (Ti/IrO<sub>2</sub>-Ta<sub>2</sub>O<sub>5</sub>) as anode. The geometric area of electrode participating in the reaction

was 3 cm<sup>2</sup>. Various mixing rates were used in the presence of compressed air (0.8 L min<sup>-1</sup>) as shown in Fig. 4-1C. 50 mg L<sup>-1</sup> of Na<sub>2</sub>SO<sub>4</sub> was used as electrolyte with 0.5 mM Fe<sup>2+</sup> (FeSO<sub>4</sub>·7H<sub>2</sub>O) as catalyst and sulfuric acid was used to adjust the pH value less than 3.

**d) Reduction of oxygen to H<sub>2</sub>O<sub>2</sub> at carbon felt cathode with operative parameters:**

Various mixing rates were used: 0, 300, 600 and 800 rpm. 50 mM Na<sub>2</sub>SO<sub>4</sub> was used as supporting electrolyte. Carbon felt (thickness 4 mm) was used as cathode and saturated calomel electrode (SCE) as reference electrode. A DSA-O<sub>2</sub> (Ti/IrO<sub>2</sub>Ta<sub>2</sub>O<sub>5</sub>) anode was used for most of experiments. DSA-Cl<sub>2</sub> (Ti/RuO<sub>2</sub>-De), graphite, Boron Doped Diamond (BDD) and carbon felt anodes were also tested, in order to compare the effect of the anode material on the anodic oxidation of H<sub>2</sub>O<sub>2</sub>. Various electrodes with different wet surfaces were used (1, 2, 4, 6, 8 and 10 cm<sup>2</sup>) in order to evaluate the effect of the area of both cathode and anode on the process. The “wet surface” refers to the geometric area of the electrode wet by the water solution. Electrolyses were performed at room temperature and pH of 3 by addition of sulfuric acid in order to be under operating conditions similar to that of electro-Fenton process.

### 4.2.3 Analysis

**a) Limiting current density**

$$j_{lim} = nFD_m\left(\frac{C_0}{\sigma}\right) \quad (4-1)$$

where n is the number of electrons, F the Faraday constant (96487 C mol<sup>-1</sup>), D<sub>m</sub> the diffusion coefficient of phenol in aqueous solution (9.48 × 10<sup>-10</sup> m<sup>2</sup> s<sup>-1</sup>), C<sub>0</sub> initial concentration of phenol and σ the thickness of diffusion layer.

**b) TOC abatement and current efficiency**

The TOC abatement and current efficiency are computed according to Eq. 4-2 and Eq. 4-3, respectively.

$$X_{TOC} = \frac{(\Delta TOC)_t}{TOC_0} 100 \quad (4-2)$$

$$CE = \frac{nFVTOC_0}{i_{app}At} X_{TOC} \quad (4-3)$$

where  $(\Delta TOC)_t$  is the decay of the TOC ( $\text{mol L}^{-1}$ );  $TOC_0$  initial total organic carbon ( $\text{mol L}^{-1}$ );  $i_{app}$  the applied current density ( $\text{A m}^{-2}$ );  $t$  the residence time of solution in the cell (h);  $V$  the effective volume of the solution (L);  $A$  the wet surface of the electrode ( $\text{m}^2$ ).

### c) $\text{H}_2\text{O}_2$ current efficiency

The concentration of  $\text{H}_2\text{O}_2$  was determined from the light absorption of the Ti(IV)– $\text{H}_2\text{O}_2$  coloured complex at  $\lambda=409$  nm, using  $\text{O}_5\text{STi}\cdot\text{H}_2\text{SO}_4$  from Fluka. The current efficiency  $CE$  for the generation of  $\text{H}_2\text{O}_2$  was defined as Eq. 4-4:

$$CE = nFV[\text{H}_2\text{O}_2]/(I_{app} t) \quad (4-4)$$

where  $n$  is the number of electrons,  $F$  the Faraday constant ( $96,487 \text{ C mol}^{-1}$ ),  $V$  the volume of the cell,  $[\text{H}_2\text{O}_2]$  the concentration of  $\text{H}_2\text{O}_2$ ,  $i_{app}$  (A) the applied current and  $t$  (s) the residence time of the solution in the cell.

### d) Energy consumption (EC)

The energy consumption (EC) for the abatement of TOC is defined by Eqs. 4-5a and 4-5b.

$$EC = \frac{\Delta E_{cell} I t}{(\Delta TOC)_t} \quad (4-5a)$$

$$EC = \frac{\Delta E_{cell} I t}{1000V} \quad (4-5b)$$

where  $\Delta E_{cell}$  is the average cell potential (V);  $I$  the current intensity (A);  $V$  the volume of the solution ( $\text{m}^3$ ).

The analytical equipment used in the above experiments is reported in Table 4-3.

Table 4-3. Experimental apparatus

Name	Company
TOC-L CSH/CSN analyzer	Japan Shmadzu
Cary 60 UV-Vis spectrophotometric	America Agilent
pH- meter	Italy Hanna
HPLC	America Agilent
AMEL2053 potentiostat	Italy Amel
CP225D electronic balance	Germany Sartorius
MR3000 magnetic stirrer	Germany Heidolph

## 4.3 Results and discussion

### 4.3.1 IOAC with Ti/RuO<sub>2</sub> anode

First experiments were performed in phenol (100 mg L<sup>-1</sup>) wastewater containing a quite small concentration (50 mg L<sup>-1</sup>) of NaCl. The concentration of phenol and TOC in the solution were determined after 6 h of electrolysis with an applied current intensity of 4.1, 8.2 and 16.4 mA (current density  $j$  1.36, 2.73 and 5.45 mA cm<sup>-2</sup>, respectively).

As shown in Fig. 4-2A, the degradation of phenol depends on the applied current intensity [3-5]. Just a small part of phenol was degraded with low applied current intensity due to the low charge passed and the low formation of active chlorine. The phenol concentration reduced from 100 to 88 mg L<sup>-1</sup> in 6 h with 4.1 mA, and the TOC abatement was only about 5 %. The phenol concentration decreased to 78.7 mg L<sup>-1</sup> and 56.9 mg L<sup>-1</sup> when the current intensity increased to 8.2 and 16.4 mA, respectively. Accordingly, as shown in Fig. 4-2B, the TOC abatement increased to 8% and 12% respectively.



At Ti/RuO<sub>2</sub> in the presence of chlorides the organic compounds are oxidized by both direct oxidation at the anode and by electro-generated active chlorine. The initial pH is about 5 ~ 6, and increased to about 7 at the end of the electrolysis, where ClO<sup>-</sup> plays a leading role; however, as Silva and co-workers pointed out [6], the oxygen evolution reaction leads to a slightly acidic environment on the anode surface, which increases the concentration of HClO and Cl<sub>2</sub>.

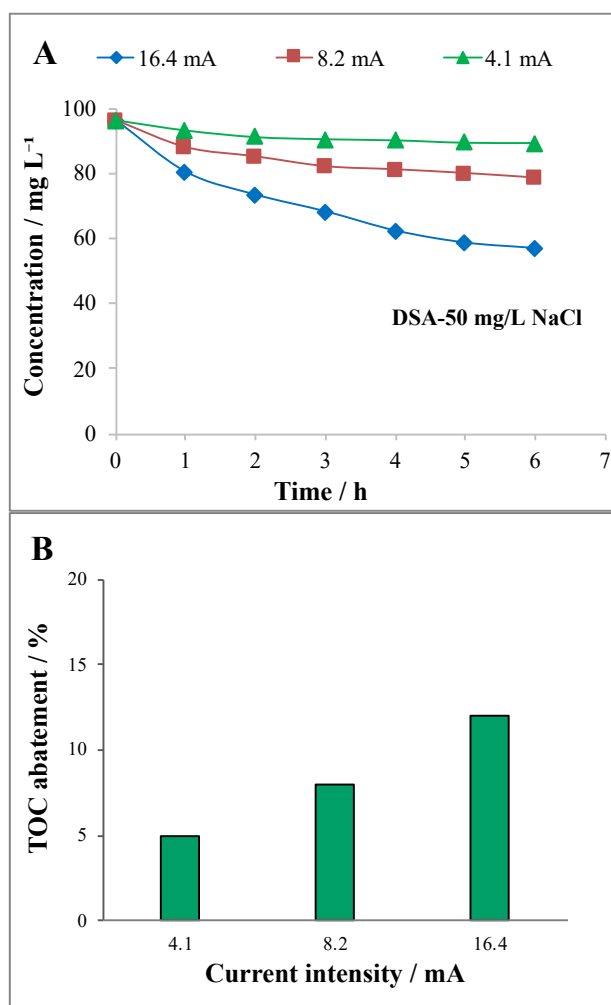


Fig. 4-2 Effect of current intensity on the concentration of phenol (A) and TOC (B), as a function of time. Operative conditions: DSA-Ti/RuO<sub>2</sub> as the anodes, Ni as the cathode, supporting electrolyte 50 mg L<sup>-1</sup> NaCl, rotational rate 600 rpm, room temperature, initial phenol concentration 100 mg L<sup>-1</sup>.

In order to evaluate the effect of NaCl concentration, a series of electrolyses was repeated in the presence of 100 g L<sup>-1</sup> NaCl electrolyte; as shown in Fig. 4-3A, the phenol

was completely removed in 2 and 4 h with 16.4 and 8.2 mA current intensity, respectively, while the concentration of phenol was 4 mg L<sup>-1</sup> after 6 h with 4.1 mA.

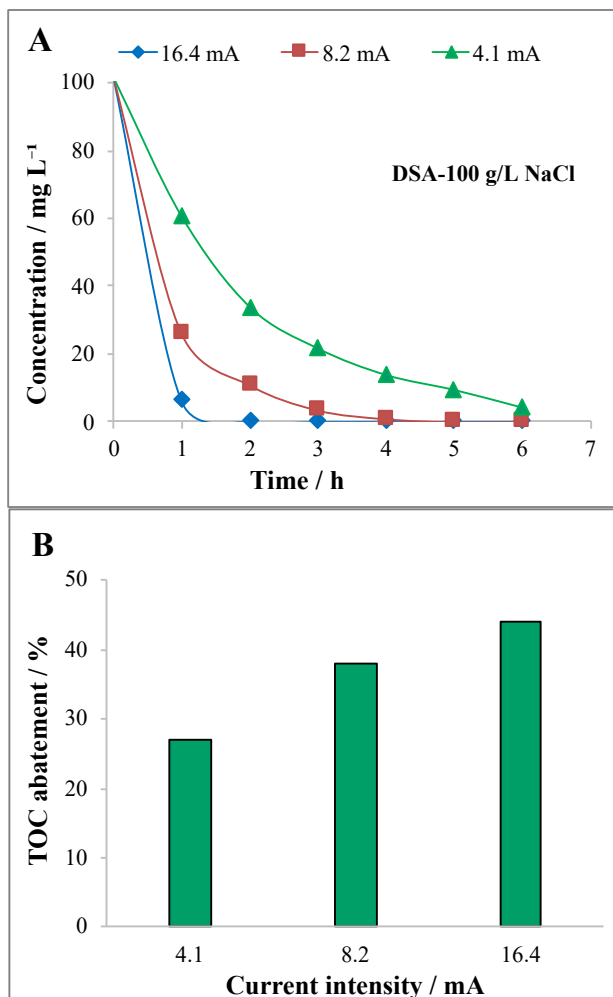


Fig. 4-3 Effect of current intensity on the concentration of phenol (A) and TOC(B), as a function of time. Operative conditions: DSA-Ti/RuO<sub>2</sub> as the anodes, Ni as the cathode, supporting electrolyte 100 g L<sup>-1</sup> NaCl, rotational rate 600 rpm, room temperature, initial phenol concentration 100 mg L<sup>-1</sup>.

As shown in Fig. 4-3B, when the current intensity increased from 4.1 mA to 8.2 and 16.4 mA, the TOC abatement increased from 27% to 38% and 44%. Overall, the mineralization (TOC abatement) of phenol is significantly affected by the higher concentration of chlorides in the wastewater (please compare Fig. 4-2B and 4-3B), due to the larger formation of active chlorine.

In order to evaluate the effect of the nature of the anode, some experiments were repeated with DSA-O<sub>2</sub> (Ti/IrO<sub>2</sub>-Ta<sub>2</sub>O<sub>5</sub>) anode. The two DSA electrodes show a little different oxygen evolution potentials and chlorine evolution potentials (Ti/RuO<sub>2</sub> 1.36±0.02 V and 1.10±0.02 V vs. SCE, respectively, while Ti/IrO<sub>2</sub>-Ta<sub>2</sub>O<sub>5</sub> 1.39±0.02 V and 1.11±0.02 V vs. SCE) respectively) [7].

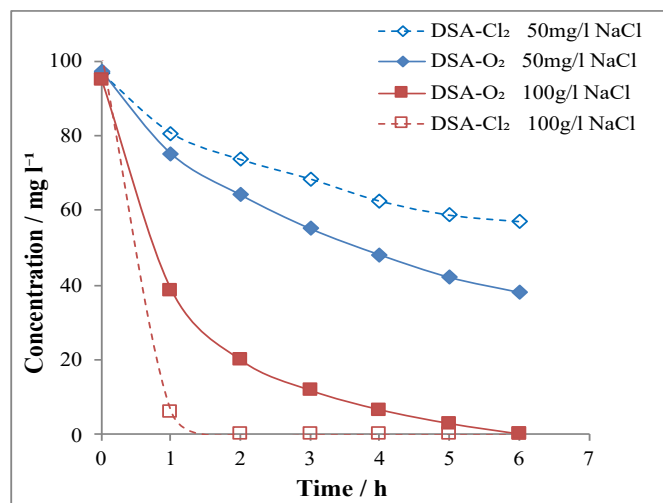


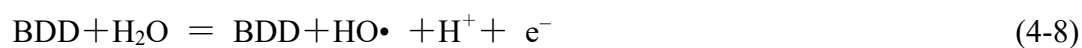
Fig. 4-4 Effect of different anodes on phenol removal from wastewater containing 50 mg L<sup>-1</sup> and 100 g L<sup>-1</sup> NaCl electrolyte. Operative conditions: DSA-Cl<sub>2</sub> (Ti/RuO<sub>2</sub>) and DSA-O<sub>2</sub> (Ti/IrO<sub>2</sub>-TaO<sub>5</sub>) as the anode, Ni as the cathode, rotational rate 600 rpm, room temperature, initial phenol concentration 100 mg L<sup>-1</sup>.

As shown in Fig. 4-4, a higher phenol abatement was obtained by Ti/IrO<sub>2</sub>-Ta<sub>2</sub>O<sub>5</sub> anode with 50 mg L<sup>-1</sup> NaCl electrolyte. The phenol concentration decreased from 100 to 38 and 56.9 mg L<sup>-1</sup> with Ti/IrO<sub>2</sub>-Ta<sub>2</sub>O<sub>5</sub> and Ti/RuO<sub>2</sub> respectively in 6 h. On the contrary, the phenol abatement was higher with Ti/RuO<sub>2</sub> than that of Ti/IrO<sub>2</sub>-Ta<sub>2</sub>O<sub>5</sub> with 100 g L<sup>-1</sup> NaCl electrolyte. The phenol was degraded completely in 2 and 6 h with Ti/RuO<sub>2</sub> and Ti/IrO<sub>2</sub>-Ta<sub>2</sub>O<sub>5</sub> respectively. The different effect of the nature of the anode at different NaCl concentrations could be due to the fact that at low NaCl concentration the prevalent oxidation mechanism is likely to be the direct anodic oxidation, while at high NaCl concentration it is the oxidation by electro-generated active chlorine whose formation is favored at Ti/RuO<sub>2</sub>.

### 4.3.2 EO with BDD anode

The tests were carried out in the phenol containing wastewater with 50 mg L<sup>-1</sup> NaCl electrolyte. The concentration of phenol and TOC were determined after 6 h with the applied current intensity of 4.1, 8.2 and 16.4 mA (current density of 1.36, 2.73 and 5.45 mA cm<sup>-2</sup> respectively). As shown in Fig. 4-5A, the concentration of phenol decreased from 100 to 2 mg L<sup>-1</sup> after 6 h. The abatement of phenol was slightly lower with 4.1 mA. At the same time, the removal rate of TOC in the solution increased with the increase of current intensity. As shown in Fig. 4-5B, the abatement of TOC was 36%, 66% and 83% when the current intensity was 4.1, 8.2 and 16.4 mA, respectively. Compared with the DSA-Ti/RuO<sub>2</sub> anode used in 4.3.1, the BDD anode was more effective in removing TOC from the wastewater, indeed, the organic pollutants in the wastewater can be almost completely converted into CO<sub>2</sub> and H<sub>2</sub>O [8-10].

It was observed that among all electrodes, the BDD anode had the highest oxygen evolution potentials and highest chlorine evolution potentials (1.98±0.02 V and 1.28±0.02 V vs. SCE, respectively) [7], which supported the idea that the BDD anode was the most efficient for pollutant degradation by direct anodic oxidation. It is supposed that the anodic degradation of organics on BDD is mainly due to the electro-generation of hydroxyl radical (Eq. 4-6). The researchers have demonstrated that HO• is loosely adsorbed on the surface of BDD anode (Eq. 2-7) and distributed in the diffusion layer (Eq. 4-8) [11,12]. The organic is degraded to CO<sub>2</sub> and H<sub>2</sub>O (Eq. 4-9 ~ 10) [13,14]. Many researchers have demonstrated that BDD anodes allow complete mineralization of several pollutants such as ammonia, cyanide, phenols, aniline, hydrocarbons, dyes, surfactants, drugs, pesticides, etc.



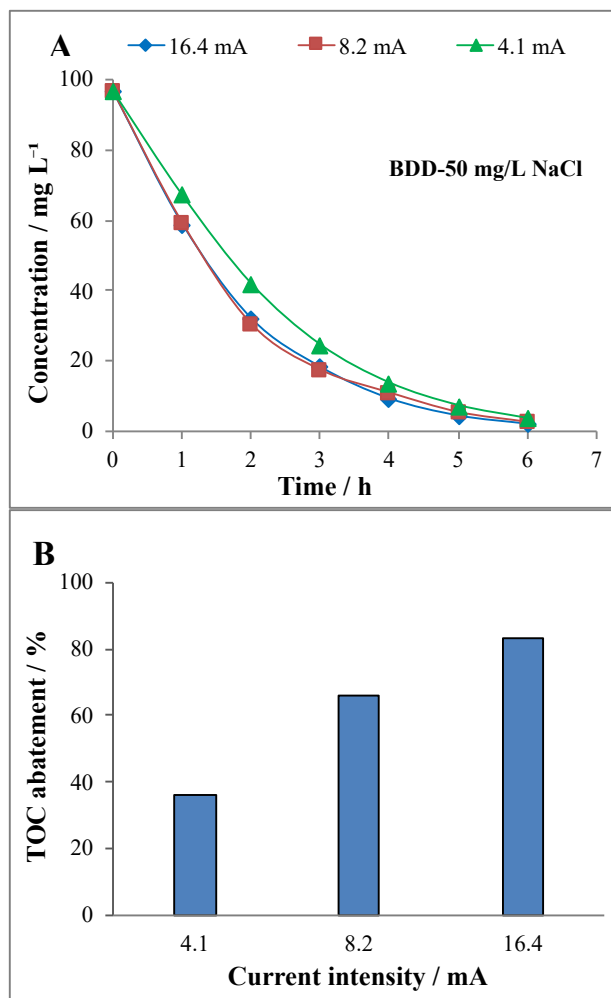
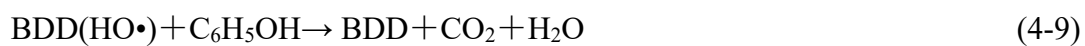


Fig. 4-5 Effect of current intensity on the concentration of phenol (A) and TOC (B) as a function of time. Operative conditions: BDD as the anode, Ni as the cathode, supporting electrolyte 50  $\text{mg L}^{-1}$  NaCl, rotational rate 600 rpm, room temperature, initial phenol concentration 100  $\text{mg L}^{-1}$ .

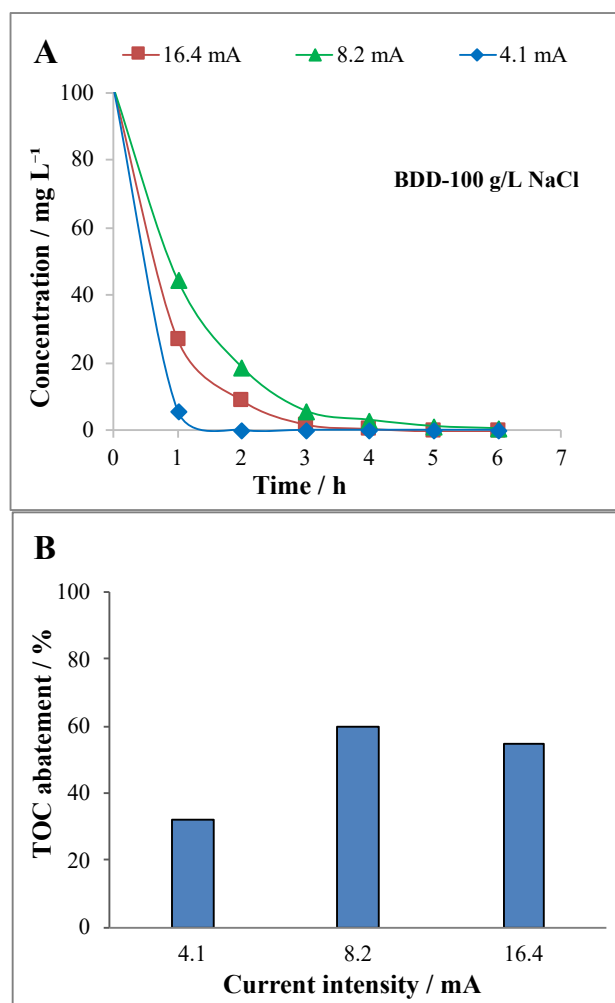


Fig. 4-6 Effect of current intensity on the concentration of phenol (A) and TOC (B) with 100 g L<sup>-1</sup> NaCl electrolyte. Operative conditions: Ti/RuO<sub>2</sub> as the anodes. Ni as the cathode, supporting electrolyte 100 g L<sup>-1</sup> NaCl, rotational rate 600 rpm, room temperature, initial phenol concentration 100 mg L<sup>-1</sup>.

As shown in Fig. 4-6A, phenol was completely removed in 2, 4 and 6 hours at 16.4, 8.2 and 4.1 mA, respectively, using 100 g L<sup>-1</sup> NaCl as electrolyte, and the removal rate was significantly higher than that achieved with 50 mg L<sup>-1</sup> NaCl, thus showing that electro-generated active chlorine can contribute to the oxidation of phenol also at BDD anodes. As shown in Fig. 2-6B, TOC abatement of 32%, 60% and 55% were obtained when the current intensity was 4.1, 8.2 and 16.4 mA, respectively. Hence, the TOC abatement with 100 g L<sup>-1</sup> NaCl was lower than that obtained at 50 mg/l NaCl, especially at high current densities. This is probably due to the fact that at high concentrations of NaCl and high current densities the indirect oxidation by electro-generated active chlorine prevails on

the direct anodic oxidation by hydroxyl radicals that at BDD anodes is more effective for mineralization purposes.

In summary, in the presence of chloride ions in the wastewater, the coexistence of active chlorine and  $\text{HO}\cdot$  produced on the anode surface must be considered in the electrochemical destruction mechanism. Especially with high current intensity, oxidation occurs mainly by indirect electrochemical oxidation by active chlorine, which makes difficult to mineralize the organic pollutants completely.

### 4.3.3 Energy efficiency analysis

- **Comparison of the electrochemical reaction rates and current efficiency**

Fig. 4-7 shows the average reaction rates at DSA ( $\text{Ti/RuO}_2$ ) and BDD anodes, respectively, with  $50 \text{ mg L}^{-1}$  and  $100 \text{ g L}^{-1}$  NaCl-containing wastewater. As shown in Fig. 4-7A, the reaction rate at BDD was significantly higher than that at DSA with  $50 \text{ mg L}^{-1}$  NaCl electrolyte. The corresponding reaction rates at BDD and DSA were 35 and  $7.6 \text{ mol/L}\cdot\text{h}$  using  $16.4 \text{ mA}$  current intensity, respectively.

As shown in Fig. 4-7B, similar reaction rates were obtained at DSA ( $\text{Ti/RuO}_2$ ) and BDD anodes when the wastewater contained  $100 \text{ g L}^{-1}$  NaCl, especially when the current intensity was  $8.2$  and  $16.4 \text{ mA}$ .

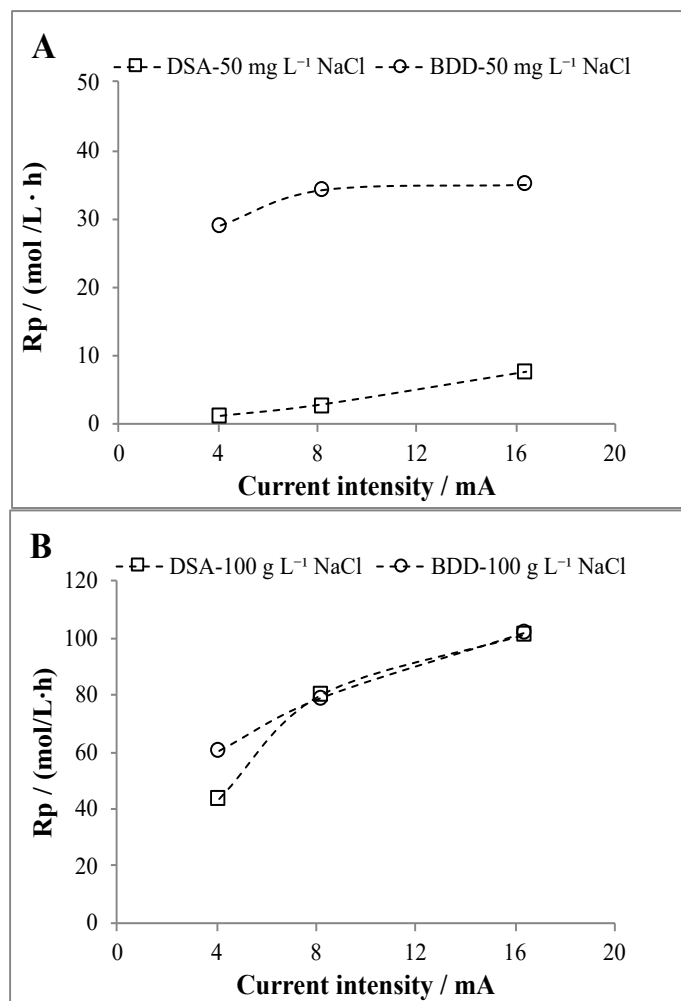


Fig. 4-7 Effect of current intensity on the reaction rate at 50 mg L<sup>-1</sup>(A) and 100 g L<sup>-1</sup>(B) electrolyte. Operative conditions: Ti/RuO<sub>2</sub> and BDD as the anodes, Ni as the cathode, rotational rate 600 rpm, room temperature, initial phenol concentration 100 mg L<sup>-1</sup>.

Fig. 4-8 shows the change of the final current efficiency with current intensity with DSA (Ti/RuO<sub>2</sub>) and BDD anode in phenol wastewater containing 50 mg L<sup>-1</sup> and 100 g L<sup>-1</sup> NaCl electrolyte, respectively. As shown in Fig. 4-8A, the current efficiency at DSA electrode was 10%, 8% and 6%, and at BDD 62%, 64% and 40%, with 4.1, 8.2 and 16.4 mA current intensity, respectively. As shown in Fig. 4-8B, the difference of current efficiency between BDD and DSA anodes were small with 100 g L<sup>-1</sup> NaCl electrolyte, especially when the current intensity was 16.4 mA, since in these conditions the role of the direct anodic oxidation by hydroxyl radicals becomes very small.



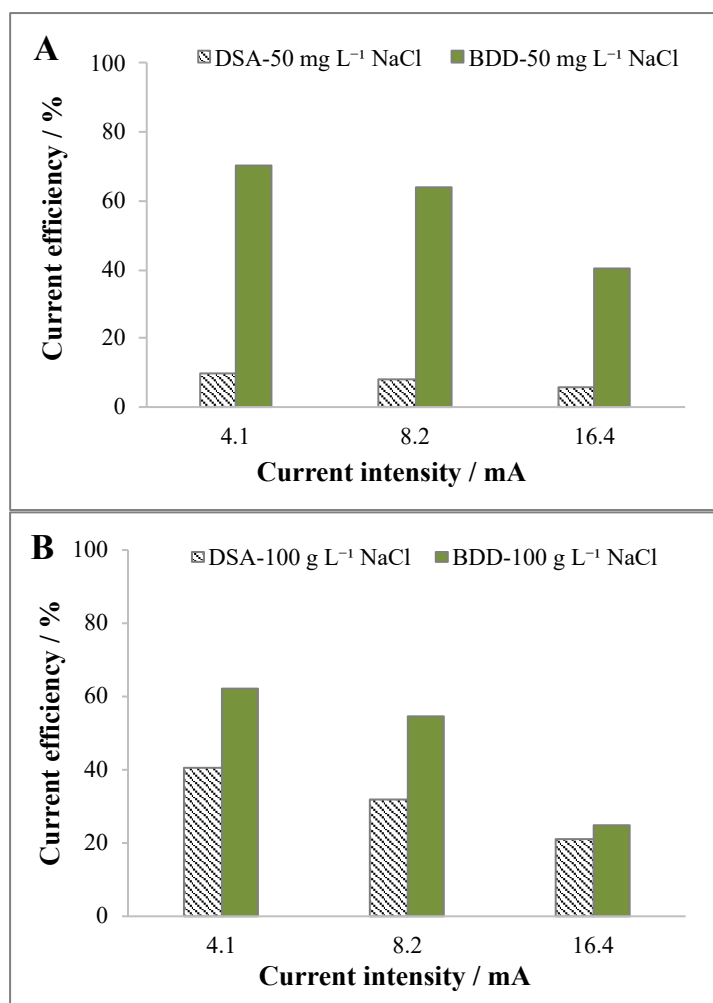
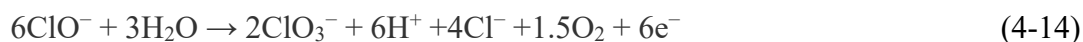


Fig. 4-8 Effect of current intensity on the current efficiency at 50 mg L<sup>-1</sup>(A) and 100 g L<sup>-1</sup> (B) electrolyte. Operative conditions: Ti/RuO<sub>2</sub> and BDD as the anodes, Ni as the cathode, rotational rate 600 rpm, room temperature, initial phenol concentration 100 mg L<sup>-1</sup>.

As shown in Fig. 4-8 in all tested conditions the current efficiency decreased with the current. For low concentrations of NaCl, this result is mainly to show a higher impact of the oxygen evolution parasitic reaction as Eq. 4-11.



For high concentrations of NaCl this should be due to various parasitic reactions including the formation of chlorate (Eq.12 ~16) [15-17].



- **Energetic and technical comparison**

In order to compare the different adopted routes, the removal of TOC, cell potential and energy consumption, were reported in Table 4-4. The average cell potential achieved with a low concentration of NaCl was very high due to the low conductivity of the solution. As a consequence, very high energy consumptions were recorded. The BDD anode gave a drastically higher removal of TOC and, consequently, a lower energy consumption with respect to DSA (Ti/RuO<sub>2</sub>) anode. When the electrolyses were repeated with a high concentration of NaCl, smaller cell potentials were obtained at both anodes, because of the high conductivity of the solution, resulting in lower energy consumptions. BDD gave slightly higher removals of the TOC. However, due to the higher cell potentials recorded, the energy consumption at BDD anode was higher than that achieved at DSA. Furthermore, BDD anodes present very large investment costs. Hence, on overall, DSA anodes seem more feasible at least at high concentrations of NaCl.

Table 4-4 Technological and economic comparison of different anode materials (BDD, Ti/RuO<sub>2</sub>) in the treatment of high and low salt (50 mg L<sup>-1</sup>, 100 g L<sup>-1</sup>NaCl) wastewater with phenol

Electrolyte	Electrode	j / mA	$\Delta E_{cell} / V$	TOC abatement/ %	EC / kW·h g TOC <sup>-1</sup>	EC / kW·h m <sup>-3</sup>
50 mg L <sup>-1</sup> NaCl		4.1	14	5	1.19	5.74
	DSA(Ti/RuO <sub>2</sub> )	8.2	27	8	2.86	22.14
		16.4	49	12	6.93	80.36
		4.1	5	36	0.06	2.05
	BDD	8.2	15.4	66	0.2	12.63
		16.4	32.7	83	0.67	57.24
100 g L <sup>-1</sup> NaCl		4.1	2.5	27	0.048	1.03
	DSA(Ti/RuO <sub>2</sub> )	8.2	2.6	38	0.064	2.13
		16.4	2.7	44	0.099	4.43
		4.1	3.3	32	0.042	1.35
	BDD	8.2	3.4	60	0.049	2.79
		16.4	3.5	55	0.111	5.74

#### 4.3.4 Electro-Fenton process

Electro-Fenton process is among the most known and popular EAOPs. It has been developed upon an extensive study over the last 25 years, with particularly remarkable contributions by Brillas and Oturan's group [18]. This process has been proposed to achieve the implementation of a new and powerful advanced oxidation method that overcomes the drawbacks of the classical Fenton process. It allows the continuous in situ electrogeneration of H<sub>2</sub>O<sub>2</sub> and/or regeneration of Fe(II) at the cathode, thus avoiding the use of high amounts of H<sub>2</sub>O<sub>2</sub> and Fe(II) salt [19,20].

The electrolyses were performed with 50 mg L<sup>-1</sup> Na<sub>2</sub>SO<sub>4</sub> as supporting electrolyte, Fe<sub>2</sub>SO<sub>4</sub>·7H<sub>2</sub>O (0.5 mM) as catalyst, DSA-O<sub>2</sub> (Ti/IrO<sub>2</sub>-Ta<sub>2</sub>O<sub>5</sub>) and carbon felt as anode and cathode respectively, a synthetic wastewater with 100 mg L<sup>-1</sup> initial phenol concentration. Sulfuric acid was used to adjust the pH to about 3.

As shown in Fig. 4-9A, the removal efficiency of phenol in the electro-Fenton process was related to the current intensity and time passed. When the current intensity increased from 4.1 to 8.2 mA, the concentration of phenol in the solution decreased from 13.11 to 0.87 mg L<sup>-1</sup> in 6 h; when the current intensity was 16.4 mA, the phenol was completely removed in 4 h. Similarly, the TOC removal was 16%, 28% and 41% with 4.1, 8.2 and 16.4 mA respectively. This is mainly due to the increased amount of charge passed and as a consequence of the amount of H<sub>2</sub>O<sub>2</sub> produced at the cathode (Eq. 1-2) resulting the increase of the amount of HO• produced (Eq. 1-3).

As shown in Fig. 4-9B, when the current intensity was 16.4 mA, the TOC abatement was 41%. As shown in Fig. 4-10, the current efficiency in the electro-Fenton reaction was rather low. The optimum current efficiency of 31% was obtained when the current intensity was 4.1 mA.

Numerous parasitic reactions take place, including: the reduction of H<sub>2</sub>O<sub>2</sub> to H<sub>2</sub>O (Eq. 4-19), the homogeneous decomposition of H<sub>2</sub>O<sub>2</sub> (Eq. 4-20) and the hydrogen evolution reaction of cathode (Eq. 4-21).



On the other hand, since experiments were carried out in a conventional undivided reactor, as shown in Eq. 4-22 and 4-23, H<sub>2</sub>O<sub>2</sub> is decomposed to peroxy radical HO<sub>2</sub>• at the anode, and then decomposed to O<sub>2</sub>.

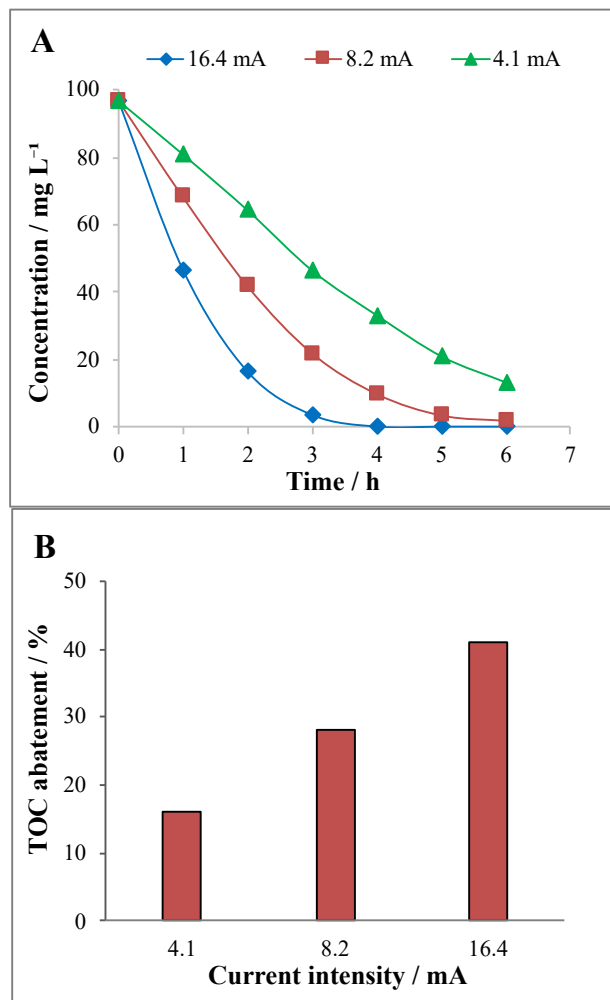


Fig. 4-9 Effect of current density on the abatement of the phenol(A) and TOC (B) achieved by EF process. Operative conditions: DSA-O<sub>2</sub> (Ti/IrO<sub>2</sub>-Ta<sub>2</sub>O<sub>5</sub>) as the anode, carbon felt as the cathode, supporting electrolyte 50 mg L<sup>-1</sup>Na<sub>2</sub>SO<sub>4</sub>, rotational rate 600 rpm, room temperature, initial phenol concentration 100 mg L<sup>-1</sup>.

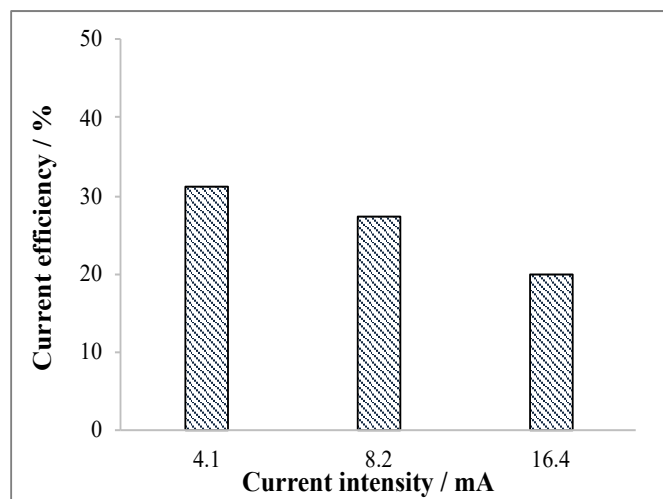


Fig. 4-10 Effect of current intensity on the current efficiency achieved by EF process. Operative conditions: DSA-O<sub>2</sub> (Ti/IrO<sub>2</sub>-Ta<sub>2</sub>O<sub>5</sub>) as the anode, carbon felt as the cathode, supporting electrolyte 50 mg L<sup>-1</sup>Na<sub>2</sub>SO<sub>4</sub>, rotational rate 600 rpm, room temperature, initial phenol concentration 100 mg L<sup>-1</sup>.

In addition, Oturan and co-workers [21] identified the main intermediates in the degradation of organic pollutants by electro-Fenton with carbon felt cathode. They found that various by-products are produced after electro-Fenton electrolysis, including malonic acid, formic acid, acetic acid and other simple substances, as well as hydroquinone, 1,2-naphthoquinone, 4-aminophenol and 4-aminobenzenesulfonic acid aromatic products.

The accumulation of H<sub>2</sub>O<sub>2</sub> in the solution is much lower than the amount of H<sub>2</sub>O<sub>2</sub> produced in the process of EF, which is the main reason for the low organic removal and current efficiency. These parasitic reactions are expected to be strengthened by the increase of current intensity, resulting in a further reduction of current efficiency. In order to increase the accumulation of H<sub>2</sub>O<sub>2</sub> in the EF process, we report in the following a systematic study on the effect on the electro-generation of hydrogen peroxide of various parameters (such as the nature and the area of the anode, the ratio between the cathode and anode surface, the current density and the mixing rate) that can affect the anodic oxidation of H<sub>2</sub>O<sub>2</sub>. A quite simple and conventional undivided cell equipped with a carbon felt cathode was used for experiments in order to focus the study on these

parameters that can be, however, of general relevance for various kinds of cells and cathodes.

#### **4.3.5 Effect of the ratio between the anode and the cathode surfaces and of other operative parameters on H<sub>2</sub>O<sub>2</sub> electro-generation**

- **Effect of the ratio between the cathode and the anode surfaces for potentiostatic electrolyses**

First experiments were performed using carbon felt as cathode with a surface of 8 cm<sup>2</sup> and a DSA anode with the same surface. A potentiostatic alimention was used. In order to select the working potential, some preliminary short electrolyses were carried out at different working potentials (-0.7, -0.9, -1.1 and -1.3 V vs. SCE). The working potential of -0.9 V vs. SCE was selected since it gave the highest final concentration of H<sub>2</sub>O<sub>2</sub>. A current intensity of about 17 mA, corresponding to a current density of about 2.2 mA cm<sup>-2</sup> was obtained.

As shown in Fig. 4-11A, the reduction of oxygen gives rise to the formation of H<sub>2</sub>O<sub>2</sub> whose concentration increased with the charge passed up to a plateau value close to 2 mM. As previously mentioned in the literature, the plateau is reached when the cathodic generation rate of hydrogen peroxide (Eq. 1-3) is equal to the rate of its decomposition by cathodic reduction reaction (Eq. 4-19) disproportionation (Eq. 4-20) and anodic oxidation (Eq.4-22~23).

Hence, the current efficiency for the hydrogen peroxide generation decreased with the time from about 24% after 1 h to about 11% after 3 h (Fig. 4-11B). In order to evaluate the effect of the ratio between the cathode and the anode surfaces, the electrolyses were repeated using a cathode with an area of 8 cm<sup>2</sup> and various anodes with an area of 8, 6, 4 and 2 cm<sup>2</sup>, corresponding to a ratio between the cathode and the anode surface  $A_{cat}/A_{an}$  of 1, 1.33, 2 and 4, respectively. The working potential was maintained to -0.9 V vs. SCE. As shown in Fig. 4-11A, the reduction of the anode surface (i.e., the increase of  $A_{cat}/A_{an}$ )

gave rise to a drastic enhancement of the hydrogen peroxide concentration. In particular, after 3 h, the concentration of  $\text{H}_2\text{O}_2$  was about 2.1, 3.5, 5 and 7.3 mM for values of  $A_{\text{cat}}/A_{\text{an}}$  of 1, 1.33, 2 and 4 (corresponding to a surface of the anode of 8, 6, 4 and 2  $\text{cm}^2$ ), respectively. In order to rationalize these results, it is important to focus on the fact that, if the cathode potential is not too high, the main cause for the hydrogen peroxide degradation is likely to be its anodic oxidation (Eq. 4-22~23). Hence, the decrease of the anode surface is expected to limit the rate of such anodic process.

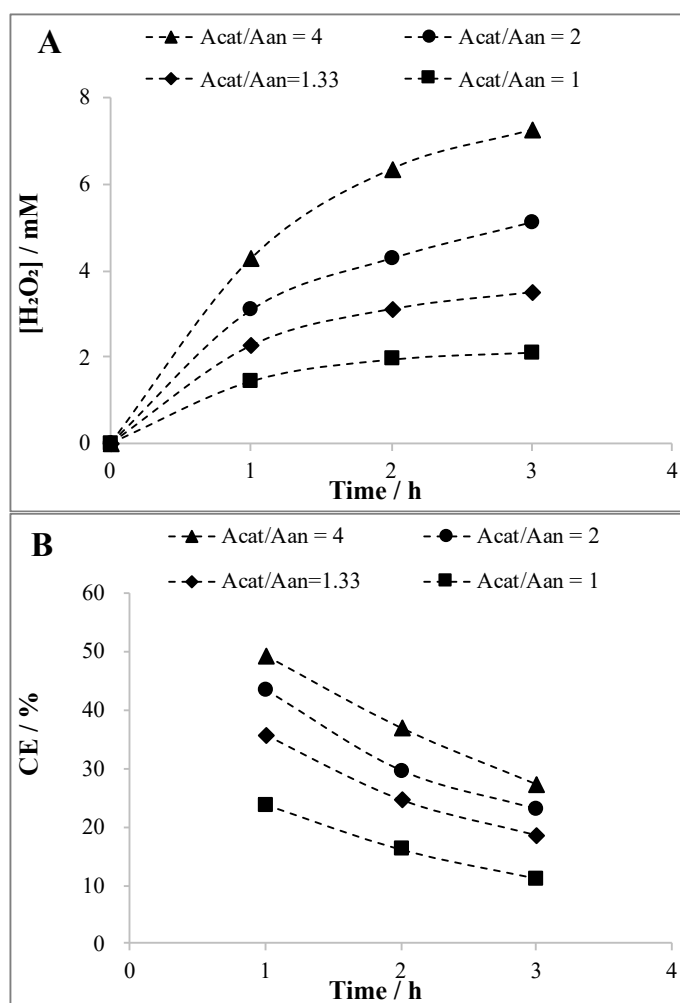


Fig. 4-11  $\text{H}_2\text{O}_2$  production (A) and current efficiency (B) as a function of electrolysis time for experiments performed at  $-0.9$  V vs. SCE with different values of the surfaces of the anode. Anode: DSA/Ti/IrO<sub>2</sub>-Ta<sub>2</sub>O<sub>5</sub> (2, 4, 6 and 8  $\text{cm}^2$ ); cathode: carbon felt (8  $\text{cm}^2$ ) for a ratio between the cathode and the anode surface  $A_{\text{cat}}/A_{\text{an}}$  of 4, 2, 1.33 and 1, respectively. Rotational rate 600 rpm, air 0.8 L min<sup>-1</sup>.



In particular, assuming, in a first approximation approach, that both the cathodic generation of  $\text{H}_2\text{O}_2$  and its anodic oxidation take place under the kinetic control of the mass transfer (of oxygen for the cathodic process and of  $\text{H}_2\text{O}_2$  for the anodic one), at steady-state conditions, the rate of the mass transfer of oxygen to the cathode surface and that of  $\text{H}_2\text{O}_2$  to the anode should assume the same values (see Eq. 4-24):

$$k_m(\text{O}_2) [\text{O}_2]_b A_{\text{cat}} = k_m(\text{H}_2\text{O}_2) [\text{H}_2\text{O}_2]_b A_{\text{an}} \quad (4-24)$$

where  $[\text{H}_2\text{O}_2]_b$  and  $[\text{O}_2]_b$  are the concentrations of  $\text{H}_2\text{O}_2$  and  $\text{O}_2$ , respectively, in the bulk of the solution,  $k_m(\text{O}_2)$  and  $k_m(\text{H}_2\text{O}_2)$  are the mass transfer coefficients for  $\text{O}_2$  and  $\text{H}_2\text{O}_2$ , respectively, and  $A_{\text{cat}}$  and  $A_{\text{an}}$  are the wet surfaces of cathode and anode, respectively. Hence, the steady-state concentration of  $\text{H}_2\text{O}_2$ , under the above-mentioned assumptions, can be computed by Eq. 4-25 [22].

$$[\text{H}_2\text{O}_2]_b = [\text{O}_2]_b (k_m(\text{O}_2)/k_m(\text{H}_2\text{O}_2)) A_{\text{cat}}/A_{\text{an}} = a A_{\text{cat}}/A_{\text{an}} \quad (4-25)$$

where  $a = [\text{O}_2]_b (k_m(\text{O}_2)/k_m(\text{H}_2\text{O}_2))$  can be simply estimated, in a first approximation approach, for the experiments performed with  $A_{\text{cat}}/A_{\text{an}} = 1$ . Indeed, in spite of the strong approximations used, the theoretical predictions based on Eq. 4-25 show a not bad agreement with experimental results (Fig. 4-12).

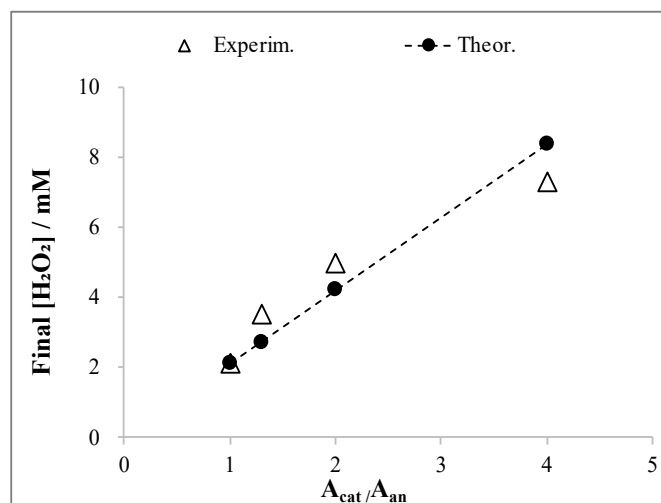


Fig. 4-12 Comparison between the final concentrations of  $\text{H}_2\text{O}_2$  and the theoretical predictions based on Eq. 28 with  $a = 2.1$  mM.

- **Effect of the  $A_{\text{cat}}/A_{\text{an}}$  ratio for galvanostatic electrolyses**

Galvanostatic alimentation is more suitable than potentiostatic one for applicative purposes, since in commercial cells reference electrodes are often avoided to reduce the costs and galvanostatic alimentation is simpler to be adopted. Hence, the effect of  $A_{\text{cat}}/A_{\text{an}}$  ratio was studied also using galvanostatic alimentation under the following conditions.

- (a) A first series of experiments was performed using a surface of the cathode of  $8 \text{ cm}^2$  and a surface of the anode of 8, 6, 4 and  $2 \text{ cm}^2$  (corresponding to a  $A_{\text{cat}}/A_{\text{an}}$  ratio of 1, 1.33, 2 and 4) with a fixed value of the current (40 mA with a current density computed with respect to the cathode of  $5 \text{ mAcm}^{-2}$ ). On overall, lower concentrations of hydrogen peroxide were obtained (Fig. 4-13A and B) with respect to the electrolyses performed under potentiostatic conditions reported in Fig. 4-11. This result is probably due to the fact that these galvanostatic electrolyses took place with a working potential of about -1.0 to -1.2 V vs. SCE (Fig. 4-13B), significantly more negative than that adopted under potentiostatic electrolyses, thus favoring the cathodic reduction of  $\text{H}_2\text{O}_2$  to water [23]. More relevant, also in this case, the reduction of the anode surface (i.e., the enhancement of the  $A_{\text{cat}}/A_{\text{an}}$  ratio) resulted in a drastic enhancement of the  $\text{H}_2\text{O}_2$  concentration. As an example, the enhancement of  $A_{\text{cat}}/A_{\text{an}}$  from 1 to 4 resulted in an increase of the stationary concentration of hydrogen peroxide from about 0.8 to 2.2 mM (Fig. 4-13B).

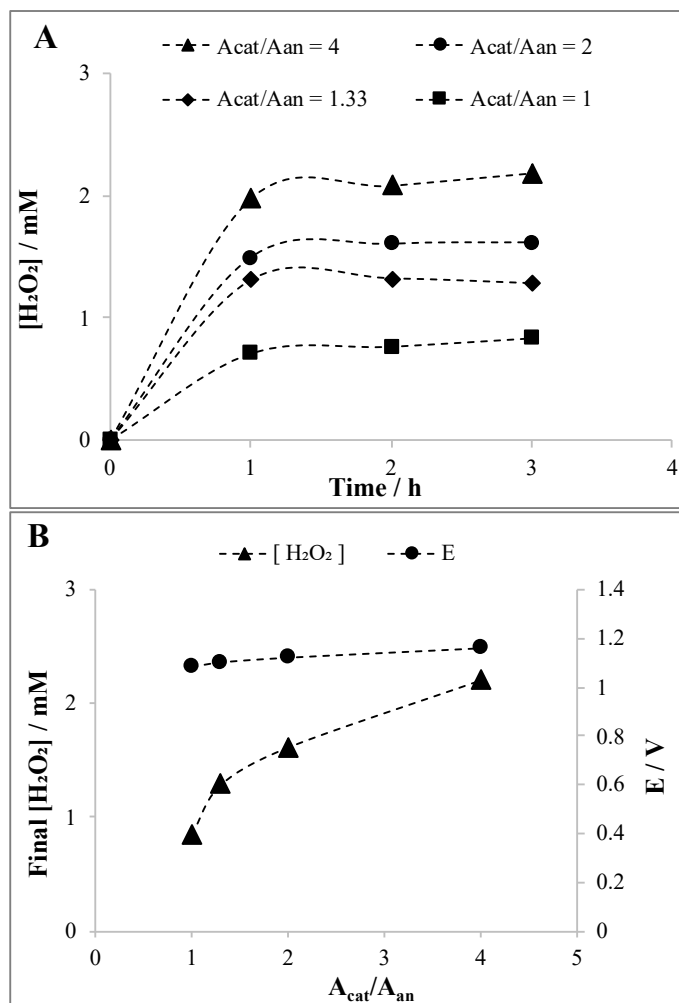


Fig. 4-13 Effect of the  $A_{cat}/A_{an}$  ratio on the  $H_2O_2$  production for amperostatic electrolyses. (A) production of  $H_2O_2$  vs. time and (B) final  $H_2O_2$  concentration and the working potential. Electrolyses performed at 40 mA with a surface of the cathode of  $8 \text{ cm}^2$  and different values of the surfaces of the anode (8, 6, 4 and  $2 \text{ cm}^2$  corresponding to  $A_{cat}/A_{an}$  of 1, 1.33, 2 and 4, respectively) using a constant value of the current density computed with respect to  $A_{cat}$  ( $j_{cat} = 5 \text{ mA cm}^{-2}$ ). DSA as anode, carbon felt as cathode, rotational rate 600 rpm, air  $0.8 \text{ L min}^{-1}$ .

(b) A second set of experiments was performed using a constant value of the anode surface  $A_{an}$  of  $2 \text{ cm}^2$  and changing the value of the cathode surface  $A_{cat}$  from 2 to  $10 \text{ cm}^2$  (in order to have  $A_{cat}/A_{an}$  from 1 to 5). The current intensity was selected in order to maintain a constant value of the current density computed with respect to  $A_{cat}$  ( $i_{cat} = 5 \text{ mA cm}^{-2}$ ). Hence, in this case, the experiments with higher values of the  $A_{cat}/A_{an}$  ratio were performed with higher current intensities, that gave rise to higher

ohmic drops and consequently to higher working potentials (Fig. 4-14). As shown in Fig. 4-14, in this case the plot  $\text{H}_2\text{O}_2$  concentration vs.  $A_{\text{cat}}/A_{\text{an}}$  gave a curve with a maximum for a value of the ratio of 2. This result is due to two opposite effects: (i) for low  $A_{\text{cat}}/A_{\text{an}}$  ratio, relatively low working potentials were recorded (Fig. 4-14) and, as above observed, the increase of  $A_{\text{cat}}/A_{\text{an}}$  ratio resulted in higher concentrations of  $\text{H}_2\text{O}_2$ ; (ii) experiments performed with higher  $A_{\text{cat}}/A_{\text{an}}$  ratio occurred with higher working potential that favour the hydrogen peroxide reduction to water (Eq. 4-19). In particular, for  $A_{\text{cat}}/A_{\text{an}}=2$  (i.e.,  $A_{\text{cat}}=4$  and  $A_{\text{an}}=2$   $\text{cm}^2$ ), the final hydrogen peroxide was about 3.8 mM and occurred with a current intensity of 10 mA, a cell potential of about 2.5 V and a working potential close to -0.9 V vs. SCE. On the other hand, for  $A_{\text{cat}}/A_{\text{an}}=5$  (i.e.,  $A_{\text{cat}}=10$  and  $A_{\text{an}}=2$   $\text{cm}^2$ ), the current intensity was 50 mA, the cell and the working potential about -3.2 and -1.2 V, respectively, and the final hydrogen peroxide concentration was about 1.4 mM. Furthermore, since the current density was fixed for the cathode, the increase of  $A_{\text{cat}}/A_{\text{an}}$  ratio was achieved imposing higher current densities for the anode, thus favoring the anodic oxidation of hydrogen peroxide.

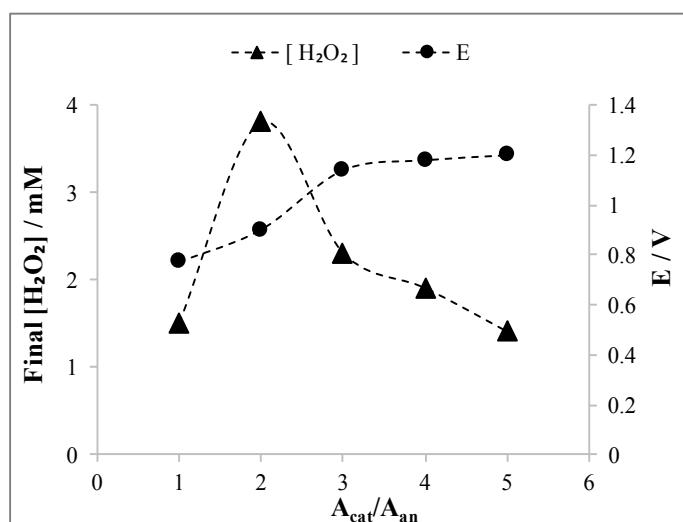


Fig. 4-14 The final  $\text{H}_2\text{O}_2$  concentration and the working potential for electrolyses performed with a surface of the anode of 2  $\text{cm}^2$  and different values of the surfaces of the cathode (2, 4, 6, 8 and 10  $\text{cm}^2$  corresponding to  $A_{\text{cat}}/A_{\text{an}}$  of 1, 2, 3, 4 and 5 respectively) using a constant value of the current density computed with respect to  $A_{\text{cat}}$  ( $j_{\text{cat}} = 5$   $\text{mA cm}^{-2}$ ). DSA as anode, carbon felt as cathode, rotational rate 600 rpm, air 0.8  $\text{L min}^{-1}$ .

- **Effect of the current density**

In order to evaluate the effect of the current density  $i$  on the process, a set of electrolyses was carried out with an area of the cathode and of the anode of 4 and 2 cm<sup>2</sup>, respectively, for a  $A_{\text{cat}}/A_{\text{an}}$  ratio of 2, at the following current densities: 1.25, 3, 5, 5.75, 8.75, 10.5, 13.75 mAcm<sup>-2</sup> (in the range of current intensity 5-55 mA). As shown in Fig. 4-15A, the curve final concentration of hydrogen peroxide vs. current density presents a maximum for 5.75 mA cm<sup>-2</sup>, which corresponds to a concentration of H<sub>2</sub>O<sub>2</sub> of about 4.2 mM and to a working potential of about -0.9 V. Indeed, for the lowest values of current density (i.e., for less negative values of the working potential), the cathodic reduction of oxygen occurs under the kinetic control of the charge transfer or under a mixed kinetic regime, and the enhancement of  $i$  results in an increase of the hydrogen peroxide formation, because of the higher amount of charge passed. Otherwise, for high values of the current density (and of the working potential), from one hand, the cathodic reduction of oxygen to hydrogen peroxide does not benefit of the larger amount of charge passed since it is kinetically limited by the mass transfer of oxygen to the cathode surface, and from the other hand the higher potential favours the reduction of H<sub>2</sub>O<sub>2</sub> to water. Hence, under these conditions the increase of  $i$  results in lower stationary concentrations of hydrogen peroxide.

Fig. 4-15B reports the effect of current density on both the CE achieved after 3 h and the CE achieved when a stationary (almost constant) concentration of H<sub>2</sub>O<sub>2</sub> is obtained (named "CE stationary"). A quite small decrease of stationary CE was achieved when the current density was increased up to 5.75 mAcm<sup>-2</sup> (the value of  $i$  which corresponds to the maximum value of the H<sub>2</sub>O<sub>2</sub> concentration in Fig. 4-15A). However, when the current density was further increased, a dramatic decrease of the CE is achieved, according to the hypothesis that at high currents (and potentials) the cathodic production of hydrogen peroxide is limited by the mass transfer of oxygen to the cathode and that the following cathodic reduction of H<sub>2</sub>O<sub>2</sub> to water is favoured.

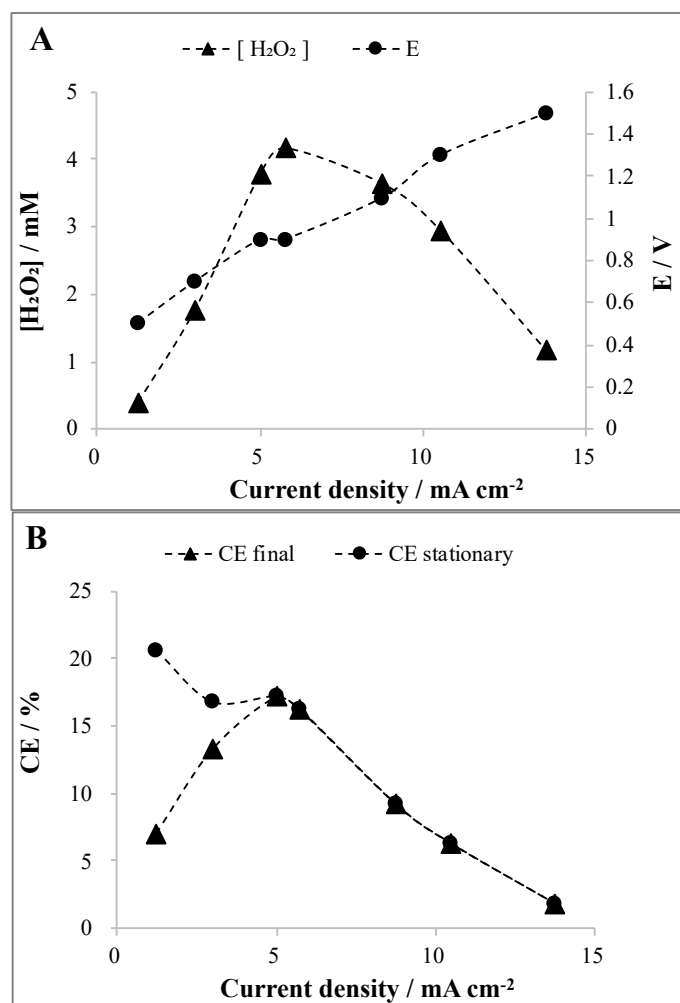


Fig. 4-15 Effect of the current density on the H<sub>2</sub>O<sub>2</sub> production. (A) reports the production of H<sub>2</sub>O<sub>2</sub> after 3 h and the working potential vs. SCE while (B) reported the CE after 3 h and the CE computed when an almost constant concentration of H<sub>2</sub>O<sub>2</sub> is reached (CE stationary). Surface of the cathode and anode 4 and 2 cm<sup>2</sup>, respectively. DSA as anode, carbon felt as cathode, rotational rate, 600 rpm, air 0.8 L min<sup>-1</sup>.

- **Effect of the mixing rate**

As previously discussed, the performances of the process are likely to be affected by the mass transfer of oxygen to the cathode surface and of hydrogen peroxide to the anode. Hence, the process is likely to be affected by the mixing. In order to evaluate the effect of the mixing rate on the process, two series of experiments were carried out with a current

density of  $5 \text{ mAcm}^{-2}$  computed with respect the surface of the cathode, various mixing rates in the range 0-800 rpm, a surface of the anode of  $2 \text{ cm}^2$  and a surface of the cathode of 4 ( $A_{\text{cat}}/A_{\text{an}}=2$ ) or 2 ( $A_{\text{cat}}/A_{\text{an}}=1$ )  $\text{cm}^2$ . As shown in Fig. 4-16, for both the two series of experiments, the higher is the mixing rate the higher is the stationary concentration of  $\text{H}_2\text{O}_2$ . As an example, for the experiments performed with  $A_{\text{cat}}/A_{\text{an}}=2$ , in the absence of mixing the stationary concentration of hydrogen peroxide was slightly lower than 0.6 mM (Fig. 4-16A) and the process occurred with a working potential close to -1.3 V vs. SCE. In the presence of a quite low stirring rate (300 rpm), the stationary concentration of  $\text{H}_2\text{O}_2$  increased up to 1.2 mM (Fig. 4-16A) and the working potential decreased to 1.16 V. A

A further enhancement of the mixing rate to 800 rpm gave rise to a strong increase of the stationary concentration of  $\text{H}_2\text{O}_2$  up to 4.2 mM (Fig. 4-16A) and to a decrease of the working potential to 0.86 V. In order to rationalize the positive effect of mixing rate on the production of  $\text{H}_2\text{O}_2$ , two main factors have to be considered:

- (a) the enhancement of the mass transfer rate of  $\text{H}_2\text{O}_2$  to the anode which favours the anodic oxidation to oxygen (Eq. 4-22~23);
- (b) the enhancement of the mass transfer rate of oxygen to the cathode, which favours the oxygen conversion to the cathode (Eq.4-19). Of course, the enhancement of the mass transfer increases the surface concentration of oxygen, thus giving rise to more positive cathode potentials, which allows to minimize the following cathode reduction of  $\text{H}_2\text{O}_2$  to water (Eq. 4-19).

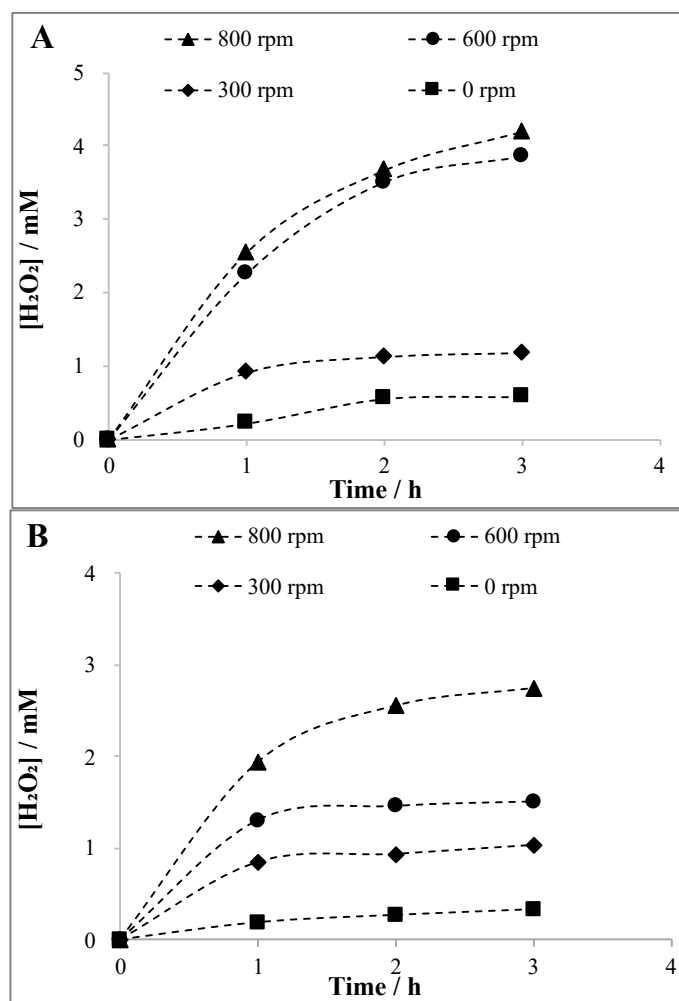


Fig. 4-16 Effect of the mixing rate on the  $H_2O_2$  production vs. time for experiments performed with an area of the cathode of 4 (A) and 2 cm<sup>2</sup> (B) and an area of the anode of 2 cm<sup>2</sup>. Current density: 5 mA cm<sup>-2</sup> computed with respect the surface of the cathode. DSA as anode, carbon felt as cathode, air 0.8 L min<sup>-1</sup>.

On overall, the experimental results show that the enhancement of the cathodic production of  $H_2O_2$  prevails with respect to the higher consumption of hydrogen peroxide at the anode. As shown in Fig. 4-16B, the increase of the mixing rates caused higher production of hydrogen peroxide also using  $A_{cat}/A_{an} = 1$ . However, these experiments gave significantly lower concentrations of  $H_2O_2$  with respect to that achieved in the series of electrolyses performed with  $A_{cat}/A_{an} = 2$ .



- **Effect of the nature of the anode**

In order to evaluate the effect of the nature of the anode on the process, a series of electrolyses was performed with the following electrodes: Ti/IrO<sub>2</sub>-Ta<sub>2</sub>O<sub>5</sub> (DSA®-O<sub>2</sub>), a Ru based anode (DSA®-Cl<sub>2</sub>), compact graphite, boron doped diamond (BDD) and carbon felt. As shown in Fig. 4-17A, the nature of the anode had a dramatic effect on the production of H<sub>2</sub>O<sub>2</sub>. The highest concentration of hydrogen peroxide was achieved with DSA-O<sub>2</sub>, which favours kinetically the water oxidation to oxygen with respect to other electrodes, thus limiting the anodic oxidation of H<sub>2</sub>O<sub>2</sub>. The utilization of DSA-Cl<sub>2</sub>, compact graphite and BDD gave rise to lower concentrations of H<sub>2</sub>O<sub>2</sub>, since oxygen evolution is less favoured with respect to DSA-O<sub>2</sub>. Very low concentrations of hydrogen peroxide were obtained using carbon felt, because of the very large effective surface of this electrode that favours the anodic oxidation of hydrogen peroxide.

Indeed, in spite of the fact that all the anodes present the same geometric surface, carbon felt has a higher value of effective area due to its three-dimensional structure. Fig. 4-17B reports the effect of the anode on the current efficiency. At carbon felt, after 3 h the CE was about 1.4%, while at DSA-O<sub>2</sub>, it was close to 17%. These results seem particularly important for the selection of the anodes in electro-Fenton processes that are in most of cases operated in undivided cells in order to avoid the cost of the membrane and to reduce the cell potentials. In particular, according to data reported in Fig. 4-17, Ti/IrO<sub>2</sub>-Ta<sub>2</sub>O<sub>5</sub> (DSA-O<sub>2</sub>) should be selected as anode for electro-Fenton process if the anodic process has to be only the oxygen evolution. It is worth to mention that BDD anode leads to lower concentration of hydrogen peroxide. However, it can be selected as anode for EF, according to the literature, if the anode has to contribute to the degradation of organics by direct electrochemical oxidation.

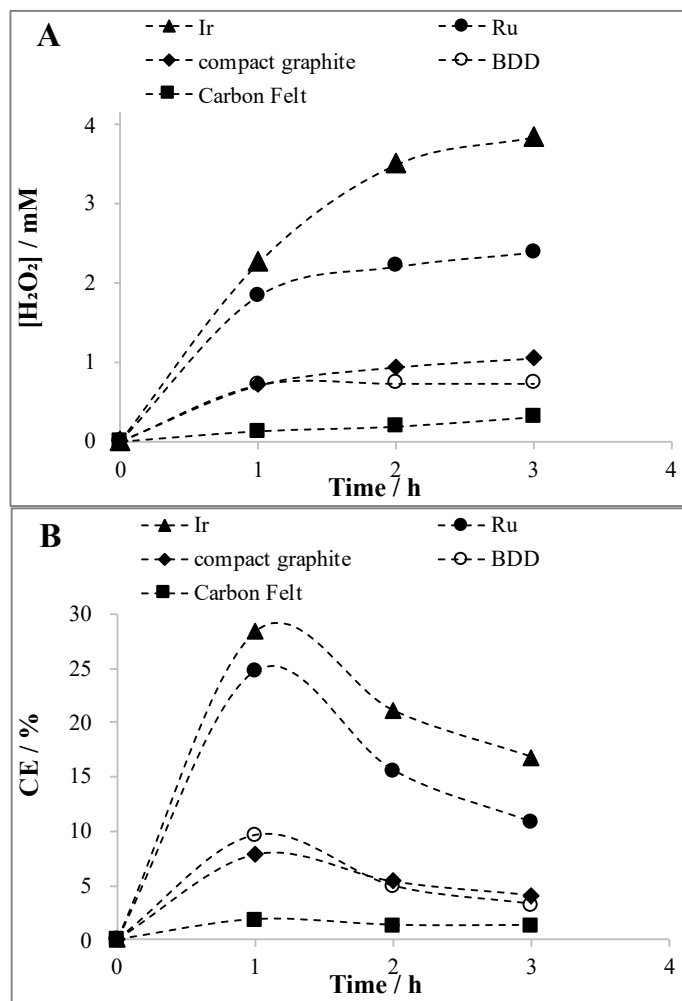


Fig. 4-17 Effect of the nature of the anode on the H<sub>2</sub>O<sub>2</sub> production (A) and CE (B) vs. time for experiments performed with an area of the cathode of 4 cm<sup>2</sup> and an area of the anode of 2 cm<sup>2</sup>. Current density: 5 mA cm<sup>-2</sup> computed with respect the surface of the cathode. Carbon felt as cathode, rotational rate 600 rpm, air 0.8 L min<sup>-1</sup>.

#### 4.4 Summary

In this chapter, DSA (Ti/RuO<sub>2</sub>) anode, BDD anode and carbon felt cathode were used to treat phenol wastewater containing high and low salt (NaCl) electrolytes by direct electrochemical oxidation, indirect electrochemical oxidation with active chlorine and electro Fenton process.

- 1) When the concentration of NaCl in the wastewater is low ( $50 \text{ mgL}^{-1}$ ), the electrochemical oxidation caused by  $\text{HO}\cdot$  plays a dominant role in the degradation process of phenol. The BDD anode has a strong ability to produce  $\text{HO}\cdot$  weakly adsorbed on the anode surface, which can completely degrade the phenol to carbon dioxide and water. However, the cell potential in the electrochemical reaction process is high due to the very low conductivity of wastewater, which leads to high energy consumption. When the current intensity was  $16.4 \text{ mA}$ , the corresponding TOC abatement reached to 83%, but the energy consumption was as high as  $57 \text{ kW}\cdot\text{h m}^{-3}$ . For the same current intensity, the TOC abatement by DSA anode was just 12%.
- 2) When the concentration of NaCl in wastewater is high ( $100 \text{ gL}^{-1}$ ), the indirect electrochemical oxidation of active chlorine plays a major role in the degradation process of phenol, and it is gradually strengthened with the increase of current intensity. The use of DSA anode is conducive to the chlorine evolution reaction, and then promotes the degradation of phenol in wastewater. However, the organic pollutants can't be removed completely, and refractory intermediate products are produced. Under the limit current intensity of  $16.4 \text{ mA}$ , the TOC abatement was 44%, and the corresponding current efficiency was 21%. Although the removal rate of TOC and current efficiency were similar to those of DSA anode, BDD seems less suitable than DSA one for electrochemical treatment of wastewater containing high concentration of NaCl electrolytes due to its higher price.
- 3) When the electro-Fenton method was used to treat the phenol wastewater, the TOC abatement was limited by the limited accumulation of  $\text{H}_2\text{O}_2$  in the solution. When the current intensity was  $16.4 \text{ mA}$ , the TOC abatement was 41%. There is a strong relationship between the accumulation of  $\text{H}_2\text{O}_2$  in solution and its decomposition at anode: increasing the ratio of cathode to anode surface area can increase the amount of  $\text{H}_2\text{O}_2$  produced by cathode and reduce the decomposition reaction of anode; an optimal value of the current density (and of the working potential) has to be selected to maximize the generation of hydrogen peroxide; in order to enhance the generation of  $\text{H}_2\text{O}_2$ , it is necessary also to increase the mixing rate. With  $\text{Ti/IrO}_2\text{-Ta}_2\text{O}_5$  anode, a stable  $\text{H}_2\text{O}_2$  concentration of up to  $7.3 \text{ mM}$  was obtained at a working potential of  $-0.9 \text{ V vs. SCE}$  and a rotating speed of  $600 \text{ rpm}$  at a ratio of anode to cathode surface  $1 (2 \text{ cm}^2): 4 (8 \text{ cm}^2)$ .

#### 4.5 Reference

- [1] Zhu X, Ni J, Li H, et al. Effects of ultrasound on electrochemical oxidation mechanisms of p-substituted phenols at BDD and PbO<sub>2</sub> anodes. *Electrochimica Acta*, 2010, 55 (20): 5569–5575.
- [2] Massa A, Hernández S, Ansaloni S, et al. Enhanced electrochemical oxidation of phenol over manganese oxides under mild wet air oxidation conditions. *Electrochimica Acta*, 2018, 273: 53–62.
- [3] Santos M J R, Medeiros M C, Oliveira T M B F, et al. Mazzetto S.E. Martínez-Huitle C.A. Castro S.S.L. . Electrooxidation of cardanol on mixed metal oxide (RuO<sub>2</sub>-TiO<sub>2</sub> and IrO<sub>2</sub>-RuO<sub>2</sub>-TiO<sub>2</sub>) coated titanium anodes: insights into recalcitrant phenolic compounds. *Electrochimica Acta*, 2016, 212: 95–101.
- [4] De Coster J, Appels L, Dewil R. Parameter evaluation of the anodic oxidation of phenol in wastewater using a Ti/RuO<sub>2</sub>-IrO<sub>2</sub> anode. *Desalination and Water Treatment*, 2017, 82: 322–331.
- [5] Polcaro A M, Vacca A, Palmas S, et al. Electrochemical treatment of wastewater containing phenolic compounds : oxidation at boron-doped diamond electrodes. *Journal of Applied Electrochemistry*, 2003, 33: 885–892.
- [6] Da Silva A J C, dos Santos E V, de Oliveira Morais C C, et al. Electrochemical treatment of fresh, brine and saline produced water generated by petrochemical industry using Ti/IrO<sub>2</sub>-Ta<sub>2</sub>O<sub>5</sub> and BDD in flow reactor. *Chemical Engineering Journal*, 2013, 233: 47–55.
- [7] Zhou M, Liu L, Jiao Y, et al. Treatment of high-salinity reverse osmosis concentrate by electrochemical oxidation on BDD and DSA electrodes. *Desalination*, 2011, 277 (1–3): 201–206.
- [8] Panizza M, Cerisola G. Electrocatalytic materials for the electrochemical oxidation of synthetic dyes. *Applied Catalysis B: Environmental*, 2007, 75: 95–101.
- [9] Maria A, Solano S, Costa C K, et al. Applied Catalysis B: Environmental Decontamination of real textile industrial effluent by strong oxidant species electrogenerated on diamond electrode: Viability and disadvantages of this electrochemical technology. *Applied Catalysis B, Environmental*, 2013, 130–131: 112–120.

- [10] Hammami S, Bellakhal N, Oturan N, et al. Chemosphere Degradation of Acid Orange 7 by electrochemically generated OH radicals in acidic aqueous medium using a boron-doped diamond or platinum anode: A mechanistic study. *Chemosphere*, 2008, 73: 678–684.
- [11] Enache T A, Chiorcea-Paquim A M, Fatibello-Filho O, et al. Hydroxyl radicals electrochemically generated in situ on a boron-doped diamond electrode. *Electrochemistry Communications*, 2009, 11 (7): 1342–1345.
- [12] Bejan D, Guinea E, Bunce N J. On the nature of the hydroxyl radicals produced at boron-doped diamond and Ebonex®anodes. *Electrochimica Acta*, 2012, 69: 275–281.
- [13] Zhang C, Xian J, Liu M, et al. Formation of brominated oligomers during phenol degradation on boron-doped diamond electrode. *Journal of Hazardous Materials*, 2018, 344: 123–135.
- [14] Jarrah N, Mu’azu N D. Simultaneous electro-oxidation of phenol, CN<sup>-</sup>, S<sup>2-</sup> and NH<sub>4</sub><sup>+</sup> in synthetic wastewater using boron doped diamond anode. *Journal of Environmental Chemical Engineering*, 2016, 4 (3): 2656–2664.
- [15] Szpyrkowicz L, Zilio-Grandi F, Naumczyk J . Application of electrochemical processes for tannery wastewater treatment. *Toxicological & Environmental Chemistry*, 1994, 44 (3–4): 189–202.
- [16] Lister M W. Decomposition of sodium hypochlorite: the uncatalyzed reaction. *Canadian Journal of Chemistry*, 1956, 34 (4): 465–478.
- [17] Neodo S, Rosestolato D, Ferro S, et al. On the electrolysis of dilute chloride solutions: Influence of the electrode material on faradaic efficiency for active chlorine, chlorate and perchlorate. *Electrochimica Acta*, 2012, 80: 282–291.
- [18] E. Brillas, I. Sirés, M.A. Oturan. Electro-Fenton process and related electrochemical technologies based on Fenton’s reaction chemistry. *Chem. Rev.*, 2009,109: 6570–6631.
- [19] Ren G, Zhou M, Liu M, et al. A novel vertical-flow electro-Fenton reactor for organic wastewater treatment. *Chemical Engineering Journal*, 2016, 298: 55–67.
- [20] Djafarzadeh N. Mineralization of an Azo Dye Reactive Red 195 by Advanced Electrochemical Electro-Fenton Process. *International Journal of Chemical Engineering and Applications*, 2015, 7 (4): 217–220.

- [21] Özcan A, Oturan M A, Oturan N, et al. Removal of Acid Orange 7 from water by electrochemically generated Fenton's reagent. *Journal of Hazardous Materials*, 2009, 163 (2–3): 1213–1220.
- [22] Scialdone O, Galia A, Gattuso C, et al. Effect of air pressure on the electro-generation of H<sub>2</sub>O<sub>2</sub> and the abatement of organic pollutants in water by electro-Fenton process. *Electrochimica Acta*, 2015, 182: 775–780.
- [23] Qiang Z, Chang J, Huang C. Electrochemical generation of hydrogen peroxide from dissolved oxygen in acidic solutions. *Water Research*, 2002, 36: 85–94.

---

## **Chapter 5. Electrochemical treatment of low conductivity real wastewater with microfluidic reactors**

### **5.1 Introduction**

The effectiveness of the electrochemical treatment of wastewater contaminated by organics depends on many factors including the electrode material. Several anodic materials have been tested, but most of them presented important drawbacks such as loss of activity (graphite), release of toxic ions ( $\text{PbO}_2$ ), low service life ( $\text{SnO}_2$ ), not complete oxidation ( $\text{IrO}_2$ ) [1]. On the contrary, synthetic boron diamond (BDD), with its high anodic stability and wide potential window, is considered to be an effective material for the direct combustion of organics in wastewater.

In the last years, it has been shown that synthetic wastewater with low conductivity can be effectively treated using filter-press flow cell with a very small inter-electrode distance (“micro cell”). Furthermore, such cells improve the removal of organic pollutants performed by both direct anodic oxidation, cathodic reduction, electro-Fenton and coupled processes. In addition, in micro-cells it is possible to achieve high conversions of the pollutants for single passage, thus allowing to operate in a continuous mode. This opened to the possibility to use a multistage system involving cells operating in series with different operating conditions/electrodes, thus allowing to maximize the current efficiency and to minimize the treatment time [2-4]. However, the utilization of micro cells for the treatment of real wastewater was not investigated up to now. Hence, in this work, the problem of wastewater with low conductivity will be investigated in detail, using a real wastewater containing organics and characterized by quite low conductivity, coming from the separation of oil and water phases performed from one company devoted to the treatment of wastewater located in the south of Sicily. Two different cells were used: a conventional undivided batch cell (“conventional cell”), often used in the labs, operated both in the absence and in the presence of a supporting electrolyte, and a micro

cell, with the main aim to evaluate if real wastewater with low conductivity can be properly treated by electro- chemical oxidation at BDD anode and to select the more promising cell and route.

## 5.2 Experimental

### 5.2.1 Experimental materials and reactor

#### a) The real wastewater

A real wastewater (initial TOC of 210 mg L<sup>-1</sup>) coming from the separation of oil and water phases performed from one company devoted to the treatment of wastewater located in the south of Sicily, with low conductivity (1.4 mS cm<sup>-1</sup>) and pH 6.2 was used. Na<sub>2</sub>SO<sub>4</sub> (0.03, 0.05, 0.1 and 0.2 M) were used as supporting electrolyte for selected experiments. The wastewater conditions are shown in Table 5-1.

Table 5-1 Results of physical and chemical analyzes of degrease wastewater used in the experiment

Name	Unit	Concentration
pH (25°C)		6.2
TOC	mg L <sup>-1</sup>	210
conductivity	ms cm <sup>-1</sup>	1.42

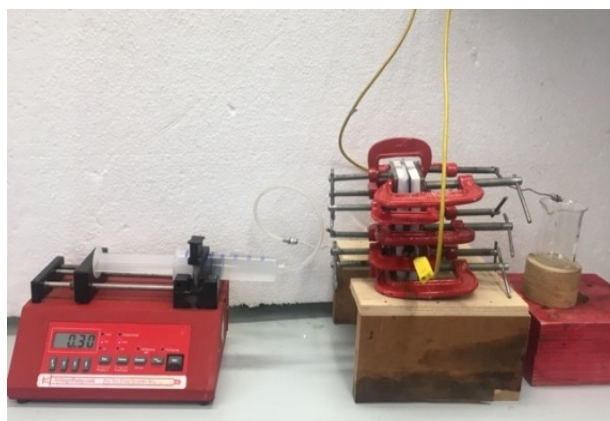
#### b) The reactor

Electrolyses at the macro-scale were performed in a cell (Fig. 4-1A) equipped with a Nickel cathode and a BDD anode (working area A =3.75 cm<sup>2</sup>) and containing 50 mL of solution. The inter-electrode gap was about 2 cm. The microreactor, shown in Fig.5-1, is constituted by:

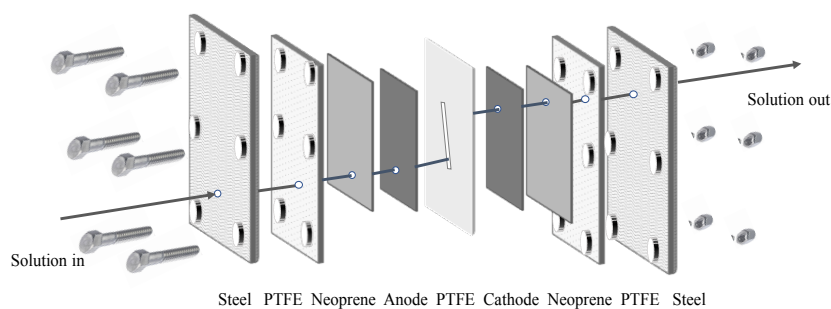
- two steel plates with two holes, to impart mechanical stability to the cell;



- two plates of teflon with 2 holes, one for inlet and one for the outlet of the fluid;
- two neoprene gaskets, each of which is interposed between the plate of Teflon containment and the electrode, which ensure the sealing and prevent any loss of solution from the cell;
- two electrodes consisting of two flat plates with the same dimensions;
- one polytetrafluoroethylene (PTFE) spacer with nominal thickness of 50  $\mu\text{m}$  inserted between two plate electrodes. Spacers were cut to define the working area ( $A = 3.75 \text{ cm}^2$ ).



A



B

Fig. 5-1 (A) System with pump, micro reactor and tubing. (B) Scheme of the micro-reactor.

## 5.2.2 Methods

Electrolyses at the macro-scale were performed under relatively vigorous stirring performed by a magnetic stirrer ( $400 \text{ rpm min}^{-1}$ ) in order to speed-up the mass transfer

of the organics to the anode surface. Experiments in the micro reactor were performed in a continuous mode with a single passage of the solution inside the cell, using a syringe pump (New Era Pump Systems, Inc.) to feed the solutions by stainless steel tubing to the cell, with a flow rate between 0.1 and 0.5 mL min<sup>-1</sup>. These flow rates were chosen in order to have treatment times for 50 mL of solution (1 h 40 min and 8 h 20 min for 0.5 and 0.1 mL min<sup>-1</sup>, respectively) of the same order of magnitude than that achieved in the conventional cell. Electrolyses were performed at room temperature and driven by an Amel 2053 potentiostat/galvanostat operated in galvanostatic mode.

### **5.2.3 Analysis**

Analyses were the same as reported in 4.2.3.

## **5.3 Results and discussion**

### **5.3.1 Electrolyses performed in conventional cell in the absence of supporting electrolyte**

First electrolyses were carried out in a conventional cell without the addition of a supporting electrolyte at a boron doped diamond (BDD) anode and a Nickel cathode at a current intensity of 60 mA (corresponding to a current density of 16 mAcm<sup>-2</sup>) for 7 h. As shown in Fig. 5-2A, a quite good but not total abatement of TOC of about 62% was achieved at the end of the electrolysis. To improve the abatement of TOC, a series of electrolyses was carried out at different current intensities (in the range 20-200 mA, corresponding to 5.3-53 mAcm<sup>-2</sup>). As shown in Fig. 5-2A, the performances of the process are drastically affected by the current intensity. In particular, the higher was the current intensity the higher was the abatement of the TOC; as an example, at the end of the electrolyses, the abatement was about 50% and 84% at 20 and 200 mA, because of the higher amount of charge passed. The very high abatements obtained at high current densities are due to the utilization of a very effective anode towards the mineralization of

organics such as BDD. In particular, at BDD the degradation of organics in the absence of salts and of added supporting electrolyte is expected to take place mainly by hydroxyl radicals generated by water oxidation. Oxygen evolution at BDD starts at about 2.3 V vs. SCE by oxidation of water and formation of hydroxyl radicals (Eq. 5-1). As discussed more in detail in the previous chapter, various authors have proposed, on the bases of the poor adsorption ability of the BDD surface, that hydroxyl radicals generated by water oxidation at BDD are free or very weakly adsorbed on the electrode surface. In the absence of organics, HO• gives rise to the evolution of oxygen (Eq. 5-2).



In the presence of organics, hydroxyl radicals are involved in their oxidation (Eq. 5-3), that of course takes place in competition with the oxygen evolution. In the case of BDD, quasi-free or weakly adsorbed HO• were shown to be particularly effective for the degradation of organics [5,6].



As shown in Fig. 5-2B, the increase of the current resulted in a decrease of the current efficiency (CE), caused by a larger involvement of the parasitic process of oxygen evolution, due to the fact that at higher currents the oxidation of organics is expected to take place under the kinetic control of the mass transfer of the organics to the anode or under a mixed kinetic control. As an example, a final CE of 13% and 2% was obtained at 20 and 200 mA, respectively.

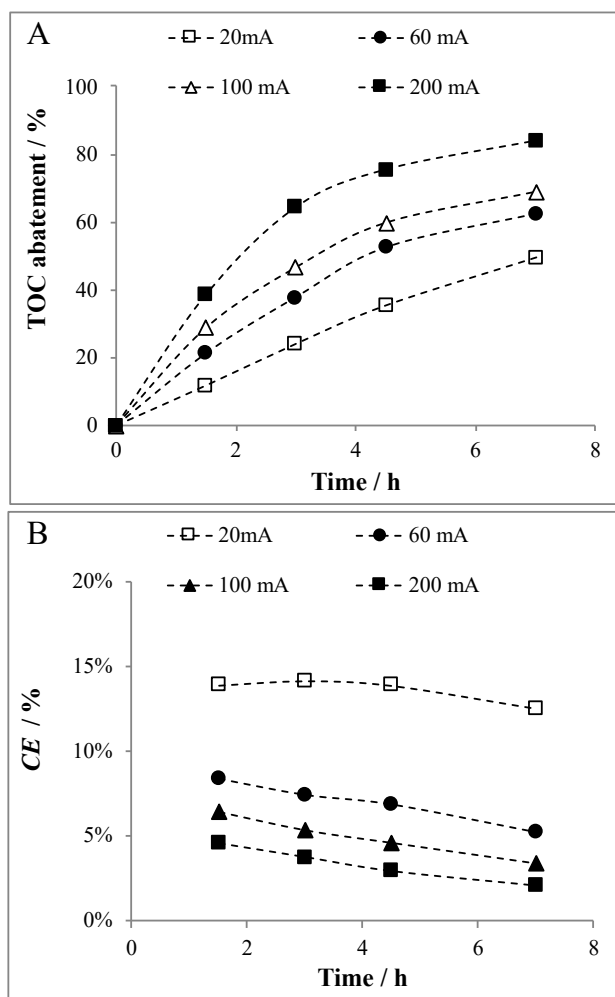


Fig. 5-2 Effect of current intensity on (A) the abatement of the TOC, (B) the current efficiency (CE) achieved in a conventional cell fed with the real wastewater (initial TOC  $210 \text{ mg L}^{-1}$ ) at BDD anode and Nickel cathode. Operative conditions: Rotational rate 400 rpm, electrode surface  $3.75 \text{ cm}^2$ , current intensity 20-200 mA.

As shown in Fig. 5-3, very high potential differences were recorded for all these experiments, because of the low conductivity of the wastewater, thus resulting in large ohmic drops in the solution. Hence, very high energetic consumptions were observed, which are not suitable from an applicative point of view. Furthermore, the increase of current intensity, which allowed to enhance the TOC removal, resulted in a dramatic increase of both cell potential and energetic consumption. The pH was measured during the experiments and it was observed a slight increase to about 7-8 at the end of the electrolyses.

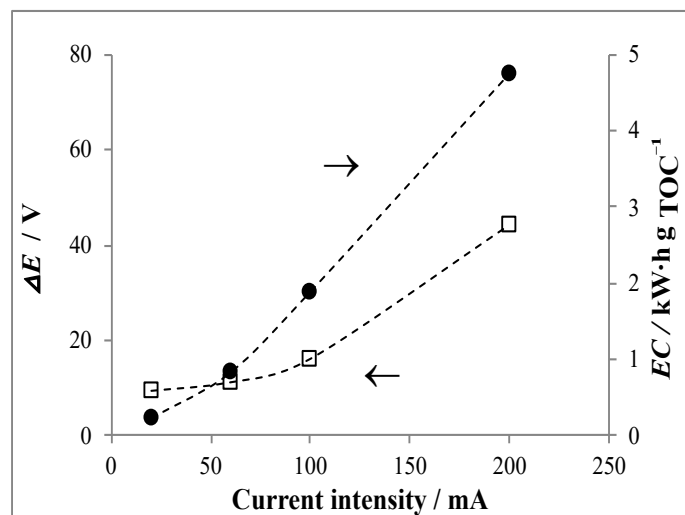


Fig. 5-3 Effect of current intensity on the the average cell potential and energetic consumption (kWh gTOC<sup>-1</sup>) fed with the real wastewater (initial TOC 210 mg L<sup>-1</sup>) at BDD anode and Nickel cathode. Operative conditions: Rotational rate 400 rpm, electrode surface 3.75 cm<sup>2</sup>, current intensity 20-200 mA.

### 5.3.2 Electrolyses performed in conventional cell in the presence of supporting electrolyte

To reduce the energetic consumption, the addition of a supporting electrolyte to the solution was evaluated. Sodium sulphate was used for its environmental compatibility. NaCl was not used, since its presence can lead during the anodic oxidation to the formation of organo-chlorinated compounds that can be more toxic than the starting organic pollutants.

To evaluate the effect of the presence of the supporting electrolyte on the process, two series of electrolyses were performed at both 20 and 200 mA, respectively, adding to the solution various concentrations of Na<sub>2</sub>SO<sub>4</sub> in the range 0-200 mM. As shown in Fig. 5-4, at 20 mA the addition of sodium sulphate had a slight positive effect on the removal of the TOC (Fig. 5-4A); as an example, the TOC removal increased from about 51% to 62%

after 7 h of electrolysis adding to the solution 0.1 M of  $\text{Na}_2\text{SO}_4$ . This positive effect can be explained considering that the anodic oxidation of electrolytes containing  $\text{SO}_4^{2-}$  at anodes with high oxygen evolution overpotential, such as boron-doped diamond or lead dioxide, leads to the generation of  $\text{S}_2\text{O}_8^{2-}$  (Eq. 5-4) [7-9], which diffuses to the bulk of the electrolyte resulting in a mediated homogeneous reaction with the organic pollutant.

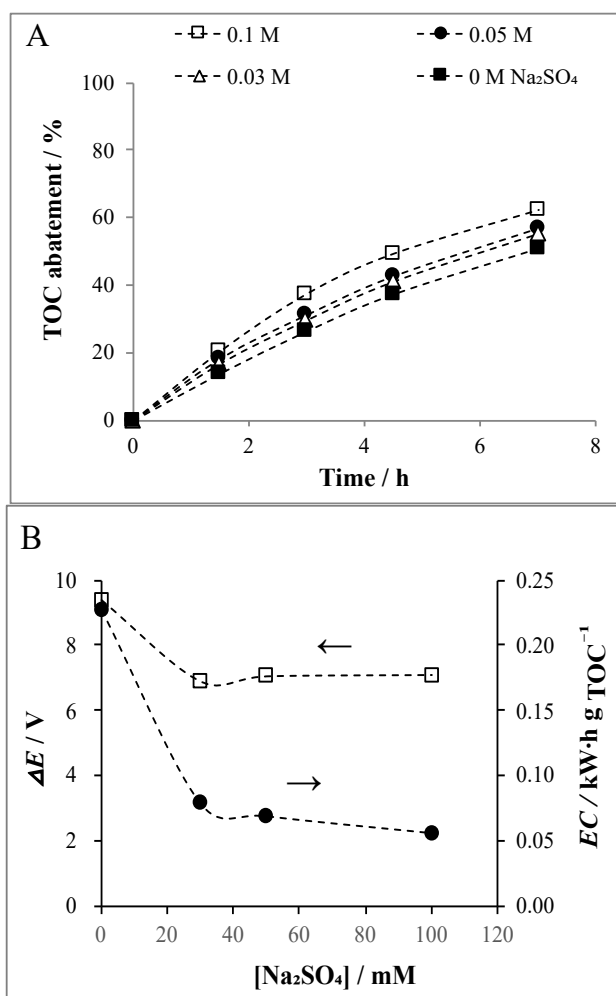


Fig. 5-4 Effect of  $\text{Na}_2\text{SO}_4$  concentration on (A) the abatement of the TOC, (B) the average cell potential and energetic consumption ( $\text{kW}\cdot\text{h g TOC}^{-1}$ ) achieved at 20 mA current intensity in a conventional cell fed with the real wastewater (initial TOC  $210 \text{ mg L}^{-1}$ ) at BDD anode and Nickel cathode. Operative conditions: Rotational rate 400 rpm, electrode surface  $3.75 \text{ cm}^2$ .

However, the small increase of the abatement of the TOC observed in the presence of large amounts of  $\text{Na}_2\text{SO}_4$  suggests that the oxidation of organics present in the wastewater by  $\text{S}_2\text{O}_8^{2-}$  is not particularly effective, because of two main reasons: (i)  $\text{S}_2\text{O}_8^{2-}$  are weak oxidants at least at room temperature and (ii) at low current density small amounts of  $\text{S}_2\text{O}_8^{2-}$  are expected to be formed. Hence, for the adopted wastewater, the degradation is likely to take place mainly by electro-generated hydroxyl radicals also in the presence of sodium sulphate, at least at low current densities.

As shown in Fig. 5-4B, the effect of the supporting electrolyte on cell potential and energetic consumption. The addition of the supporting electrolyte at 20 mA allowed to reduce dramatically the cell potential, and, as a consequence, the energetic consumption, because of the drastic reduction of ohmic drops. As an example, the addition of 0.1 M of  $\text{Na}_2\text{SO}_4$  caused a reduction of the cell potential from more than 9 V to about 4 V and of the energetic consumption from 0.23 to 0.06  $\text{kW}\cdot\text{h gTOC}^{-1}$ .

It is worth mentioning that at 200 mA, where a more relevant formation of  $\text{S}_2\text{O}_8^{2-}$  is expected, a different effect of the concentration of  $\text{Na}_2\text{SO}_4$  was observed. Indeed, as shown in Fig. 5-5A, the addition of sodium sulphate gave rise to lower abatements of the TOC. As an example, after 7 h of electrolysis, the removal of the TOC was 50% and 38% in the absence and in the presence of 0.05M  $\text{Na}_2\text{SO}_4$ . The increase of the concentration of  $\text{Na}_2\text{SO}_4$  to 0.1 and 0.2 M lead to a further decrease of the final abatement of the TOC to 21% and 9%, respectively. A negative effect of the concentration of sodium sulphate on the anodic oxidation of organic pollutants was observed also by Zhang et al. [10] for the removal of bromophenol blue under various experimental conditions. These authors in order to explain their results have pointed out that the formation of  $\text{S}_2\text{O}_8^{2-}$  can involve a reaction between  $\text{Na}_2\text{SO}_4$  and  $\text{HO}\cdot$  (Eqs. 5-5 and 6). In this frame, it seems reasonable to suppose that the presence of sulphates at high currents can reduce significantly the concentration of hydroxyl radicals close to the electrode surface, thus reducing the extent of the direct oxidation of organics by hydroxyl radicals, which are stronger oxidants than  $\text{S}_2\text{O}_8^{2-}$ .

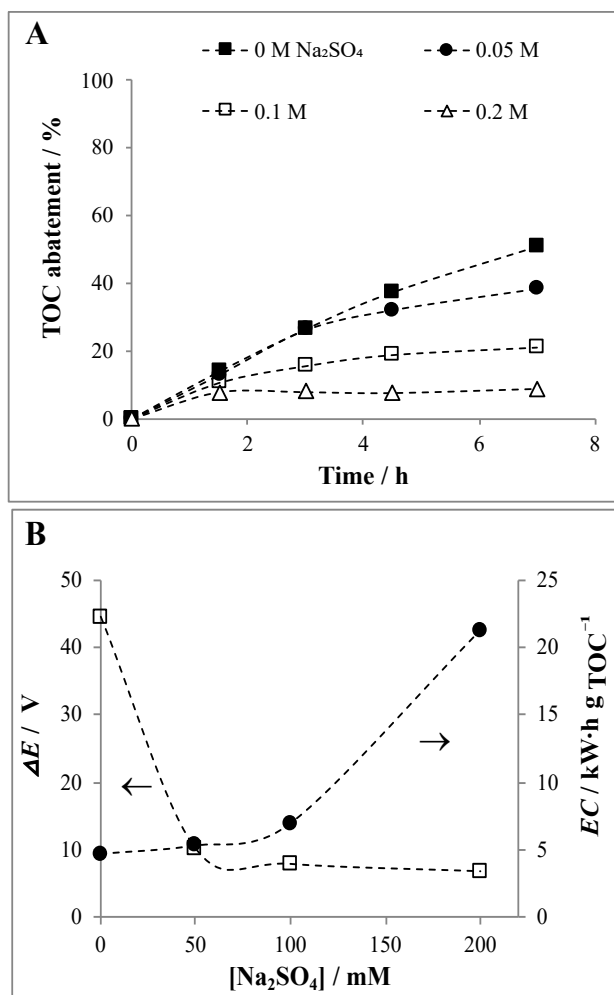
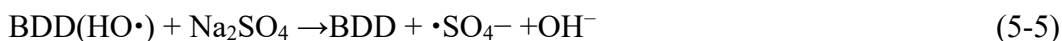


Fig. 5-5 Effect of Na<sub>2</sub>SO<sub>4</sub> concentration on (A) the abatement of the TOC, (B) the average cell potential and energetic consumption (kW·h g TOC<sup>-1</sup>) achieved at 200 mA current intensity in a conventional cell fed with the real wastewater (initial TOC 210 mg L<sup>-1</sup>) at BDD anode and Nickel cathode. Operative conditions: Rotational rate 400 rpm, electrode surface 3.75 cm<sup>2</sup>.

As shown in Fig. 5-5B, at 200 mA, the enhancement of the supporting electrolyte concentration resulted in a decrease of the cell potential but in a more complex behavior for the energetic consumptions. Indeed, the energetic consumption decreased from about 4.7 to 1.2 kW·h g TOC<sup>-1</sup>, upon enhancing the Na<sub>2</sub>SO<sub>4</sub> concentration from 0 to 0.1 M, but



increased to about  $21.2 \text{ kW}\cdot\text{h gTOC}^{-1}$  for a further increase of  $\text{Na}_2\text{SO}_4$  concentration to  $0.2 \text{ M}$ , because of the drastic reduction of the TOC abatement observed for high sulphate concentrations at high currents.

In order to find suitable operating conditions to achieve both high abatements of the TOC and low energetic consumptions, a series of electrolysis was performed at various currents (20, 60, 100 and 200 mA) with  $\text{Na}_2\text{SO}_4$  concentration of 0.05 and 0.2 M.

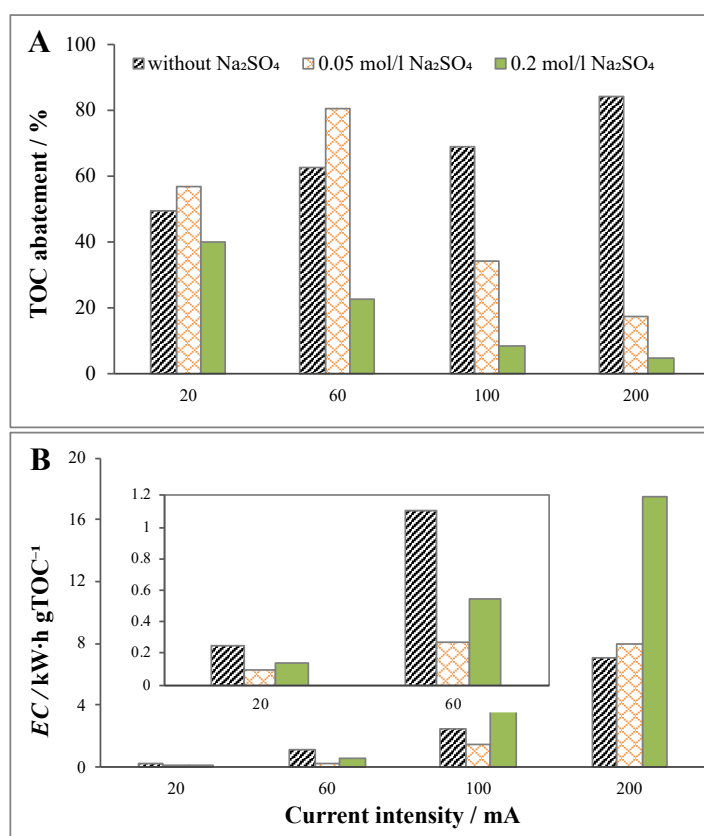


Fig. 5-6 Effect of current intensity on the (A) final abatement of the TOC and (B) energetic consumption ( $\text{kW}\cdot\text{h gTOC}^{-1}$ ) achieved after 7 h in conventional cell fed with the real wastewater (initial TOC  $210 \text{ mg L}^{-1}$ ) and  $\text{Na}_2\text{SO}_4$  (0, 0.05 or 0.2 M) at BDD anode and Nickel cathode. Operative conditions: Rotational rate 400 rpm, electrode surface  $3.75 \text{ cm}^2$ , current intensity 20-200 mA.

As shown in Fig. 5-6A, for all the adopted values of current densities, the experiments with 0.2 M of  $\text{Na}_2\text{SO}_4$  gave lower abatements with respect to that performed with 0.05 M

of  $\text{Na}_2\text{SO}_4$ , thus confirming that for the adopted wastewater, a high concentration of sodium sulphate is detrimental for the process. At 0.05 M, the curve TOC abatement vs. current presented a maximum for 60 mA. This is probably due to the fact that for low currents, the oxidation process is too slow, while for the highest values of currents the sulphates are likely to consume an excessive amount of hydroxyl radicals, thus making less effective the process.

Furthermore, as shown in Fig. 5-6B, the utilization of the lower concentration of  $\text{Na}_2\text{SO}_4$  and of 60 mA allowed to reduce drastically the energetic consumption.

### 5.3.3 Electrolyses performed in micro cells in the absence of supporting electrolyte

A series of electrolysis was performed with a micro reactor with an inter-electrode distance of 50  $\mu\text{m}$  in the absence of a supporting electrolyte at various currents (20, 60, 100 and 200 mA) and flow rates (0.1, 0.2, 0.3, 0.4 and 0.5  $\text{mL min}^{-1}$ ). As shown in Fig. 5-7A, the removal of TOC increased upon enhancing the adopted current. As an example, at 0.3  $\text{mL min}^{-1}$ , the removal of TOC was 12%, 73%, 85% and 93% at 20, 60, 100 and 200 mA, because of the larger amount of charge passed. However, at each value of the flow rate, the highest current efficiencies (CE) were obtained at 60 mA (Fig. 5-7B). As an example, at 0.3  $\text{mL min}^{-1}$ , the CE was 8%, 16%, 11% and 7% respectively at 20, 60, 100 and 200 mA. At lower currents, lower CE were caused by the low TOC removal, probably due to the fact that at too low current densities and working potentials, BDD is expected not to generate effectively hydroxyl radicals. Conversely, at high currents, a relevant part of the charge is used for oxygen evolution since the oxidation of the organics is kinetically limited by its mass transfer to the anode due to both the high current densities densities and the very low concentrations of organics achieved in the last part of the cell.

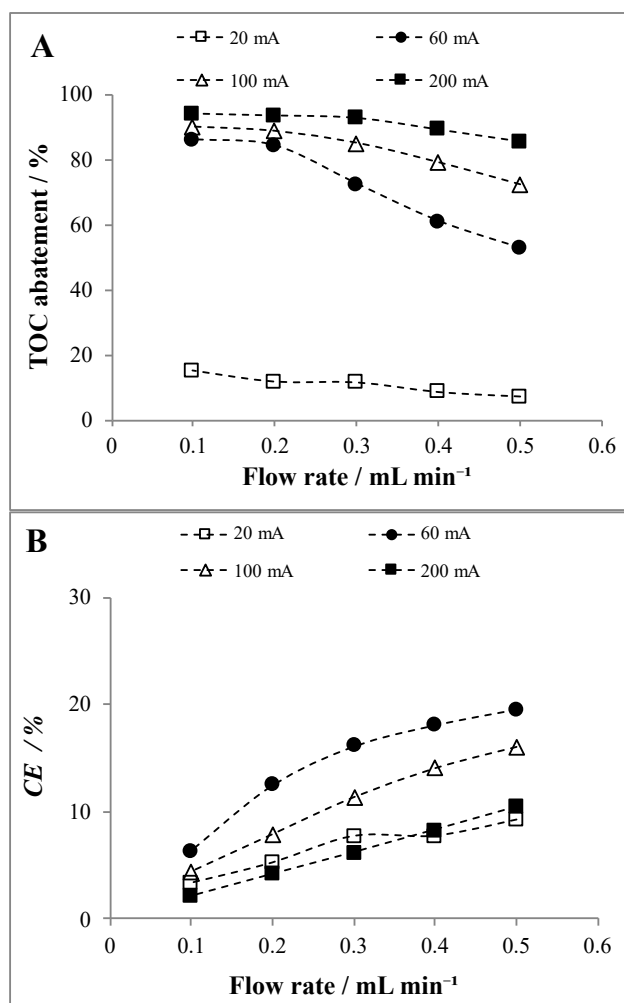


Fig. 5-7 Effect of current and flow rate on the abatement of the (A)TOC abatement (B)current efficiency achieved in a micro cell fed with the real wastewater (initial TOC 210 mg L<sup>-1</sup>). Operative conditions: BDD as anode, Nickel as cathode, flow rate 0.1-0.5 mL min<sup>-1</sup>, electrode surface 3.75 cm<sup>2</sup>, current intensity 20-200 mA.

The removal of TOC was quite low for experiments performed at 20 mA. This may be due to the fact that the degradation process of organic pollutants in wastewater was controlled by charge transfer kinetics when the current intensity and working potential were low, and the amount of HO• produced by BDD electrode was not enough to degrade the organic pollutant. On the contrary, when the current intensity was too high, the mass transfer process of organics to the anode surface determines the electrochemical degradation efficiency. As shown in Fig. 5-8, part of the charge was consumed by the parasitic reaction of oxygen evolution. As shown in Fig. 5-7B, at different flow rates, the

maximum current efficiency was always obtained at 60 mA. For example, when the flow rate is  $0.3 \text{ mL min}^{-1}$ , the current efficiency at 20, 60, 100 and 200 mA were 8%, 16%, 11% and 6%, respectively.

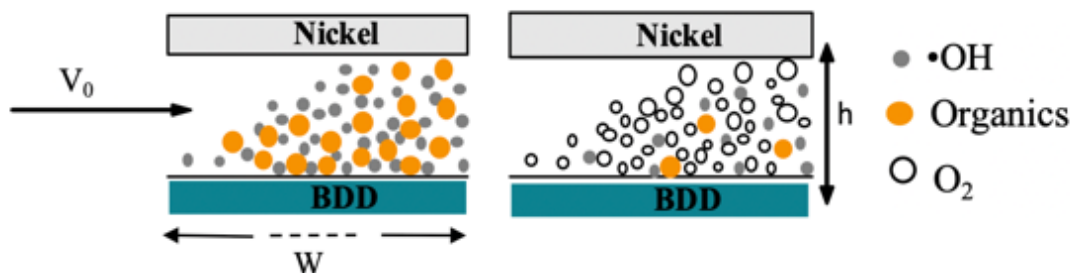


Fig. 5-8 Diagram of organic pollutants degradation by  $\text{HO}\cdot$  and oxygen evolution in microfluidic reactor (the left and the right figures refers to low and high current densities, respectively).

Fig. 5-9 reports the effect of the current at various flow rate on the cell potential and energetic consumption. The lowest energetic consumptions were achieved at 60 mA because of the relatively high abatements of TOC, the highest values of CE and the limited cell potentials (4.55 V). As shown in Fig. 5-9, the performances of the process are strongly determined also by the flow rate, which imposes from one hand the residence time and from the other hand the amount of the solution that can be treated by the cell for unit of time. A lower value of the flow rate gave higher removal of the TOC because of the longer residence time (resulting in larger amounts of charge devoted to the solution). However, the utilization of lower flow rates resulted in lower current efficiencies because of the higher impact of the parasitic processes. Indeed, at low flow rates, a significant part of the cell works in the presence of low concentrations of organics, thus favoring the parasitic evolution of oxygen. Furthermore, low flow rates gave higher energetic consumptions caused by both the lower CE and the lower amounts of solution treated for unit of time. On overall, several operating parameters allowed to achieve very high removals of the TOC (Fig. 5-7A). Indeed, an abatement higher than 80% was achieved both at 200 mA at all adopted flow rates or at 60 mA at  $0.1$  and  $0.2 \text{ mL min}^{-1}$ . As an

example, at 200 mA and 0.5 mL min<sup>-1</sup>, abatements of TOC higher than 90% were achieved coupled with relatively low energetic consumptions (0.15 kW·h gTOC<sup>-1</sup>).

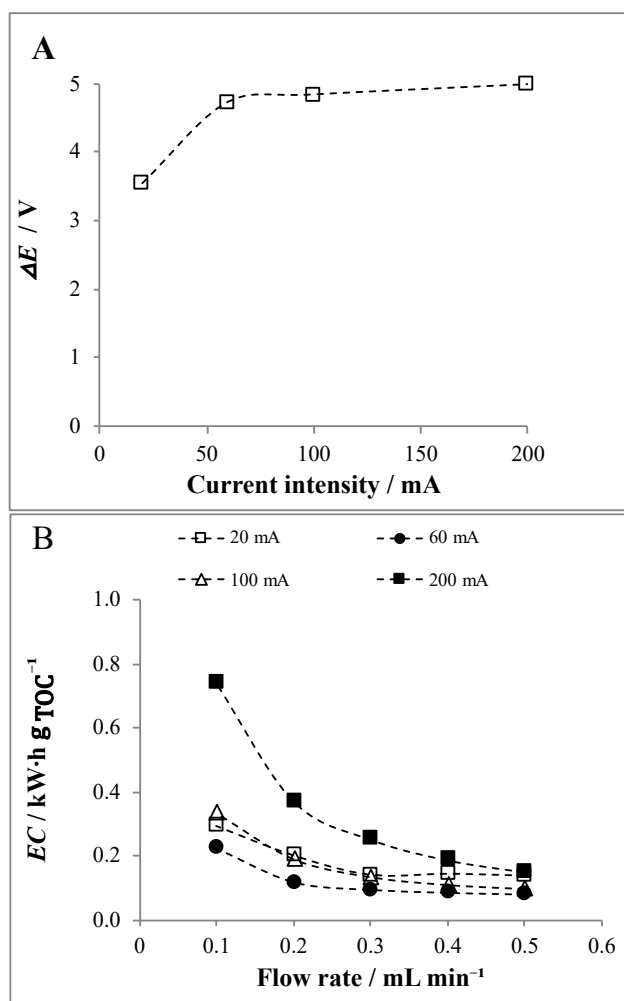


Fig. 5-9 Effect of current intensity and flow rate on the (A) cell potential (B) energy consumption achieved in a micro cell fed with the real wastewater (initial TOC 210 mg L<sup>-1</sup>). BDD as anode, Nickel as cathode, flow rate 0.1-0.5 mL min<sup>-1</sup>, electrode surface 3.75 cm<sup>2</sup>, current intensity 20-200 mA.

### 5.3.4 Technical and economical comparison between adopted routes

Fig. 5-10 reports a comparison between the adopted routes (e.g., conventional cell (i) in the absence and (ii) in the presence of 0.05 M supporting electrolyte and (iii) micro cell without the supporting electrolyte) in terms of removal of TOC, cell potential and energy consumption at various currents (60, 100 and 200 mA).

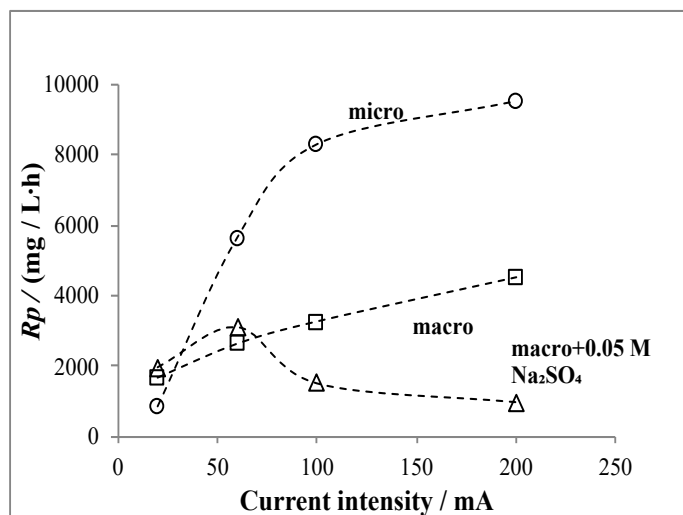


Fig. 5-10 Reaction rate using BDD anode in micro cell, macro cell and macro cell with 0.05 M  $\text{Na}_2\text{SO}_4$  vs. a current intensity. Operative conditions: Initial TOC  $210 \text{ mg L}^{-1}$ , initial conductivity  $1.42 \text{ ms cm}^{-1}$ , nickel as cathode, flow rate in the micro reactor  $0.1\text{--}0.5 \text{ mL min}^{-1}$ , the rotational rate in macro reactor is 400 rpm, electrode surface of anodes in both macro and micro reactors  $3.75 \text{ cm}^2$ .

The reaction rates of three different reaction pathways under different current intensities were shown in Fig. 5-10. Under most of adopted current densities, the reaction rate in the microfluidic reactor was significantly higher than that in the conventional reactor with or without electrolyte. Furthermore, at all the currents, the micro cell allowed to obtain the highest removals of the TOC (Fig. 5-11). Indeed, micro cells with a very small distance between the electrodes allow a significant intensification of the mass transport of the organics to the anode, thus speeding up the removal of the TOC and increasing the CE in comparison with conventional cells [11].

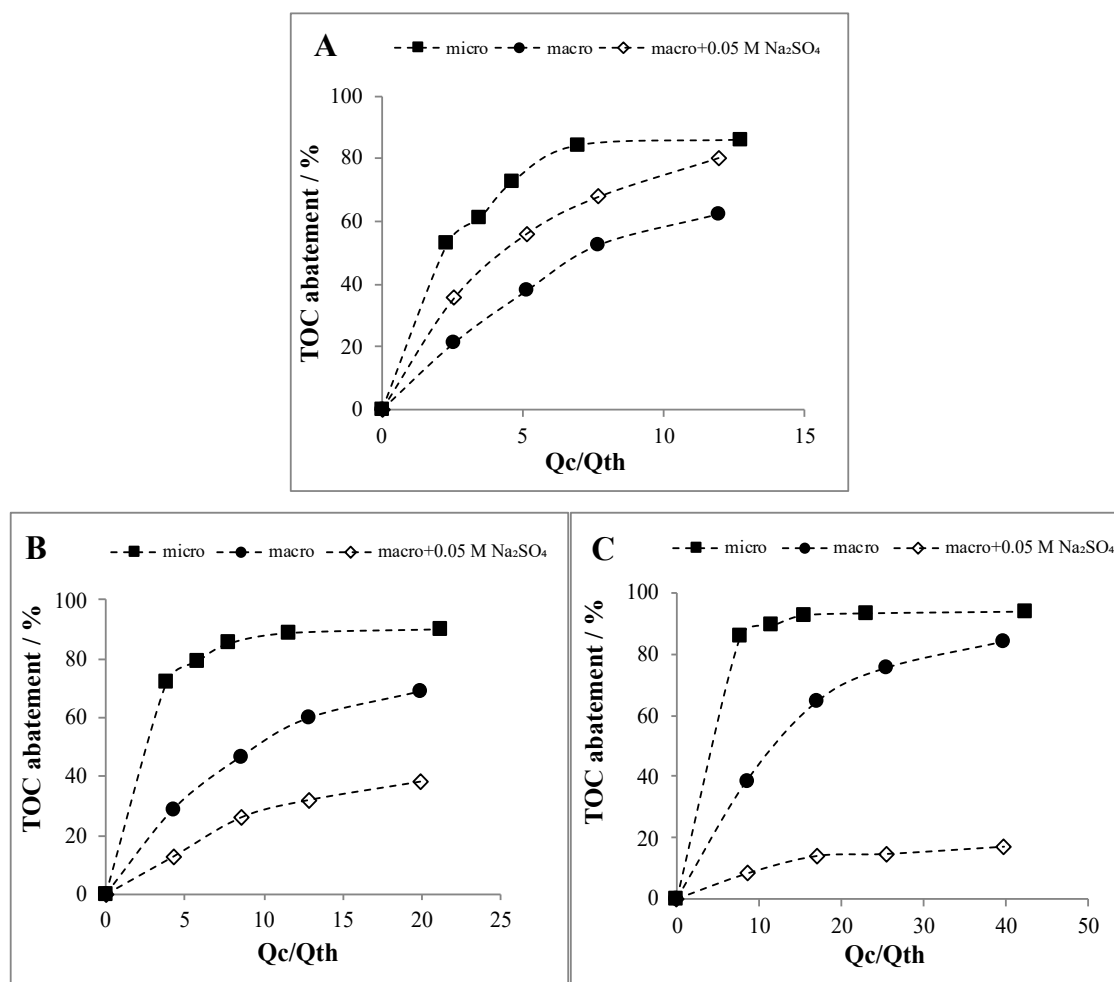


Fig. 5-11 Abatement of TOC using BDD anode in micro cell, macro cell and macro cell with 0.05 M  $Na_2SO_4$  vs. dimensionless charge  $Q_c/Q_{th}$  (ratio between the charge passed and theoretical charge necessary for the removal of organics with a CE of 100%) at various currents: (A) 60 mA, (B) 100 mA and (C) 200 mA. Operative conditions: Initial TOC 210 mg  $L^{-1}$ , initial conductivity 1.42  $ms\ cm^{-1}$ , nickel as cathode, flow rate in the micro reactor: 0.1–0.5  $mL\ min^{-1}$ , the rotational rate in macro reactor is 400 rpm, electrode surface of anodes in both macro and micro reactors 3.75  $cm^2$ .

Furthermore, small inter-electrode gaps, such as that adopted in this study (nominal distance 50  $\mu m$ ), allowed to strongly reduce the ohmic drops, also operating with water with low conductivity [12]. Indeed, as shown in Fig. 5-12, the cell potential for the macro cell in the absence of supporting electrolyte was drastically higher than that recorded with the other two routes. Furthermore, the micro cell operated in the absence of the supporting

electrolyte gave slight lower cell potentials with respect also to the macro cell operated with  $\text{Na}_2\text{SO}_4$ .

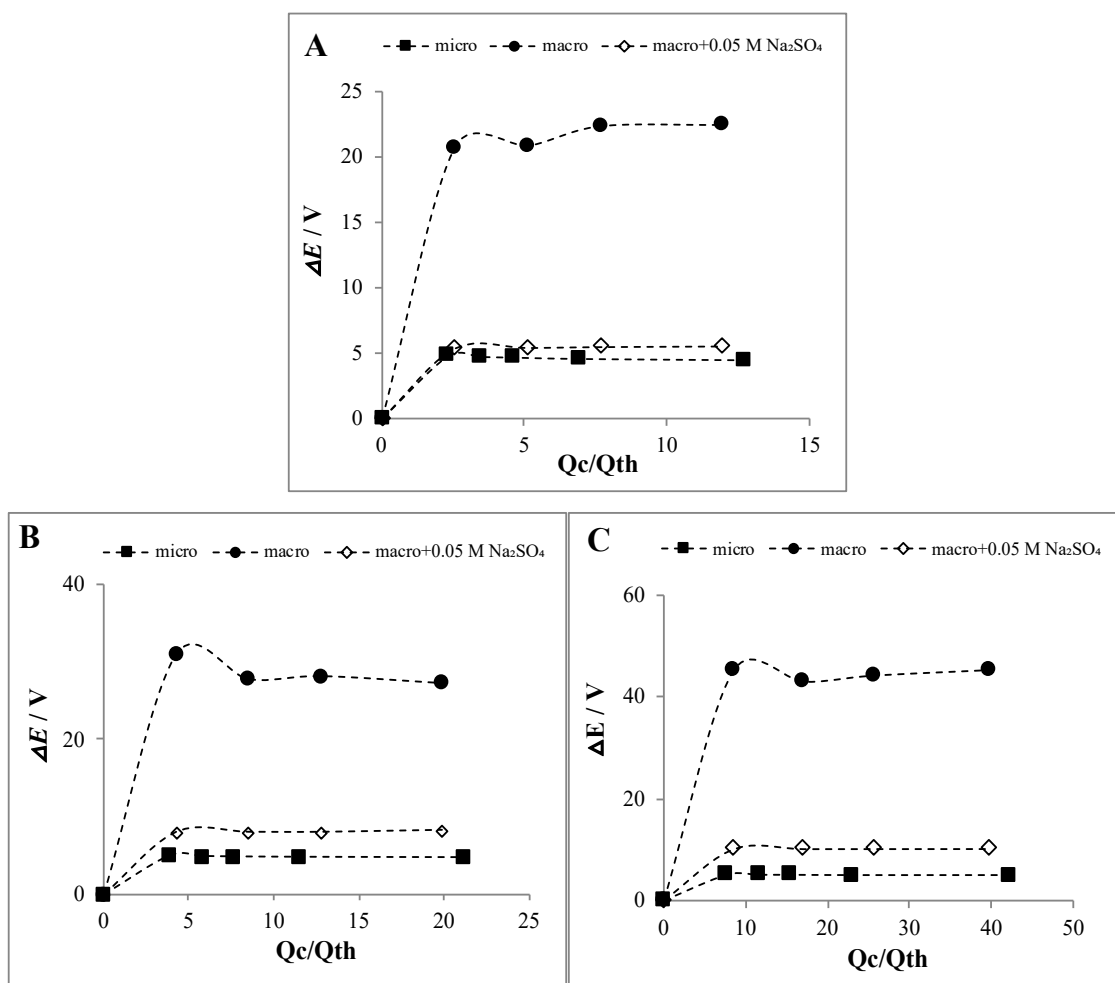


Fig. 5-12 The cell potential using BDD anode in micro cell, macro cell and macro cell with 0.05 M  $\text{Na}_2\text{SO}_4$  vs. dimensionless charge  $Q_c / Q_{th}$  (ratio between the charge passed and theoretical charge necessary for the removal of organics with a CE of 100%) at various currents: (A) 60 mA, (B) 100 mA and (C) 200 mA. Operative conditions: Initial TOC  $210 \text{ mg L}^{-1}$ , initial conductivity  $1.42 \text{ ms cm}^{-1}$ , nickel as cathode, flow rate in the micro reactor  $0.1\text{--}0.5 \text{ mL min}^{-1}$ , the rotational rate in macro reactor is  $400 \text{ rpm}$ , electrode surface of anodes in both macro and micro reactors is  $3.75 \text{ cm}^2$ .

For the energy consumption, at all currents the process performed in the conventional cell without supporting electrolyte gave very high ECs (Fig. 5-13) caused by the large ohmic drops and consequently by the high cell potentials (Fig. 5-12). The process performed with sodium sulphate gave quite low ECs comparable to that achieved in the



micro reactor only at 60 mA (Fig. 5-13A), while it gave very high ECs at 100 and 200 mA (Fig. 5-13B and C) caused by the low TOC removals.

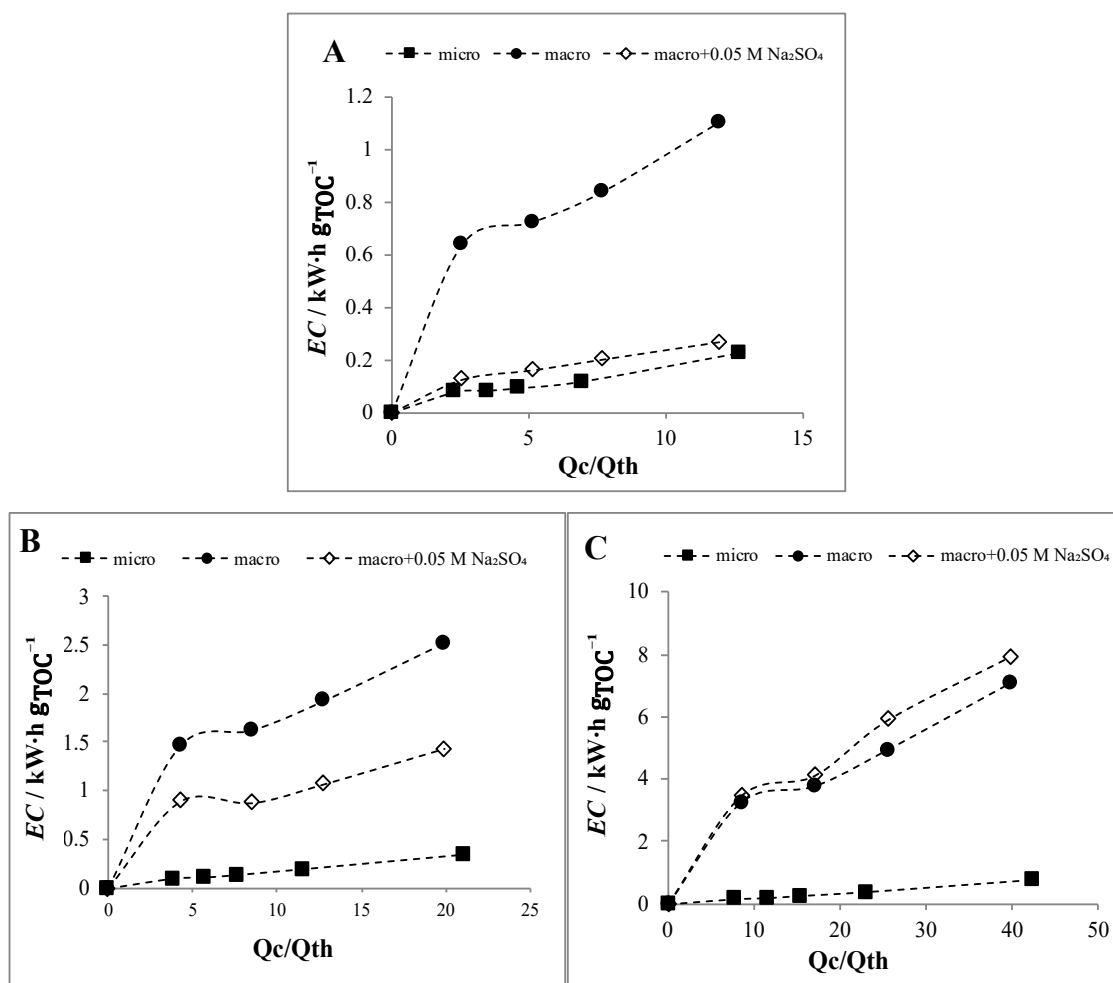


Fig. 5-13 The cell potential using BDD anode in micro cell, macro cell and macro cell with 0.05 M Na<sub>2</sub>SO<sub>4</sub> vs. dimensionless charge Qc/Qth (ratio between the charge passed and theoretical charge necessary for the removal of organics with a CE of 100%) at various currents: (A) 60 mA, (B) 100 mA and (C) 200 mA. Operative conditions: Initial TOC 210 mg L<sup>-1</sup>, initial conductivity 1.42 ms cm<sup>-1</sup>, nickel as cathode, flow rate in the micro reactor 0.1-0.5 mL min<sup>-1</sup>, the rotational rate in macro reactor is 400 rpm; electrode surface of anodes in both macro and micro reactors 3.75 cm<sup>2</sup>.

In order to compare the three adopted routes, the operating costs were estimated and reported in Table 5-2. The operating conditions for each route were selected in order to have a final abatement of the TOC of about 70 - 80%. For electrolyses performed in the conventional cell without supporting electrolyte a high abatement of the TOC was

coupled with a very high cost of treatment close to 20 €/m<sup>3</sup>, which prevents its utilization on an applicative scale. For the macro cell, in the presence of sodium sulphate, the costs and the abatements strongly depend on the adopted concentration of Na<sub>2</sub>SO<sub>4</sub> and on the current. According to previous considerations (see paragraph 5.3.2), a moderate concentration of 0.05 M and a quite low current can be selected in order to achieve both high removals of the TOC and low energetic consumptions. In this case, the cost of electric energy dropped drastically to 1.5 or 1.9 €/m<sup>3</sup> (for an abatement of the TOC of 69% and 80%, respectively) that has to be added to the cost of the supporting electrolyte that can be estimated to be about 0.4 €/m<sup>3</sup> (Table 5-2). Hence, an overall cost between 1.9 and 2.4 €/m<sup>3</sup> can be estimated for the conventional cell added with Na<sub>2</sub>SO<sub>4</sub> for an abatement of the TOC of 69% and 80% respectively. In the case of the micro cell, a quite high abatement of the TOC can be achieved in short times with respect to the macro cells and with low cell potentials, thus allowing to further reduce the operating costs to about 1 €/m<sup>3</sup>. Of course, an overall economic estimation has to take in account also the investment costs (and the price of BDD anodes that was estimated to be about 8000 €/m<sup>2</sup>), but it is worth to mention that they are expected to be quite close for the cells adopted in the study.

For the electrochemical processes, the operation cost can be assumed close to the sum of energetic one and of the cost of the supporting electrolyte. A cost of the supporting electrolyte of 52 €/ton was considered. The price of electricity strongly depends on that of the country. A cost of 0.05 € kW h<sup>-1</sup> was here considered according to [13].

Table 5-2 Main operation costs (computed for each cubic meter of treated wastewater) and other figures for the electrochemical treatment of adopted real wastewater

Route	Operative conditions	TOC removal (%)	Electric energy cost (€/m <sup>3</sup> )	Supporting electrolyte cost (€/m <sup>3</sup> )	Total operation cost (€/m <sup>3</sup> )
Macro cell without supporting electrolyte	I = 0.1 A; t = 7h	70	19.8		19.8

	I = 0.06 A;				
Macro cell with 0.05 M Na <sub>2</sub> SO <sub>4</sub>	t = 4.5 h	69	1.5	0.4	1.9
	t = 7.0 h	80	2.4		2.8
Micro cell without supporting electrolyte	I = 0.1 A; flow rate: 0.4 ml/min	79	1		1

## 5.4 Summary

The anodic treatment at a BDD anode of a real wastewater contaminated by organic pollutants and characterized by low conductivity was studied. The process was performed under three different conditions: (i) conventional cell in the absence of supporting electrolyte; (ii) conventional cell with the addition of Na<sub>2</sub>SO<sub>4</sub> as supporting electrolyte; (iii) microfluidic cell without supporting electrolyte. It was found that the performances of the process drastically depend on the adopted cell, the presence of the supporting electrolyte, the electrolysis time (or the flow rate for the micro cell) and the current.

- 1) For the experiments performed in the conventional cell in the absence of supporting electrolyte, high abatements of the TOC were achieved, which increased with the current. However, the low conductivity of the solution caused very high cell potentials that resulted in high energetic consumptions and operating costs that prevent the utilization of such route.
- 2) In order to decrease the energetic consumption, a supporting electrolyte can be added to the wastewater. A non-toxic supporting electrolyte that does not give rise to the anodic formation of toxic species has to be selected. However, this option has various disadvantages including a more difficult administrative route for the authorizations necessary to operate and the cost of the supporting electrolyte. Furthermore, we have found that in many operating conditions, the addition of Na<sub>2</sub>SO<sub>4</sub> gave rise to a lower removal of the TOC, probably caused by the fact that SO<sub>4</sub><sup>2-</sup> can react with HO• with

the formation of  $S_2O_8^{2-}$ , which are weaker oxidants than hydroxyl radicals. However, a proper selection of the concentration of sodium sulphate and of the current can allow to achieve high removals of the TOC coupled with low energetic consumptions.

- 3) When the process was operated in microfluidic cells without supporting electrolyte, very high removals of the TOC were achieved coupled with the lowest energetic consumptions, as a result of the low inter-electrode distances that allowed to reduce the ohmic drops and to intensify the mass transport of the organics to the anode.

## 5.5 References

- [1] Panizza M, Cerisola G. Direct and mediated anodic oxidation of organic pollutants. *Chemical Reviews*, 2009, 109 (12): 6541–6569.
- [2] Scialdone O, Galia A, Sabatino S, et al. Electrochemical conversion of dichloroacetic acid to chloroacetic acid in a microfluidic stack and in a series of microfluidic reactors. *ChemElectroChem*, 2015, 2 (5): 684–690.
- [3] Pérez J F, Llanos J, Sáez C, et al. A microfluidic flow-through electrochemical reactor for wastewater treatment: A proof-of-concept[J]. *Electrochemistry Communications*, 2017, 82: 85–88.
- [4] Sabatino S, Galia A, Scialdone O. Electrochemical abatement of organic pollutants in continuous-reaction systems through the assembly of microfluidic cells in series. *ChemElectroChem*, 2016, 3 (1): 83–90.
- [5] Panizza M, Cerisola G. Direct and mediated anodic oxidation of organic pollutants. *Chemical Reviews*, 2009, 109 (12): 6541–6569.
- [6] Oturan M A, Rodrigo M A, Brillas E, et al. Electrochemical advanced oxidation processes: today and tomorrow. A review. *Environmental Science and Pollution Research*, 2014, 21 (14): 8336–8367.
- [7] Panizza M, Michaud P A, Cerisola G, et al. Anodic oxidation of 2-naphthol at boron-doped diamond electrodes. *Journal of Electroanalytical Chemistry*, 2001, 507 (1–2): 206–214.

- 
- [8] Cañizares P, Gadri A, Lobato J, et al. Electrochemical oxidation of azoic dyes with conductive-diamond anodes. *Industrial and Engineering Chemistry Research*, 2006, 45 (10): 3468–3473.
- [9] Ravera M, Ciccarelli C, Gianotti V, et al. Electroassisted methods for waste destruction: Silver(II) and peroxydisulfate reagents in the electrochemically mediated oxidation of polyaromatic sulfonates. *Chemosphere*, 2004, 57 (7): 587–594.
- [10] C. Zhang, Z. He, J. Wu, D. Fu, The peculiar roles of sulfate electrolytes in BDD anode cells, *J. Electrochem. Soc.* 162 (2015) E85–E89
- [11] O. Scialdone, A. Galia, C. Guarisco, et al. Abatement of 1,1,2,2-tetra-chloroethane in water by reduction at silver cathode and oxidation at boron doped diamond anode in micro reactors. *Chemical Engineering Journal*, 2012, 189–190: 229–236.
- [12] O. Scialdone, C. Guarisco, A. Galia, et al. Anodic abatement of organic pollutants in water in micro reactors. *Journal of Electroanalytical Chemistry*, 2010, 638: 293–296.
- [13] A.S. Agarwal, Y. Zhai, D. Hill, et al. The electrochemical reduction of carbon dioxide to formate/formic acid: Engineering and economic feasibility. *ChemSusChem*, 2011,4: 1301–1310.



## **Chapter 6. Development of a process without energy inputs using a reverse electro dialysis stack and the salinity gradient of wastewaters**

### **6.1 Introduction**

In the past few years, due to the development of cheap and efficient membrane technologies, the practical application of reverse electro dialysis (RED) technology has become possible. Therefore, more and more attention has been paid to the research on the production of electricity from salinity gradient by reverse electro dialysis [1], based on the utilization of two solutions with different salt concentration in the RED stack (a high concentration solution and a diluted one, named in the following  $HC_{stack}$  and  $LC_{stack}$ , respectively). Scialdone and co-worker first demonstrated that RED can be used to generate electric energy and purify Cr (VI) - polluted wastewater at the cathode. Then, the wastewater containing acid orange 7 was treated by anodic indirect electrochemical oxidation and cathodic electro Fenton process, respectively, in a RED stack.

However, the utilization of RED for the treatment of wastewater was studied up to now using as sources of salinity gradients only seawater and freshwater and brine and seawater/freshwater. However, this imposes a strong limitation to the exploitation of such method to the cases where the industrial sites that generate/treat the wastewater are located where these salinity gradients are available and, in particular, in river estuaries and in salt ponds. Hence, in order to extend the applicability of this appealing method, other sources of salinity gradients have to be found. In this frame, it is relevant to observe that the sites that generate/treat wastewaters in most of cases are centralized plants that deal with many different kinds of liquid effluents usually characterized by different salinities. We have carried out a survey involving various companies in China and in Italy (in different sectors such as pesticides factories, petrochemistry, chemistry and oil production), and it was found that, in most of cases, wastewater with different salinity

contents are treated in the same site. For example, sites located in Sicily in industrial districts and devoted to the treatment of a large number of industrial wastewater deal at the same time with liquid effluents with a salt content close to that of freshwater as well as effluents with a NaCl concentration higher than that of seawater and in some cases close to that of brine. As a further example, petrochemical companies generate, during oil prospecting and exploitation activities, large amounts of produced waters (PW), containing numerous organics resistant to conventional biological processes, often characterized by very different salt contents; i.e., a plant located in the northeastern region of Brazil was reported to produce PW with huge differences in salinities (143650 vs. 78.7 mg L<sup>-1</sup>) [2]. Hence, it would be particularly appealing to use wastewaters with different salinities to drive the electrochemical treatment of some of these wastewaters, since it would reduce dramatically the operative costs of the process.

RED gives rise to a potential difference between the electrodes that can be used to produce electric energy and to drive redox processes at the electrodes that can be potentially used for many purposes. Hence, in this work we have studied for the first time, a RED process for the treatment of synthetic wastewaters contaminated by organics, without energy inputs, using the salinity gradient of different synthetic wastewaters.

## 6.2 Experimental

### 6.2.1 Experimental materials and reactor

#### a) Reagents

Table 6-1 Main reagents

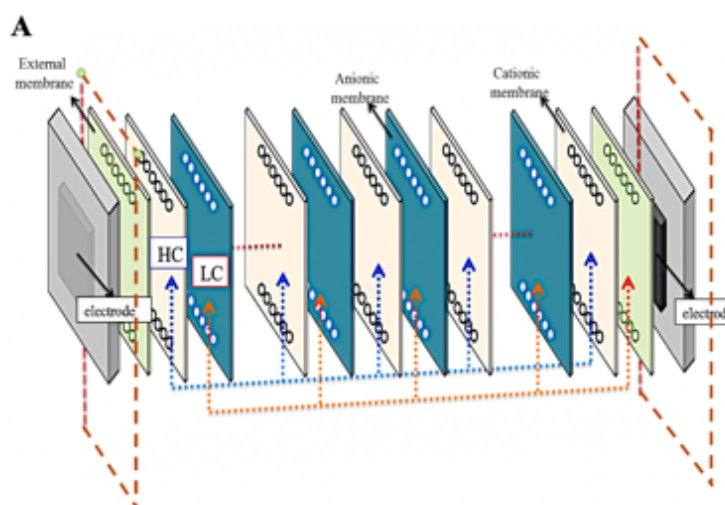
Reagents	Standards	Company
NaCl	Chemical	Sigma Aldrich
Na <sub>2</sub> SO <sub>4</sub>	Chemical	Janssen



$\text{FeSO}_4 \cdot 7\text{H}_2\text{O}$	analytical	Fluka
$\text{CHOOH}$	analytical	Sigma Aldrich
$\text{H}_2\text{SO}_4$	analytical	Sigma Aldrich

### b) Reactor

Experiments were performed in a homemade lab scale stack (as shown in Fig. 6-1A. ), equipped with anode and cathode chambers ( $10 \text{ cm} \times 10 \text{ cm} \times 2 \text{ mm}$ ), usually 60 anion- and 61 cation-exchange membranes (kindly donated by Fujifilm), gasket integrated with spacers (Deukum, 0.28 mm thickness) and two external membranes to separate electrode compartments and side ones, creating 60 pairs of alternating high concentrated ( $\text{HC}_{\text{stack}}$ ) and low concentrated ( $\text{LC}_{\text{stack}}$ ) chambers. Two external anionic membranes from Selemion were used. The exposed area of each exchange membrane was  $100 \text{ cm}^2$ . Two peristaltic pumps (General Control SpA) continuously fed the  $\text{HC}_{\text{stack}}$  and  $\text{LC}_{\text{stack}}$  solutions at a flow rate of 260 or  $200 \text{ mL min}^{-1}$ . Two hydraulic circuits were used for electrode solutions and the two electrode solutions ( $\text{HC}_{\text{an}}$  and  $\text{LC}_{\text{cat}}$ ) were continuously recirculated to the electrode compartments and to two different reservoirs (see Fig. 6-1B), by two peristaltic pumps (General Control SpA) with a flow rate of  $200 \text{ mL min}^{-1}$ . Ion exchange membranes and the electrode tested during the lab experiments are reported in Table 6-2.



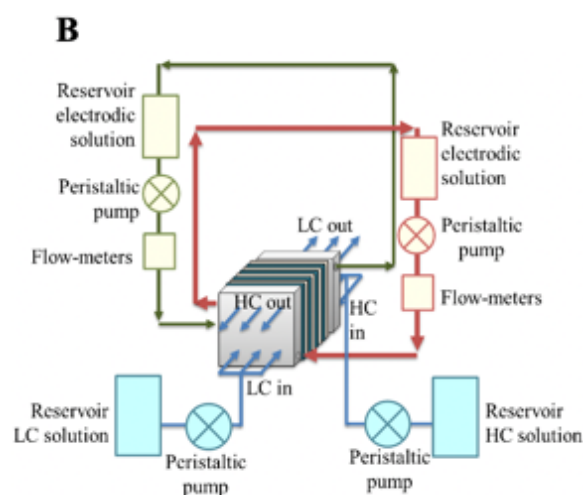


Fig. 6-1 (A)The main components of the RED system. (B)Scheme of the device with four different circulating solution: HC, LC, anodic and cathodic solution.

Table 6-2 Ion exchange membranes and the electrode tested during the lab experiments

Name	Company
cationic exchange membrane	FujiFilm
anionic exchange membrane	FujiFilm
external cationic exchange membrane	NAfion
external anionic exchange membrane	Selemion
DSA(Ti/RuO <sub>2</sub> -IrO <sub>2</sub> )	Magneto
Carbon felt	Carbone Lorraine

The Fig. 6-2 shows a photo of the main components used to assemble a stack to reverse electro dialysis.

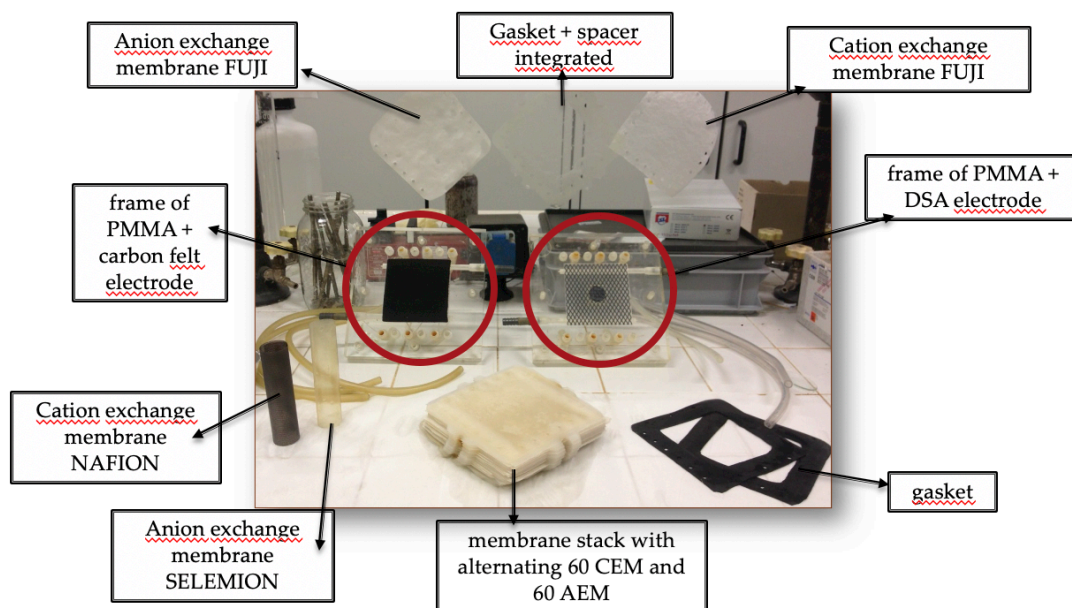


Fig. 6-2 Photo that reports the main components of a RED stack assembled with 60 cell pairs of membrane.

## 6.2.2 Methods

### a) RED system

Synthetic wastewaters were prepared dissolving NaCl and formic acid into deionized water. Experiments were performed with two solutions with high (HC) and low (LC) concentrations of NaCl, respectively, similar to that reported for wastewater coming from oil production [2]. In particular, for HC the concentration of NaCl was 120 or 143 g L<sup>-1</sup>, while for LC 50 or 78 mg L<sup>-1</sup>. For results reported in the 6.3.4, the concentration of NaCl in the LC solution was strongly changed in the range 78 mg L<sup>-1</sup> - 16 g L<sup>-1</sup>, in order to evaluate the effect of the salinity gradient on the performances of the process. Both solutions presented a TOC content of 120 mg L<sup>-1</sup> obtained by the addition of formic acid. Formic acid was chosen as model organic pollutant since carboxylic acids present a quite high resistance to electrochemical processes. HC and LC solutions were sent both to the

stack (and called  $HC_{stack}$  and  $LC_{stack}$ , respectively) and to the electrode compartments. In particular, HC was sent to the anode ( $HC_{an}$ ) and LC to the cathode ( $LC_{cat}$ ).  $FeSO_4 \cdot 7H_2O$  (0.5 mM) was added to  $LC_{cat}$  to catalyze electro-Fenton (EF) process, adjusting the pH value to 3 (by addition of  $H_2SO_4$ ). DSA anode and carbon felt cathode were assembled as shown in Fig. 6-3. In addition, the cathodic electrolytic solution was fed with air.

### b) Conventional system (1 membrane reactor)

Using a single membrane system, the electrolyte of anode and cathode chamber is 200 mL, the solution contains  $143 \text{ g L}^{-1}$  NaCl, and 10 mM formic acid. An external electric energy is supplied by a potentiostat. The experiments were performed at different supplied potentials.

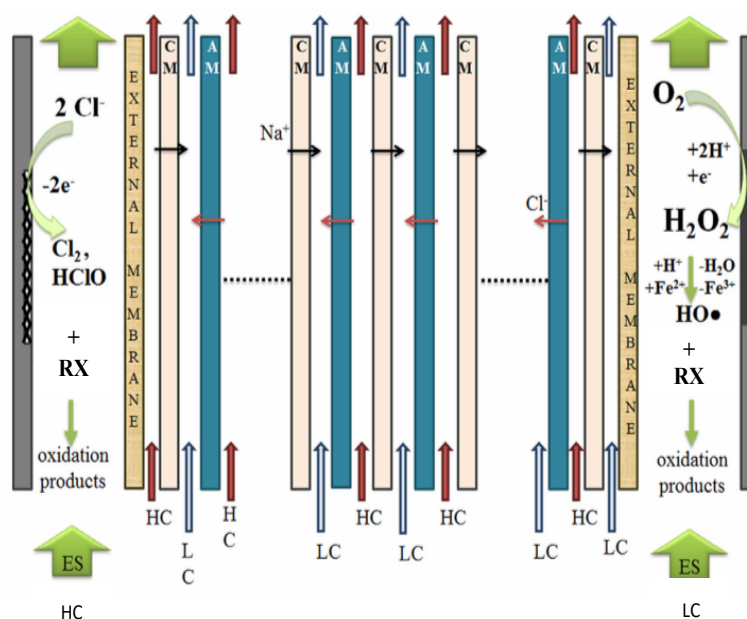


Fig. 6-3 Reports the scheme of RED stack showing cationic, anionic and external membranes, electrodes, the main reactions occurring in the electrodic compartments, concentrated (HC), diluted (LC) and electrodic solutions (ES) flowing in the stack and the ionic flux generated by the salt gradients. Anion-exchange membranes (AMs) and cation-exchange membranes (CMs) are used to selectively drive the flow of positive ions to the right (toward the cathode) and the negatively charged ions to the left (toward the anode). The flow of these charged ions is converted in a flow of electrons at the electrodes that sustain the electro-generation of oxidants.

### 6.2.3 Analysis

The potential drop across a fixed external resistance and the current intensity were measured by a multimeter Simpson. The overall external resistance was given by the contribution of an external resistance (range 0.5–38.5 Ohm) and that of cables and an amperometer (with an estimated resistance of about 3.2 Ohm). Power was calculated by multiplying the electrical current and the total cell potential. Reported power and current densities were based on the cathode geometric area (100 cm<sup>2</sup>). To evaluate the formic acid concentration, Agilent HP 1100 HPLC fitted out with Rezex ROA-Organic Acid H+ (8%) column at 55°C and coupled with a UV detector (210 nm) was used; 0.005 N H<sub>2</sub>SO<sub>4</sub> water solution at solution pH 2.5 was eluted at 0.6 mL min<sup>-1</sup> as mobile phase. A pure standard of formic acid was adopted to calibrate the instrument for its quantitative determination. The total organic carbon (TOC) was analyzed by a TOC analyzer Shimadzu VCSN ASI TOC-5000 A.

The thermodynamic potential generated in the stack is given by Eq. 3-1.

The power density is given by Eq. 6-1:

$$P = \Delta E I / A \quad (6-1)$$

where  $\Delta E$  is the potential between external load resistance.  $I$  is the current intensity of the system.  $A$  is the electrode areas (0.01 m<sup>2</sup>).

The organic abatement is given by Eq. 6-2:

$$X = 100 (C_0 - C_t) / C_0 \quad (6-2)$$

where  $C_0$  is the initial concentrations of formic acid (mol L<sup>-1</sup>) inside the electrochemical cell and  $C_t$  is the concentrations of formic acid after electrolysis time  $t$ .

A calibration curve for the relationship between NaCl and conductivity in the solution was prepared (Appendix B). The concentration of NaCl was calculated by the standard curve by measuring the conductivity of the solution.

## 6.3 Results and discussion

### 6.3.1 Treatment of two wastewaters using their salinity gradient to drive the process

As described in detail in the previous section, the case study chosen for this study involved two synthetic wastewaters with a TOC concentration of 120 mg L<sup>-1</sup> and very different NaCl contents close to those reported for two industrial wastewaters produced during oil exploitation activities in the same site. An anodic and a cathodic process were used to remove organics for HC (HC<sub>an</sub>) and LC (LC<sub>cat</sub>), respectively:

- (i) the anodic process was based on the electro-generation of active chlorine by oxidation of chlorides at DSA anodes with the formation of free chlorine, hypochlorous acid and/or hypochlorite, depending on the pH (Eq. 6-3 and 4), that can oxidize the organics (Eq. 6-5).



In particular, according to the literature [3], HOCl is the main specie present in the solution for a pH between 2 and 7, as happened in our case.

- (ii) an electro-Fenton (EF) process was carried out in the cathode compartment. As reported in detail in 4.3.3, EF consists in the two-electron reduction at carbonaceous electrodes of oxygen to hydrogen peroxide that is converted in a strong oxidant, the hydroxyl radical, in the presence of catalytic amounts of iron (II) at a pH of 2–3 that

can effectively oxidize the organics[4].

As described in literature, iron specie can be complexed by  $\text{Cl}^-$  and/or  $\text{HO}\cdot$  and at pH higher than 3 the precipitation of  $\text{Fe}(\text{OH})_{3(s)}$  is expected [4]. The same HC and LC solutions were, in addition, delivered to the membrane pairs of the stack and named  $\text{HC}_{\text{stack}}$  and  $\text{LC}_{\text{stack}}$  with the aim to generate the cell potential necessary to drive redox processes.

The same HC and LC solutions were, in addition, delivered to the membrane pairs of the stack and named  $\text{HC}_{\text{stack}}$  and  $\text{LC}_{\text{stack}}$  with the aim to generate the cell potential necessary to drive redox processes.

In the first experiment, the external load resistance value was changed in the range of  $0.5\text{-}205\ \Omega$  (connected with adjustable resistor) and the external load resistance value was selected in order to obtain the maximum power density is selected. As shown in Fig. 6-4, the maximum power density was obtained at  $38.5\ \Omega$  external load resistance.

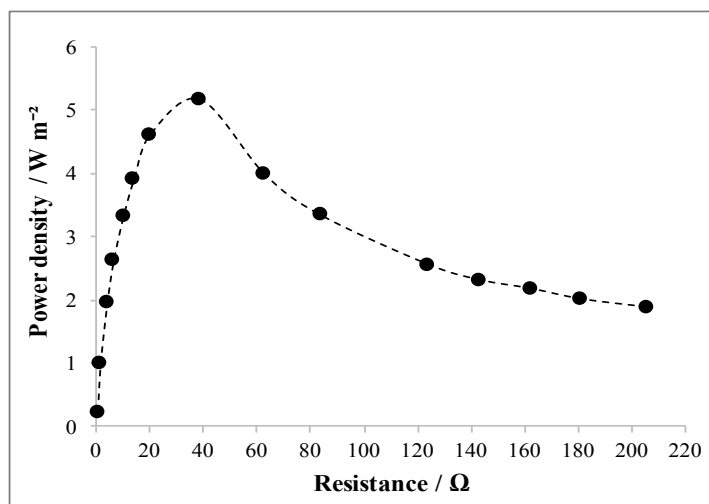


Fig. 6-4 Plot of power densities (computed as the ratio between the power and the geometric area of electrode) vs. external resistance varied between  $0.5\text{-}205\ \Omega$ .

The experiments were performed feeding HC ( $120\ \text{g L}^{-1}$ ) and LC ( $50\ \text{mg L}^{-1}$ ) solutions to the stack, equipped with 60 membrane pairs and an external resistance of  $38.5\ \text{Ohm}$ ,

to provide the salinity gradient; the solutions were continuously recirculated up to the end of the experiments. As shown in Fig. 6-5A, at the beginning of the experiment, a cell potential  $\Delta E$  close to 3 V and a current density  $i$  of about  $7.6 \text{ A m}^{-2}$  were achieved.  $\Delta E$  and  $i$  decreased with the time passed and reached after 5 h about 2.2 V and  $3.8 \text{ A m}^{-2}$ , respectively, because of the decrease of the salinity gradient (Fig. 6-5B). Indeed, when HC and LC solutions go through the stack, a small passage of NaCl from the concentrated solution to the diluted one occurs. Since HC and LC solutions are continuously recirculated to the stack, it leads to a progressive dilution of HC and to a concentration of LC with the time. Indeed, as shown in Fig. 6-5B, after 6 h the concentration of HC decreased from 120 to about  $114 \text{ g L}^{-1}$  while that of LC increased from  $50 \text{ mg L}^{-1}$  to about  $4.3 \text{ g L}^{-1}$ . Hence the salinity ratio  $[\text{NaCl}]_{\text{HC}}/[\text{NaCl}]_{\text{LC}}$  decreased from 2400 to about 27, due mainly to the increase of the concentration of NaCl in LC, causing the decrease of  $\Delta E$ .

As shown in Fig. 6-6, both solutions were effectively treated. Indeed, after 6 h, a removal of TOC was achieved in both anode and cathode compartments; in particular, after 6 h, the removal of TOC was more than 90% for anolyte and about 40% for catholyte.

Hence, these preliminary results allow to point out that the electrochemical treatment of two wastewater, contaminated by organic pollutants and characterized by very different salt contents, can be in principle achieved without energy inputs using the salinity gradient between the two wastewaters. However, the processes present two main drawbacks:

- i) while the removal of TOC was very fast in the anolyte (about 60% after 2 h), it was very slow in the catholyte (less than 10% after 2 h and about 40% after 4 h);
- ii) about 20 L of wastewater were used for both HC and LC fed to the stack to treat just 0.2 L in the electrode compartments: hence, only about 1% of the solution used in the stack was effectively treated. Furthermore,  $\text{HC}_{\text{stack}}$  and  $\text{LC}_{\text{stack}}$  presented at the end of the experiments a reduced salinity gradient that make them



less suitable to be again employed to treat other volumes of wastewater.

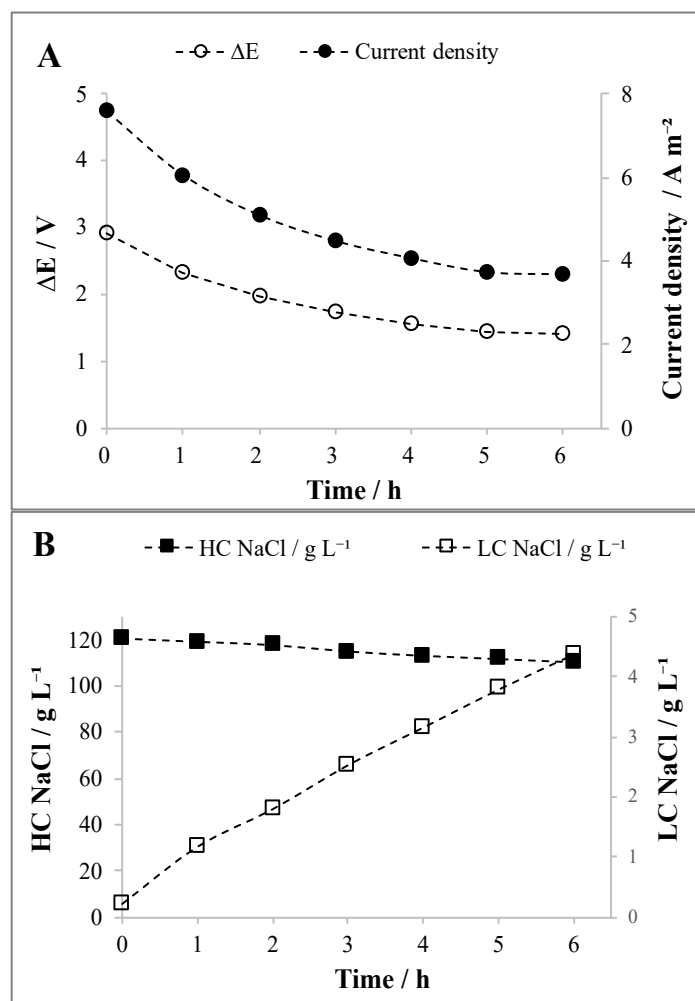


Fig. 6-5 The trend of  $\Delta E$  and  $i$  (A), of concentrations of NaCl in  $\text{HC}_{\text{stack}}$  and  $\text{LC}_{\text{stack}}$  (B) vs. time are reported. RED performed with HC (NaCl concentration  $120 \text{ g L}^{-1}$ ) and LC (NaCl concentration  $50 \text{ mg L}^{-1}$ ) fed to the stack (20 L each, flow rate  $260 \text{ mL min}^{-1}$ ), respectively, in the anode and cathode compartments (0.2 L each, flow rate  $200 \text{ mL min}^{-1}$ ). Number of membrane pairs 60, external resistance  $38.5 \text{ Oh}$ , carbon felt as cathode, DSA(Ti/RuO<sub>2</sub>-IrO<sub>2</sub>) as anode, Fe<sup>2+</sup> (0.05 mM) was added to the catholyte to catalyze EF.

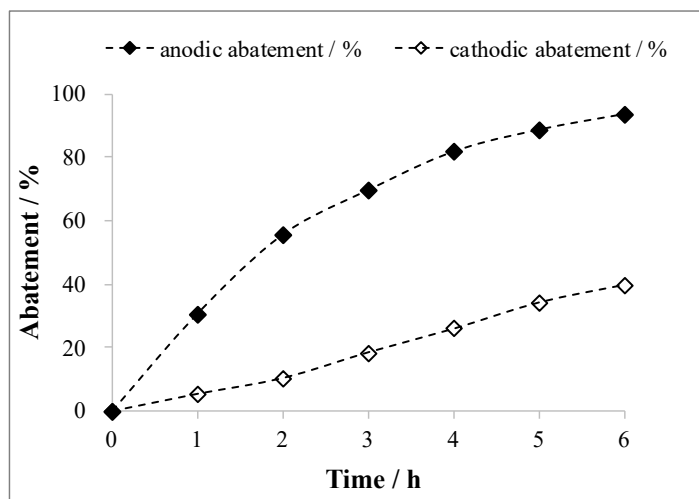


Fig. 6-6 The abatement of TOC in the catholyte and in the anolyte vs. time are reported. RED performed with HC (NaCl concentration  $120 \text{ g L}^{-1}$ ) and LC (NaCl concentration  $50 \text{ mg L}^{-1}$ ) fed to the stack (20 L each, flow rate  $260 \text{ mL min}^{-1}$ ), respectively, in the anode and cathode compartments (0.2 L each, flow rate  $200 \text{ mL min}^{-1}$ ). Number of membrane pairs 60, external resistance 38.5 Ohm, carbon felt as cathode, DSA(Ti/RuO<sub>2</sub>-IrO<sub>2</sub>) as anode, Fe<sup>2+</sup> (0.05 mM) was added to the catholyte to catalyze EF.

Hence, in order to solve or minimize these problems, a series of experiments was performed changing the operating conditions of the process.

### 6.3.2 Effect of external resistance

A series of experiments was carried out changing the external resistance  $R_e$  in the range 1.5 - 38.5 Ohm. As shown in Fig. 6-7, the decrease of  $R_e$  resulted, as expected, in a decrease of the initial value of  $\Delta E$  (from 3 V at 38.5 Ohm to 1.5 V at 10 Ohm) and to a correspondent increase of the initial  $i$  (from  $7.6 \text{ A m}^{-2}$  at 38.5 Ohm to  $15.1 \text{ A m}^{-2}$  at 10 Ohm).

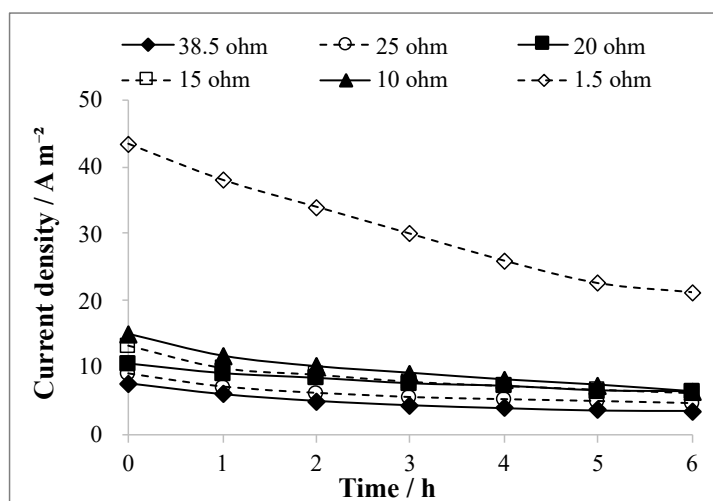


Fig. 6-7 Effect of external resistance  $R_e$  on the current density. RED performed with HC ( $\text{NaCl}$  concentration  $120 \text{ g L}^{-1}$ ) and LC ( $\text{NaCl}$  concentration  $50 \text{ mg L}^{-1}$ ) fed to the stack (20 L each, flow rate  $260 \text{ mL min}^{-1}$ ) and, respectively, in the anode and cathode compartments (0.2 L each, flow rate  $200 \text{ mL min}^{-1}$ ). Number of membrane pairs 60, carbon felt as cathode, DSA( $\text{Ti/RuO}_2\text{-IrO}_2$ ) as anode,  $\text{Fe}^{2+}$  ( $0.05 \text{ mM}$ ) was added to the catholyte to catalyze EF.

As shown in Fig. 6-8, the decrease of  $R_e$  and the corresponding increase of  $i$  gave rise to an increase of the TOC removal in the anodic compartment, due to the higher current density that speed up the generation of active chlorine at the anode. As an example, after 1 h the removal of TOC was 31%, 57% and 85% with 38.5, 10 and 1.5 Ohm, respectively. A more complex trend was observed for the abatement in the cathodic compartment. In this case, the removal of TOC increased lowering  $R_e$  from 38.5 to 20 Ohm and decreased for a further decrease of  $R_e$ . In particular, with  $R_e = 20 \text{ Ohm}$ , quite high abatements were achieved in both compartments at the end of the experiments (about 100% and 70% in the anode and cathode compartments, respectively). The presence of a maximum in the plot TOC removal vs.  $R_e$  for the cathodic compartment is due to the fact that, according to literature, EF process can be optimized at intermediate values of  $i$  [5].

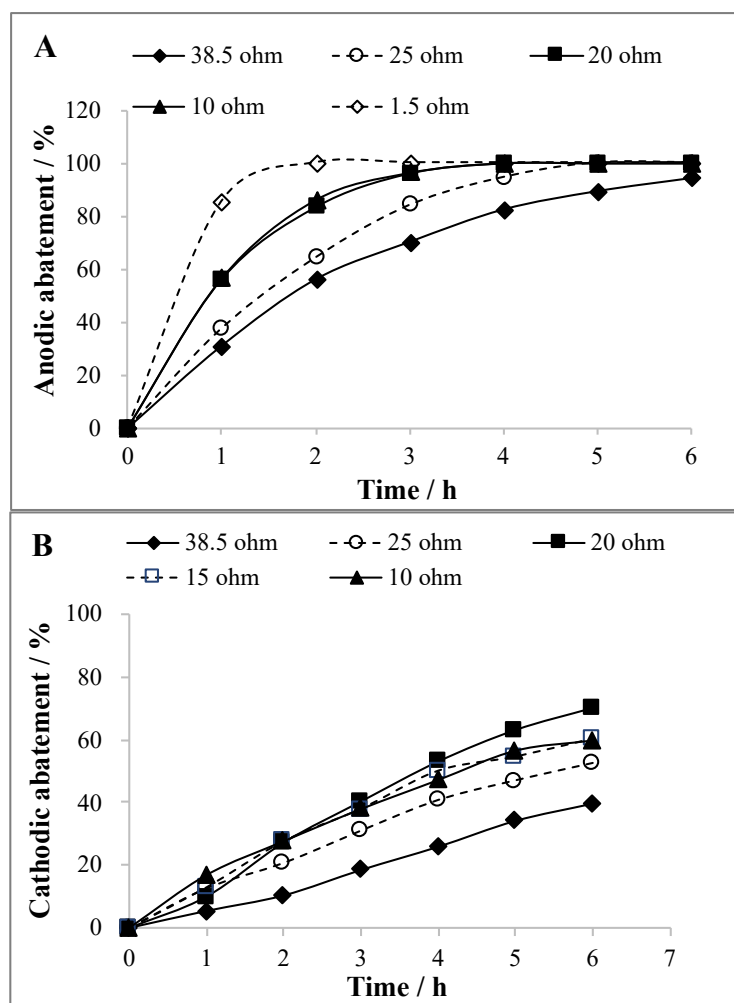


Fig. 6-8. Effect of external resistance  $R_e$  on abatement of TOC in the cathode (A) and in the anode (B) compartments. RED performed with HC (NaCl concentration  $120 \text{ g L}^{-1}$ ) and LC (NaCl concentration  $50 \text{ mg L}^{-1}$ ) fed to the stack (20 L each, flow rate  $260 \text{ mL min}^{-1}$ ) and, respectively, in the anode and cathode compartments (0.2 L each, flow rate  $200 \text{ mL min}^{-1}$ ). Number of membrane pairs 60, carbon felt as cathode, DSA(Ti/RuO<sub>2</sub>-IrO<sub>2</sub>) as anode, Fe<sup>2+</sup> (0.05 mM) was added to the catholyte to catalyze EF.

### 6.3.3 Optimization of the process

As above mentioned, only about 1% of the wastewaters used in the stack was effectively treated. In addition,  $HC_{\text{stack}}$  and  $LC_{\text{stack}}$  at the end of the experiments presented a reduced salinity gradient that make them less suitable to be again employed to treat other volumes of wastewater. It was also observed that  $HC_{\text{stack}}$  at the end of the test had

an increased volume, while  $LC_{\text{stack}}$  had a decreased volume due to a spontaneous passage of water caused by the salinity gradient (about 0.3 L of passage from  $LC_{\text{stack}}$  to  $HC_{\text{stack}}$ , each hour, corresponding to about 1.5% of the total volume). Hence, the system was changed in order to increase the ratio between the treated wastewater and the wastewater used in the stack to deliver the salinity gradient and trying to maintain stable conditions with the time passed (in terms of salinity gradient and current density). In particular, we decided to focus only to the treatment of HC wastewater by anodic process, by considering to use the LC solution only to provide the salinity gradient. Hence, we focused to the ratio between the volumes of  $HC_{\text{an}}$  and  $HC_{\text{stack}}$  (named  $HC_{\text{treat}}/HC_{\text{stack}}$ ). Among the various approach tested, a promising solution is illustrated in Fig. 6-9 and described in the following:

- at the beginning of the test, HC and LC were sent to the stack and, respectively, to the anodic and cathodic compartments with the main aim to optimize the treating of  $HC_{\text{an}}$  and to use  $LC_{\text{cat}}$  just to provide a cathodic redox process; hence, the operative conditions were selected to speed up the anodic treatment in order to achieve a high removal of organic contents in 1 h;
- after 1h, a part of  $HC_{\text{stack}}$  was withdrawn (about 0.3 L) in order to recover its initial volume (20 L) and a part of the withdrawn solution (0.2 L) was sent to the anodic compartment to replace the solution treated in the first hour; in addition,  $LC_{\text{stack}}$  solution was partially substituted with fresh one, in order to restore its initial volume and increase its salinity content;
- the operations carried out after 1h, were repeated each hour. In particular  $LC_{\text{stack}}$  solution was partially substituted with fresh one, in order to restore its initial volume and obtain an almost stable salinity content under steady-state conditions.

This approach (described in Fig. 6-9) allowed to achieve a good stability of operating conditions after a transitory stage (about 4 h) for all the monitored time (tests were carried out for 10 h).

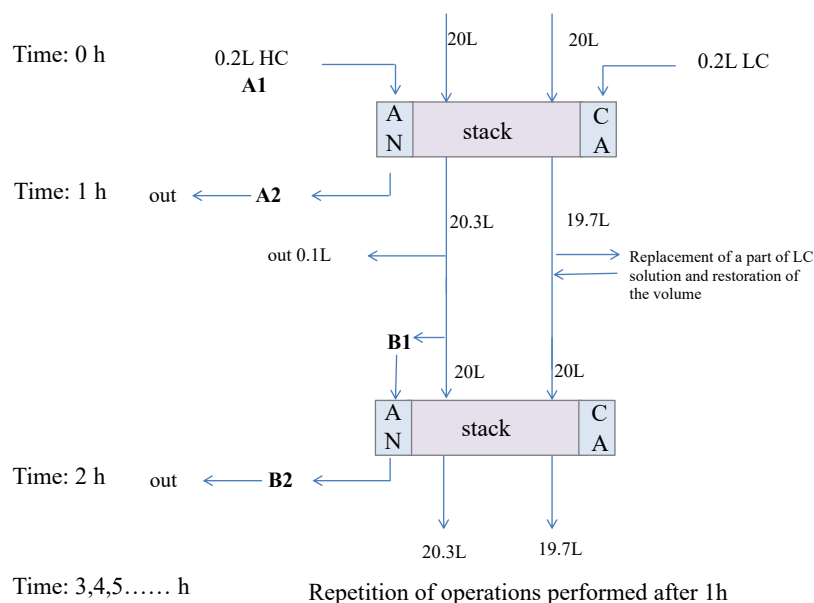


Fig. 6-9 Scheme of the process. RED performed with HC (NaCl concentration  $120 \text{ g L}^{-1}$ ) and LC (NaCl concentration  $50 \text{ mg L}^{-1}$ ) fed to the stack (20 L each, flow rate  $260 \text{ mL min}^{-1}$ ) and, respectively, in the anode and cathode compartments (0.2 L each, flow rate  $200 \text{ mL min}^{-1}$ ). Number of membrane pairs 60, carbon felt as cathode, DSA(Ti/RuO<sub>2</sub>-IrO<sub>2</sub>) as anode, Fe<sup>2+</sup> (0.05 mM) was added to the catholyte to catalyze EF, Re = 3.7 Ohm.

Indeed, as shown in Fig. 6-10A, a quite good and constant value of the abatement of TOC was achieved ( $\sim 70\%$ ), coupled with an almost constant plateau value of both the current density ( $\sim 10 \text{ A m}^{-2}$ ) and salinity gradient ( $\sim 77$ ) (see Fig. 6-10B). It is worth to mention that the abatement of formic acid was quite good if compared with other results reported in literature for its anodic oxidation in undivided cells provided with DSA or boron doped diamond anodes [6]. It is relevant to observe that under adopted operating conditions,  $\text{HC}_{\text{treat}}/\text{HC}_{\text{stack}}$  is close to 67% under steady-state conditions vs. the 1% obtained in preliminary experiments reported in the previous paragraphs. In additions, even if LC solution was used only to provide the salinity gradient, also a slow removal of TOC was obtained for it (about 70% after 8 h).

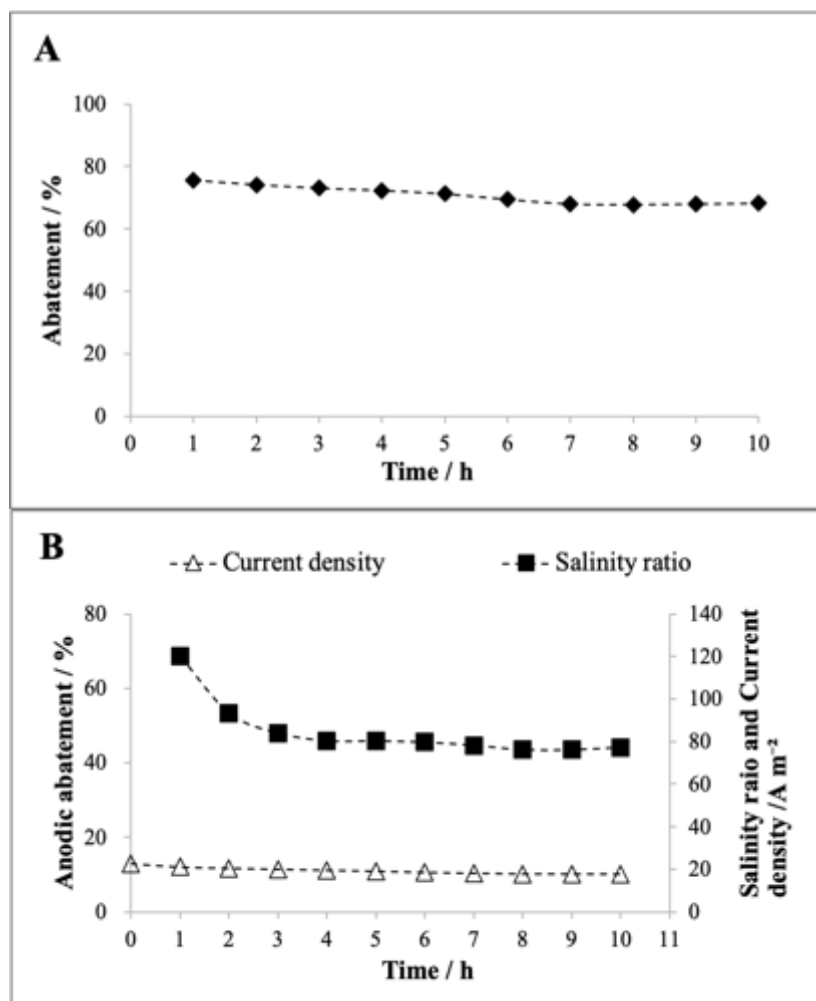


Fig. 6-10 The trend of abatement of TOC(A) in the anodic compartment, salinity ratio and current density (B) vs. time. RED performed with HC (NaCl concentration  $120 \text{ g L}^{-1}$ ) and LC (NaCl concentration  $50 \text{ mg L}^{-1}$ ) fed to the stack ( $20 \text{ L}$  each, flow rate  $260 \text{ mL min}^{-1}$ ) and, respectively, in the anode and cathode compartments ( $0.2 \text{ L}$  each, flow rate  $200 \text{ mL min}^{-1}$ ). Process performed according to the approach described in Fig. 6-9. Number of membrane pairs 60, carbon felt as cathode, DSA(Ti/RuO<sub>2</sub>-IrO<sub>2</sub>) as anode, Fe<sup>2+</sup> ( $0.05 \text{ mM}$ ) was added to the catholyte to catalyze EF,  $\text{Re} = 3.7 \text{ Ohm}$ .

### 6.3.4 Effect of the salinity ratio

Above mentioned experiments were performed using synthetic wastewaters with a quite high salinity gradient similar to some wastewater previously described in literature [2]. In order to evaluate the extendibility of the proposed approach to other wastewater

characterized by different salinity gradients, experiments were repeated with various values of the initial salinity ratio  $SR_{in}$ . In particular, a fixed HC solution was used (NaCl concentration  $143 \text{ g L}^{-1}$ ), while the concentration of NaCl in LC was changed in the range  $78 \text{ mg L}^{-1} - 16 \text{ g L}^{-1}$ , in order to have a huge range of  $SR_{in}$  (9 - 1860). The same approach described in the previous paragraph and in Fig. 6-9 was used for all these tests.

As shown in Fig. 6-11, the power generation of RED system decreased rapidly with the decrease of the SR. When the SR were 1860, 55, 18, 8, the maximum power density generated by the system were about 8.8, 5.4, 2.2 and  $0.32 \text{ W m}^{-2}$  respectively, and the maximum current intensity were also greatly reduced.

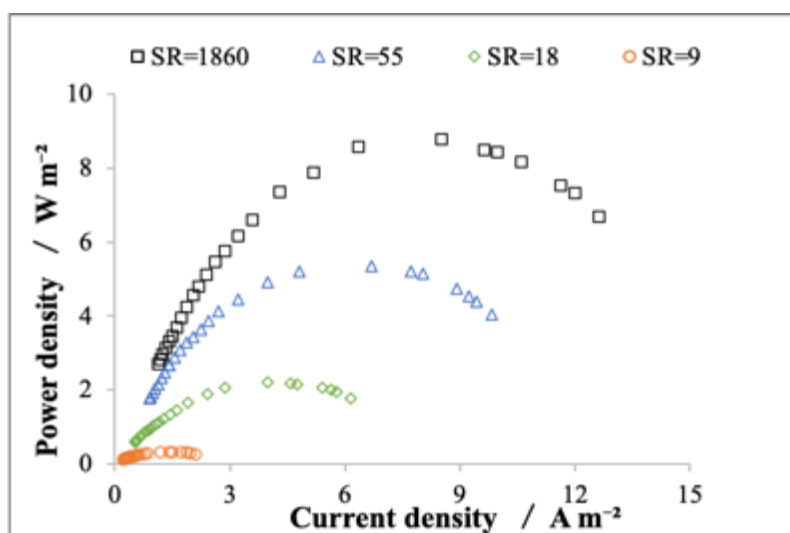


Fig. 6-11 Plot of power density vs. current density varied between  $0.5\text{-}205 \text{ }\Omega$  resistance vs. time recording a stack equipped 60 cell pairs of membranes and running in sequence with different NaCl concentration ( $78.77 \text{ mg L}^{-1}$ ,  $2.6$ ,  $8$ ,  $16 \text{ g L}^{-1}$ ) in LC. ( $143 \text{ g L}^{-1}$  NaCl in concentrated solution, external resistance  $3.7 \text{ Ohm}$ , carbon felt as cathode, DSA(Ti/RuO<sub>2</sub>-IrO<sub>2</sub>) as anode, electrode area  $100 \text{ cm}^2$ ,  $0.5 \text{ mM Fe}^{2+}$  (pH<3) in cathodic chamber).

As shown in Fig. 6-12, quite stable conditions were obtained in all the tests showing that the approach presented in the previous paragraph can allow to operate with almost constant values salinity ratio (Fig. 6-12A) and current density (Fig. 6-12B) for various values of the initial SR.



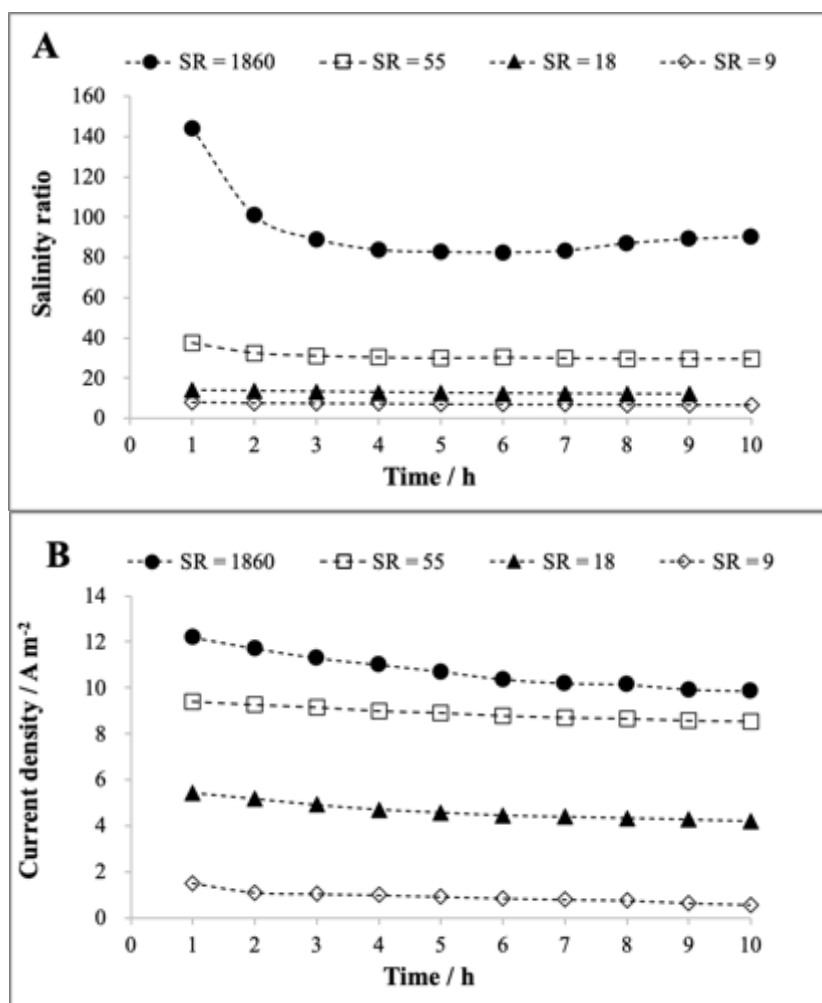


Fig. 6-12 Effect of the  $SR_m$  on SR trend (A) and current density (B) vs. time passed. RED performed with HC (NaCl concentration  $143 \text{ g L}^{-1}$ ) and various LC (NaCl concentration  $78 \text{ mg L}^{-1}$  and  $2.6, 8$  and  $16 \text{ g L}^{-1}$ ) fed to the stack ( $20 \text{ L}$  each, flow rate  $200 \text{ mL min}^{-1}$ ) and, respectively, to the anode and cathode compartments ( $0.2 \text{ L}$  each, flow rate  $200 \text{ mL min}^{-1}$ ). Process performed according to the approach described in Fig. 6-9. Number of membrane pairs 60, carbon felt as cathode, DSA (Ti/RuO<sub>2</sub>-IrO<sub>2</sub>) as anode, Fe<sup>2+</sup> ( $0.05 \text{ mM}$ ) was added to the catholyte to catalyze EF,  $R_e = 3.7 \text{ Ohm}$ .

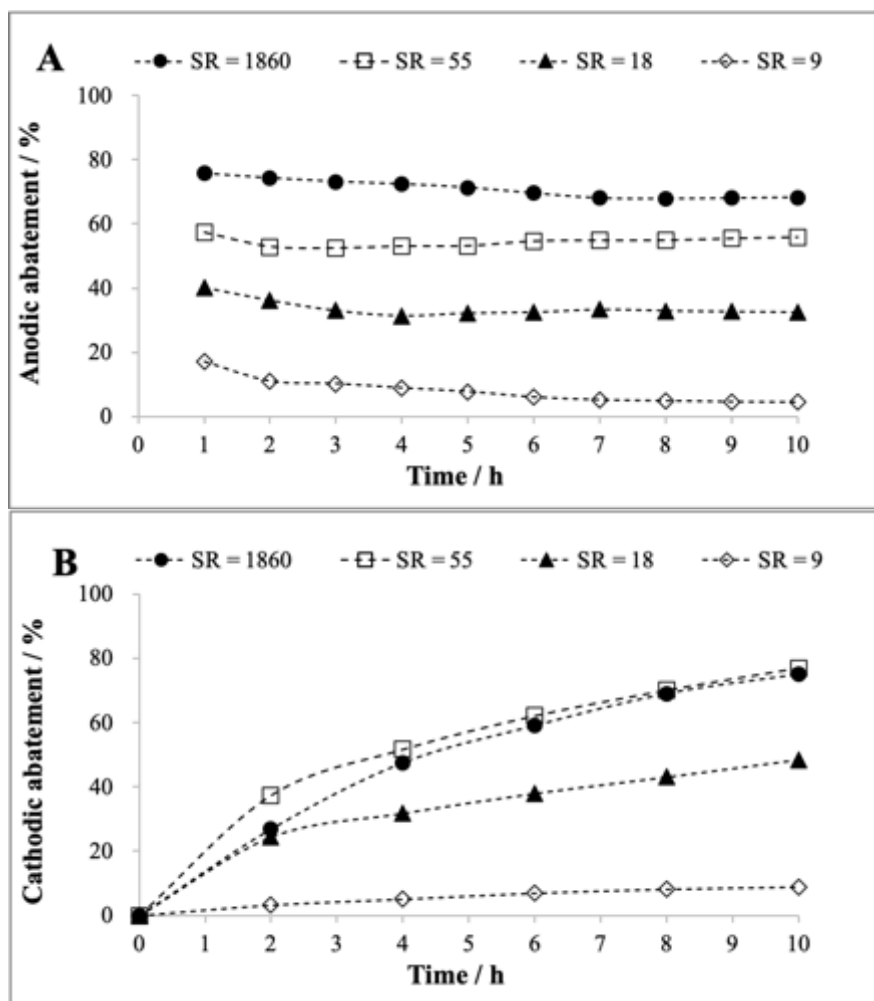


Fig. 6-13 Effect of the  $SR_{in}$  on the anodic removal of TOC (A), and cathodic removal of TOC (B) vs. time passed. RED performed with HC (NaCl concentration  $143 \text{ g L}^{-1}$ ) and various LC (NaCl concentration  $78 \text{ mg L}^{-1}$  and  $2.6, 8$  and  $16 \text{ g L}^{-1}$ ) fed to the stack ( $20 \text{ L}$  each, flow rate  $200 \text{ mL min}^{-1}$ ) and, respectively, to the anode and cathode compartments ( $0.2 \text{ L}$  each, flow rate  $200 \text{ mL min}^{-1}$ ). Process performed according to the approach described in Fig. 6-9. Number of membrane pairs 60, carbon felt as cathode, DSA ( $\text{Ti/RuO}_2\text{-IrO}_2$ ) as anode,  $\text{Fe}^{2+}$  ( $0.05 \text{ mM}$ ) was added to the catholyte to catalyze EF,  $Re = 3.7 \text{ Ohm}$ .

However, the removal of TOC strongly depended on the salinity ratio. As an example, as shown in Fig. 6-13A, for the highest  $SR_{in}$  the anodic abatement achieved every hour was close to 70% while it decreased to about 55% for  $SR_{in} = 55$ , to 33% for  $SR_{in} = 18$  and to about 5% for  $SR_{in} = 9$ . The lower removal of TOC achieved decreasing  $SR_{in}$  was due to the lower current densities. Indeed,  $i$  decreased from about 10 to 8.6, 4.4 and  $< 1 \text{ A m}^{-2}$  for initial  $SR$  1860, 55, 18 and 9. In particular, for  $SR_{in}$  of 9, the removal of TOC was

too low and, consequently, the process seems less feasible from an applicative point of view. However, for the other adopted  $SR_{in}$  the process seems feasible, even if lower  $SR_{in}$  imposes or lower removal of TOC or longer treatment times. Fig. 6-13B reports the removal of TOC for the cathodic compartment; very high removal were obtained at long times when  $SR_{in}$  were 1850 and 55.

### 6.3.5 Energy consumption assessment with 1 membrane system

A cell with an ion exchange membrane was assembled. The potentiostat was connected to add electric energy to the system. As shown in Fig. 6-14, adding 2 V applied voltage, the corresponding current density was about  $40 \text{ Am}^{-2}$ . 34%, 57%, 78% and 85% abatements were obtained after 1, 2, 3, 4 h electrolysis, respectively.

As shown in Table 6-3, formic acid removal in the anodic compartment and energy consumption of 60 cell pairs of membranes and single membrane systems were compared. In the RED system (60 cell pairs of membrane), 68%, 55%, 34% and 8% TOC abatements were obtained when the SR was 1860, 55, 18, 9, respectively, and corresponding energy consumption were 0. While using a single membrane system and the external electric energy, the TOC abatement was 34%, 57%, 78% and 85%, corresponding to 0.1, 0.11, 0.12, 0.15  $\text{kW}\cdot\text{h g TOC}^{-1}$  and 2.1, 4, 5.85, 7.8  $\text{kW}\cdot\text{h m}^{-3}$ , respectively.

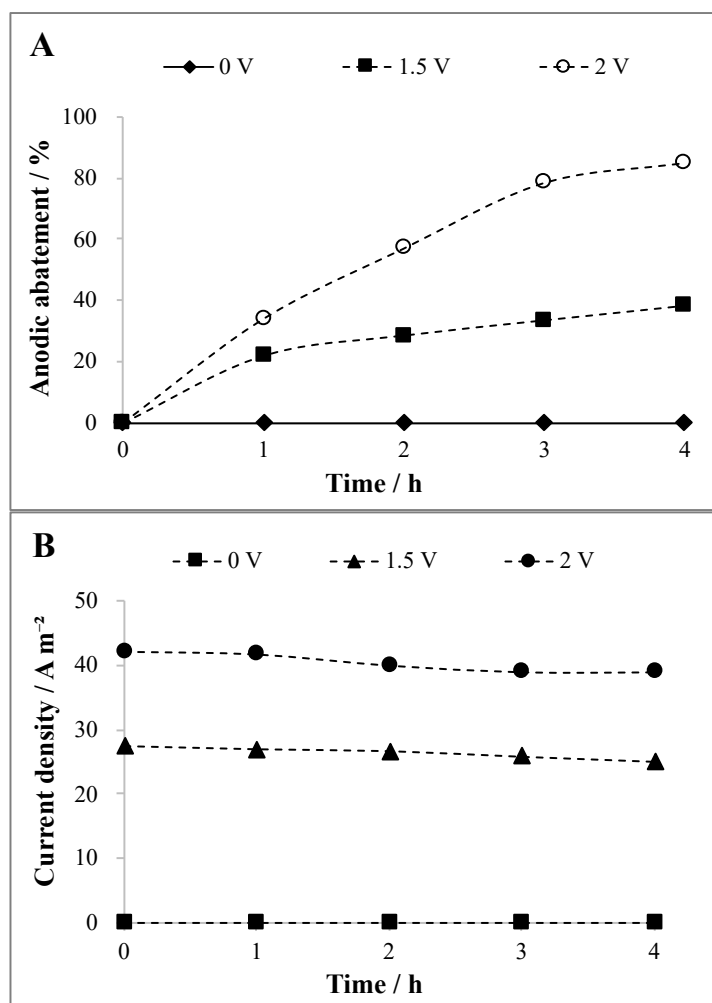


Fig. 6-14 The (A) anodic abatement of formic acid and (B) current density and vs. time and external potential with 1 membrane (143 g L<sup>-1</sup> NaCl in the solution, carbon felt as cathode, DSA(Ti/RuO<sub>2</sub>-IrO<sub>2</sub>) as anode, electrode area 100 cm<sup>2</sup>, 0.5 mM Fe<sup>2+</sup> (pH<3) in cathodic chamber).

Table 6-3 Technological and economic comparison for treating high NaCl containing formic acid wastewater with 60 cell pairs of membranes and 1 membrane

membrane	HC	LC	SR	abatement / %	energy consumption	
	(g L <sup>-1</sup> NaCl)	(g L <sup>-1</sup> NaCl)			kW·h gTOC <sup>-1</sup>	kW·h m <sup>-3</sup>
60 cell pairs of membrane	143	0.07877	1860	68	0	0
	143	2.6	55	55	0	0
	143	8	18	34	0	0
	143	16	9	8	0	0
1 membrane	143	143	1	34	0.1	2.1
				57	0.11	4
				78	0.12	5.85
				85	0.15	7.8

## 6.4 Summary

It was shown for the first time that two synthetic wastewaters with different NaCl concentration can be used in a RED system to drive anodic and cathodic processes for the removal of their organic contents. The main results achieved in the work are reported below.

- 1) The two synthetic wastewaters used to feed the salinity gradient to the stack were treated in the anodic compartment by electro-generated chlorine and in the cathodic one by electro-Fenton process. The anodic compartment was used for the waster with high NaCl content and the cathodic one for that with low NaCl concentration. A good removal of TOC was achieved for both compartments.
- 2) The decrease of the external resistance allowed to increase the current density and to achieve a very high removal of TOC in the anodic compartment in short times.
- 3) It was shown that the rate of removal of organics strongly depends on the salinity gradient between the two waters.
- 4) It was possible to develop a set-up that gives continuous and stable operations with the time that allows to treat about 2/3 of one of the two wastewaters used to provide the salinity gradient.

Further studies will be necessary for the optimization of the method. In particular, the utilization of real wastewaters will be useful for a fully evaluation of the proposed approach.

## 6.5 References

- [1] Saleem M W, Jande Y A C, Kim W S. Performance optimization of integrated electrochemical capacitive deionization and reverse electrodialysis model through a series pass desorption process. *Journal of Electroanalytical Chemistry*, 2017, 795: 41–50.
- [2] Da Silva A J C, dos Santos E V, de Oliveira Morais C C, et al. Electrochemical treatment of fresh, brine and saline produced water generated by petrochemical industry using Ti/IrO<sub>2</sub>-Ta<sub>2</sub>O<sub>5</sub> and BDD in flow reactor. *Chemical Engineering Journal*, 2013, 233: 47–55.
- [3] Deborde M, Von Gunten U. Reactions of chlorine with inorganic and organic compounds during water treatment kinetics and mechanism: a critical review. *Water Research*. 2008, 42:13-51.
- [4] Martínez-Huitle C A, Ferro, S. Electrochemical oxidation of organic pollutants for the wastewater treatment: direct and indirect processes. *Chemical Society Review*. 2006, 35: 1324-1340.
- [5] Scialdone O, Albanese A, D'Angelo, et al. Investigation of electrode material e redox couple systems for reverse electrodialysis processes. Part II: experiments in a stack with 10-50 cell pairs. *Journal of Electroanalytical Chemistry*, 2013, 704: 1-9.
- [6] Scialdone O, Galia A, Randazzo S. Oxidation of carboxylic acids in water at IrO<sub>2</sub>-Ta<sub>2</sub>O<sub>5</sub> and boron doped diamond anodes. *Chemical Engineering Journal*, 2011, 174: 266-274.

---

## **Chapter 7. First utilization of Assisted Reverse Electrodialysis for CO<sub>2</sub> electrochemical conversion and treatment of wastewater**

### **7.1 Introduction**

In recent years, some authors have proposed to use salinity gradients to sustain redox processes for the synthesis of chemical or the treatment of wastewater adopting RED stacks assembled with relatively few membrane pairs and salinity gradients available in nature or in industrial plants, thus saving the electric energy necessary for conventional electrolysis processes. In particular, some groups have shown that it is possible to use river, seawater and/or brine solutions to treat various kinds of wastewater both in lab-scale devices and in a pilot-plant scale, while others have shown that RED can be used for the generation of hydrogen using both natural salinity gradients and thermolytic solutions regenerated by waste heat [1-6]. In the previous chapter, it has been observed that plants devoted to the treatment of industrial wastewater deal often with waters characterized by different salinity and the relative salinity gradient can be used to depurate part of these wastewaters by RED, allowing potentially a huge saving of energy.

However, the development of redox processes driven by salinity gradients is strongly limited, in order to use not too large and too expensively RED stacks, to cases where small cell potentials are required and large salinity gradients are available, thus not allowing to exploit the energy present in waters with limited salinity gradients or to help processes that require high cell potentials. In this context, we have studied for the first time the utilization of assisted reverse electrodialysis (A-RED) in order to use a larger range of salinity gradients to sustain electrolysis processes characterized also by high cell potentials.

In A-RED, an external current is applied in the direction of the diffusional transport of ions which follows chemical potential gradients, thus allowing to couple the external electric energy and the energy coming from salinity gradient [7]. A-RED, which was

successfully proposed up to now only for desalination process, can be potentially used to decrease the required membrane area and/or to use lower salinity gradients and/or to achieve high overall cell potentials for the electrochemical synthesis of a large range of products. Furthermore, from a theoretical point of view, the system is expected to perform better than just the combination of electric and electrochemical driving forces. In particular, the utilization of A-RED was proposed and successfully used for the first time for two very different purposes: (i) the treatment of synthetic wastewater contaminated by organics; (ii) the conversion of carbon dioxide to high added value products. These processes were chosen as particularly promising examples, since an improvement of economics is necessary for the passage on an applicative scale, which could potentially be achieved using salinity gradients available in industrial plants.

## 7.2 Experimental

### 7.2.1 Experimental materials and reactor

#### a) Reagents

Table 7-1. Main reagents

Reagents	Standards	Company
HNO <sub>3</sub>	analytical	Romil
air	99.999% purity	Rivoira

Other reagents are the same as Table 6-1.

#### b) Reactor

The reactor is the same as 6.2.2. The stack was connected with a fixed external resistance (0.3 or 3.7 ohm) and a potentiostat (Amel 2053 potentiostat/galvanostat) which can supply the electricity energy and record the voltage and current intensity. In addition,



in order to evaluate the energy consumption saved by RED system, some electrolyses were repeated in the same stack described above with the same apparatus but using the same solutions in HC and LC or with just 1 membrane. The two electrode chambers (10 cm × 10 cm × 2 mm) contained a Tin foil cathode, (1.0 mm thick, assay > 99%, metals basis, was used for experiments devoted to conversion of carbon dioxide and treatment of wastewater, respectively) and a titanium meshes coated with Ru–Ir anode (geometric surface area 10 cm × 10 cm).

Table 7-2 Electrode tested during the lab experiments

Name	Company
Tin foil	CARLO ERBA Reagents S.r.l..Italy

Others the same as Table 6-2.

## 7.2.2 Methods

The schematically shown in Fig. 7-1. Synthetic wastewaters were prepared dissolving NaCl and formic acid (120 mg L<sup>-1</sup>) into deionized water (lab-utility, conductivity < 0.5 μS cm<sup>-1</sup>). Formic acid was chosen as organic model compound, according to the literature, since carboxylic acids are rather resistant to oxidation by electrochemical methods. For experiments devoted to the anodic treatment of synthetic wastewater, solutions used in HC and LC compartments were prepared by dissolving NaCl (143 g L<sup>-1</sup> in HC and 16, 32, 64 and 143 g L<sup>-1</sup> in LC) into deionized water. LC solution was sent also to the cathodic compartment. For experiments devoted to the conversion of CO<sub>2</sub> to HCOOH, solutions used in HC and LC compartments were prepared by dissolving NaCl (150 g L<sup>-1</sup> in HC and 0.05, 0.5 and 150 g L<sup>-1</sup> in LC) into deionized water. HC solutions was sent also to the anodic compartment. Cathodic solution contained 0.1 M Na<sub>2</sub>SO<sub>4</sub> as supporting electrolyte at a solution pH = 4 and was fed with 0.25 L min<sup>-1</sup> CO<sub>2</sub>. H<sub>2</sub>SO<sub>4</sub> was used to set the pH, measured with a HANA pH-meter. Before each experiment, tin foil was subjected to mechanically smoothing treatment, chemically treated with 11%vol HNO<sub>3</sub> (HNO<sub>3</sub>, Assay

67%-69%.) water solution for 2 min and washed with an ultrasound bath in deionized water for 5 min. In addition, the cathodic electrolytic solution was fed with air or CO<sub>2</sub> for experiments devoted to the anodic treatment of synthetic wastewater or the conversion of CO<sub>2</sub>, respectively.

For each tested operative condition, at least 2 experiments were performed to be sure that reproducible results were achieved with a difference between the results lower than 5%.

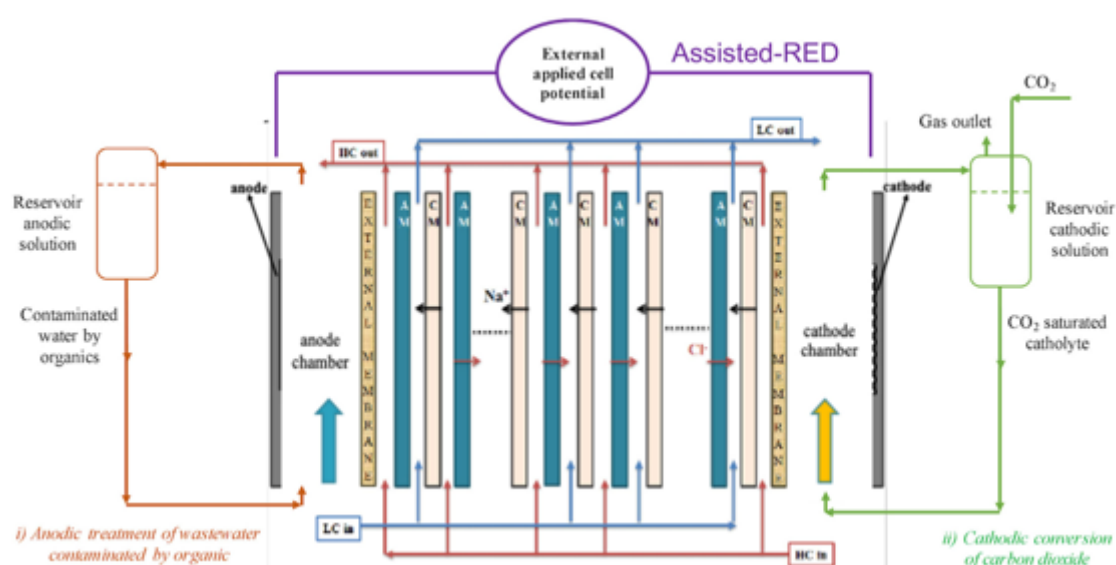


Fig. 7-1 Schematic representation of a RED stack showing cationic (CM), anionic (AM) and external membranes, electrodes, electrode chambers and concentrated (HC), diluted (LC) and electrode solutions (ES) flowing in the stack and the ionic flux generated by the salt gradients. Assisted-RED process is carried out by applying an external additional cell potential between the two electrodes in the direction of the diffusional transport of ions (purple circuit); RED process is performed without any external additional cell potential. i) The orange circuit refers to the anodic treatment of wastewater contaminated by organics; ii) the green circuit is related to the cathodic conversion of CO<sub>2</sub> (in this case CO<sub>2</sub> was bubbled in the reservoir electrolyte tank and continuously recirculated to the cathodic compartment).

### 7.2.3 Analysis

The potential drop across a fixed external resistance and the current intensity were measured by a multimeter Simpson. The overall external resistance was given by the contribution of an external resistance (range 0.5–38.5 Ohm) and that of cables and an amperometer (with an estimated resistance of about 3.2 Ohm). Power was calculated by multiplying the electrical current and the total cell potential. Reported power and current densities were based on the cathode geometric area (100 cm<sup>2</sup>). To evaluate the formic acid concentration, Agilent HP 1100 HPLC fitted out with Rezex ROA-Organic Acid H<sup>+</sup> (8%) column at 55°C and coupled with a UV detector (210 nm) was used; 0.005 N H<sub>2</sub>SO<sub>4</sub> water solution at solution pH 2.5 was eluted at 0.6 mL min<sup>-1</sup> as mobile phase. A pure standard of formic acid was adopted to calibrate the instrument for its quantitative determination. The total organic carbon (TOC) was analyzed by a TOC analyzer Shimadzu VCSN ASI TOC-5000 A.

The organic abatement (X) was defined by Eq. 6-3:

## 7.3 Results and discussion

### 7.3.1 Anodic treatment of synthetic wastewater

The first case-study involved the anodic treatment of a synthetic wastewater with an initial TOC content of 120 mg L<sup>-1</sup> with the aim of reducing its TOC content. The process is based on (i) the anodic oxidation of organics at the anode and (ii) above all on the electro-generation of active chlorine by oxidation of chlorides at dimensional stable anodes that results, for solution pH between 2 and 7, mainly in the formation of hypochlorous acid (Eqs. 6-3~5), that is able to oxidize organics (Eq. 6-6).

E° for chlorides reduction to chlorine is 1.36 V vs. SHE and a small overpotential is expected at adopted Ru based anodes. At the cathode, for small current densities, the

reduction of oxygen solubilized in water is expected (working potential between -0.2 and -0.4 V at carbonaceous cathodes) while for high currents, when the oxygen reduction becomes limited by mass transfer, the hydrogen evolution takes place needing larger potentials. A series of RED, electrolysis and A-RED experiments were performed for 3 h changing both the salinity gradient and the external applied cell potential in order to evaluate for the first time the utilization of A-RED for the treatment of wastewater contaminated by organics and to compare its performances with that of RED and electrolysis. The removal of TOC and the energetic consumption related to the external applied cell potential were recorded in order to evaluate the performances of the process. First, RED experiments were carried out (without external supply of cell potential). In the absence of salinity gradient, neither current nor abatement of TOC were observed, thus showing that no mineralization is achieved without the activation of the anodic redox process. In the presence of salinity gradients, a current density is observed, thus allowing the oxidation of formic acid and the reduction of TOC. Indeed, the presence of the salinity gradient in a stack assembly of N membrane pairs results in an electromotive force E given by Eq. 7-1:

$$E = 2N a R T \ln (SR) / F \quad (7-1)$$

where R is the gas constant, T the absolute temperature, a is the average permselectivity of the membrane pair, SR is the ratio between the solute activities in concentrated and diluted solutions, respectively, and F the Faraday constant.

In particular, for  $SR = 9$ , an initial current density close to  $9 \text{ A m}^{-2}$  and a high removal of TOC was achieved, which reached 90% after 3 h. For lower SR, both the current density and the removal of TOC decreased (Fig. 7-2A). As an example, the initial current density decreased from about 9 to  $3 \text{ A m}^{-2}$ , when the SR decreased from 9 to 4.4. Indeed, according to Eq. 7-1, a decrease of the SR results in a lower electromotive force and, as a consequence, in lower current densities. In particular, the removal of TOC for  $SR = 2.2$  was very low (about 10% after 3 h), thus showing that this low salinity gradient is not sufficient for the effective treatment of the synthetic wastewater in the adopted stack.

Fig. 7-2B reports some electrolyses carried out in the same stack without salinity gradient (SR = 1), supplying different cell potentials (1.5, 2.0 and 2.5 V) for 3 h by a potentiostat. For an applied cell potential of 2.5 V, a quite high abatement close to 80% was observed after 3 h, but a relatively high energetic consumption was necessary ( $0.28 \text{ kW}\cdot\text{h gTOC}^{-1}$ ). At 2.0 V the final abatement was still quite good (about 70% with an energetic consumption of  $0.21 \text{ kW}\cdot\text{h gTOC}^{-1}$ ); conversely, when the cell potential was decreased to 1.5 V, the removal of TOC was quite low (33%), showing that this cell potential is not high enough to provide an effective mineralization of organics.

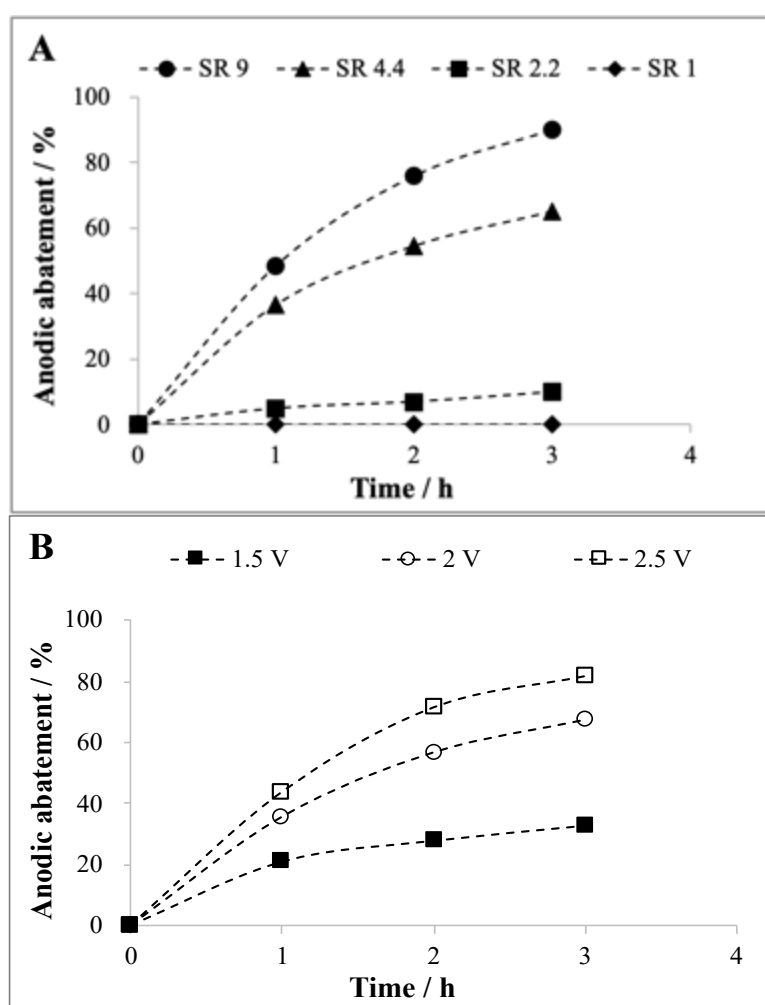


Fig. 7-2 Removal of TOC in the anodic compartment achieved by RED (2A) or electrolysis (2B). RED was performed with SR = 9, 4.4, 2.2 and 1.0. Number of membrane pairs 60. Electrolyses were performed in the same stack at different cell potentials (1.5, 2.0 and 2.5 V with SR = 1).

Fig. 7-3 reports the results achieved by A-RED, performing a series of experiments with different salinity gradients (2.2, 4.4 and 9) and external cell potentials supplied by the potentiostat. Hence, in this case, an external current is applied in the direction of the diffusional transport of ions which follows chemical potential gradients, thus allowing to couple the external electric energy and the energy coming from salinity gradient. In particular, an external cell potential of 1.0 or 1.5 V, insufficient to sustain effectively the standalone electrolytic process, was provided to the stack by the potentiostat.

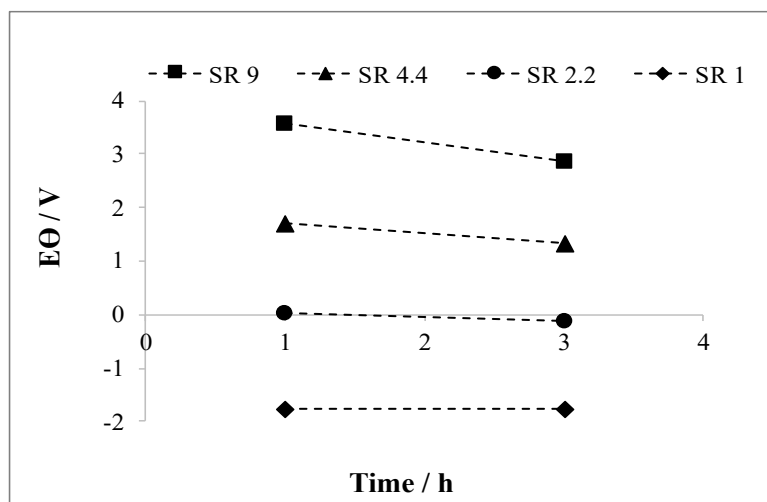


Fig. 7-3 Theory potential obtained by Eq. 5-1. RED was performed with SR = 9, 4.4, 2.2 and 1.0. Number of membrane pairs 60. Electrolyses were performed in the same stack at different cell potentials (1.5, 2.0 and 2.5 V with SR = 1).

Fig. 7-4A and 4B show that, for both 1 and 1.5 V, the enhancement of the salinity ratio resulted in an increase of the abatement of TOC for any value of the time passed. At 1.0 V, the presence of a salinity gradient allowed a significant removal of TOC (Fig. 7-4A). Very good abatements of TOC were achieved after 3 h with SR = 9 (abatement close to 95%) and 4.4 (abatement close to 85%). It is worth to mention that the coupling of a low SR of 2.2 and of a low cell potential of 1.0 V, that gave quite low abatements (< 10%), respectively, in RED (Fig. 7-2A) and in electrolysis (Fig. 7-2B) standalone processes, allowed to obtain an abatement close to 50% by A-RED (Fig. 7-4A), thus showing the potential synergy of salinity gradient and external supply of energy.

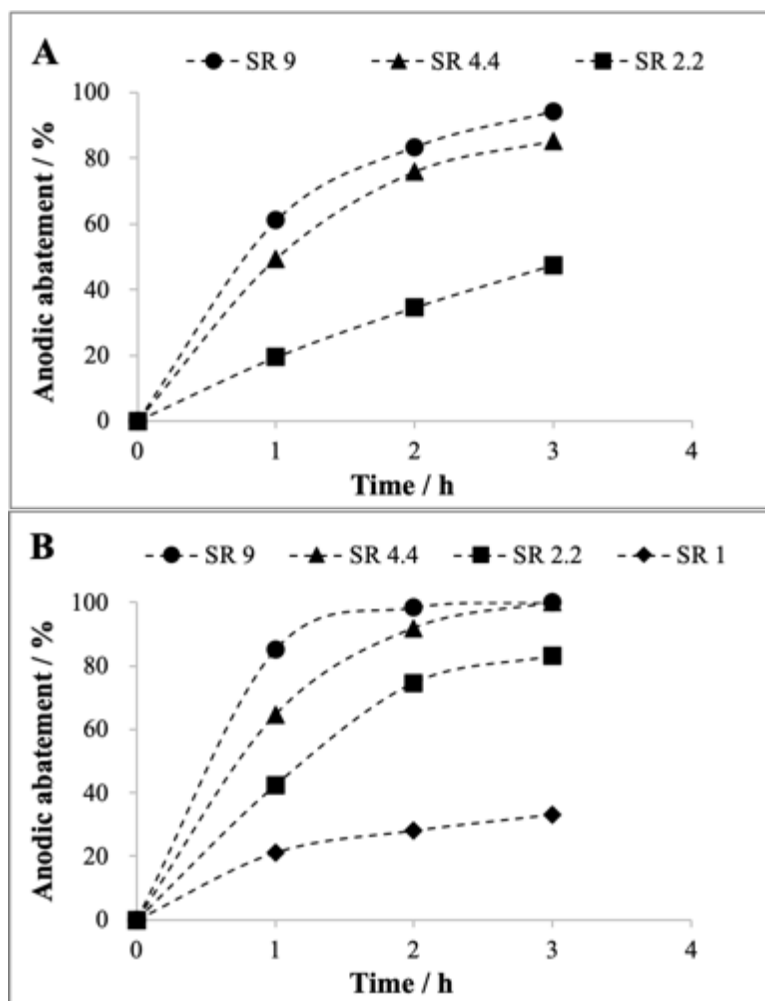


Fig. 7-4 Removal of TOC in the anodic compartment achieved by A-RED with an external supply of cell potential of 1 V (A) or 1.5 V (B). A-RED performed with SR = 9, 4.4, 2.2 and 1.0. Number of membrane pairs 60.

At 1.0 V, the presence of a salinity gradient allowed appreciable current densities (Fig. 7-5A). The utilization of salinity gradients allowed to increase the current density (Fig. 7-5B) and to achieve very good abatements (Fig. 7-4B) for all adopted SR (after 3 h, 100% for SR = 4.4 or 9 and 83% for SR = 2.2).

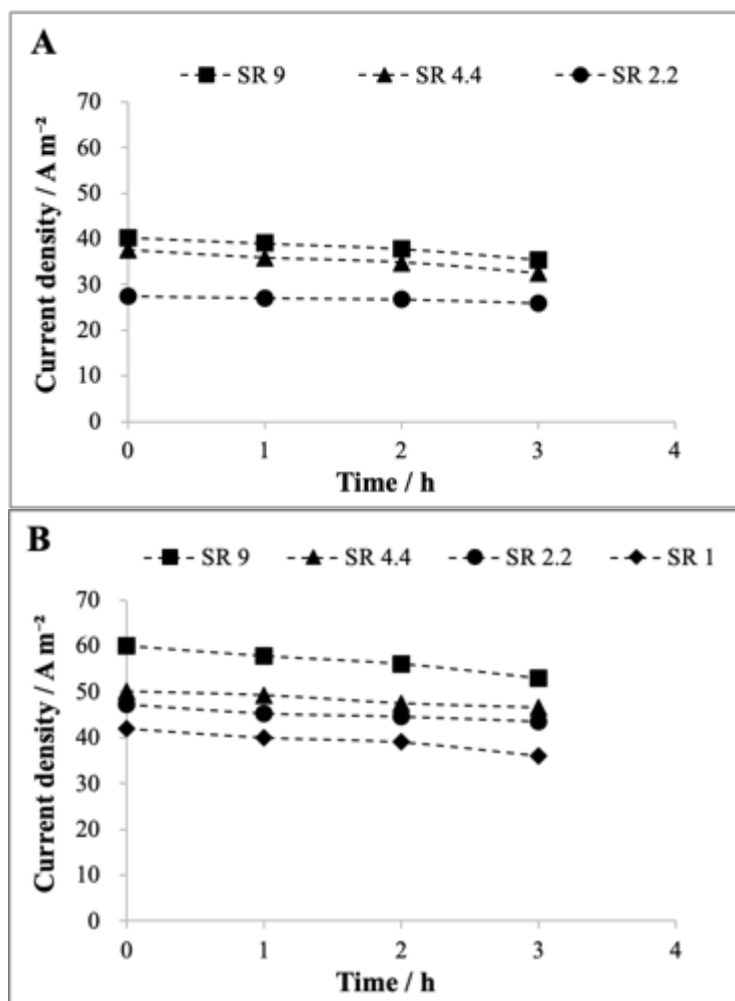


Fig. 7-5 Current density achieved by A-RED with an external supply of cell potential of 1 V (A) or 1.5 V (B). A-RED performed with SR = 9, 4.4, 2.2 and 1.0. Number of membrane pairs 60.

In all these cases, a quite low final energetic consumption (computed by the energetic consumption necessary to reduce the TOC content of 1 g) was achieved (Fig. 7-6A). In particular, the lowest energetic consumption of 0.04 kW·h gTOC<sup>-1</sup> was obtained at SR = 9. At 1.5 V, where the standalone electrolysis gave an abatement close to 33%, Furthermore, a significant reduction of the energetic consumption (Fig. 7-6B) was observed in the presence of the salinity gradient, with respect to electrolysis process. In particular, at 1.5 V the utilization of a low salinity gradient SR = 2.2 allowed to increase the removal of TOC from 33% to 85% and to reduce the energetic consumption of about 45%. Hence, it can be concluded that A-RED gives higher removal of TOC than both



electrolysis and RED processes, using lower SR with respect to RED and lower cell potentials supplied by the potentiostat with respect to electrolysis.

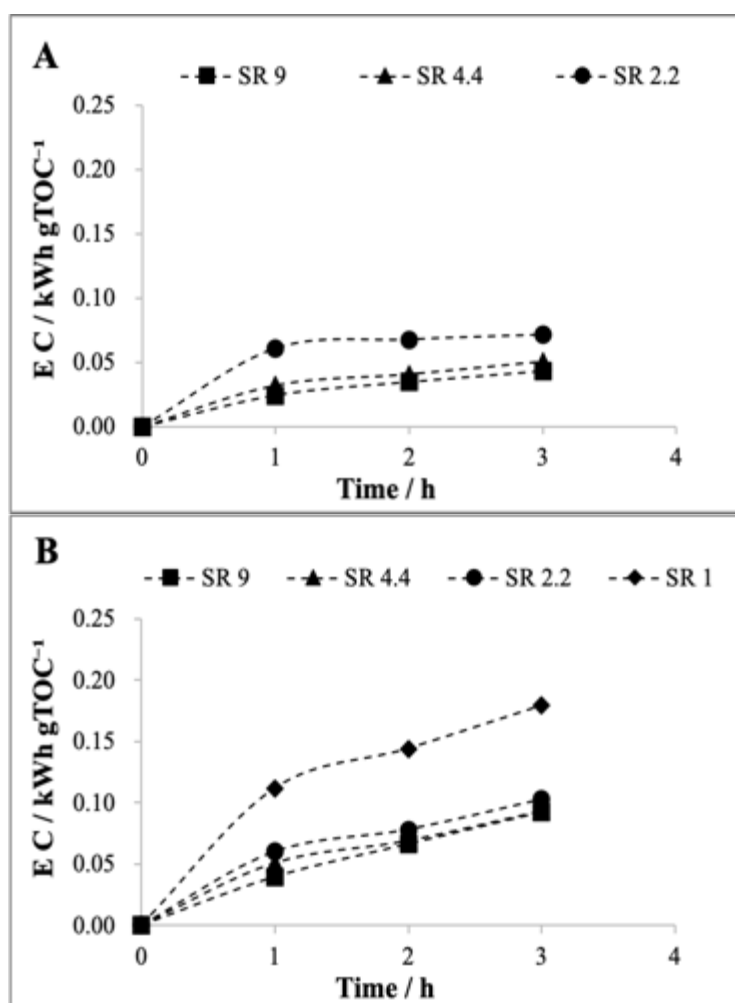


Fig. 7-6 Energetic consumption achieved by A-RED with an external supply of cell potential of 1V (A) or 1.5 V (B). A-RED performed with SR = 9, 4.4, 2.2 and 1.0. Number of membrane pairs 60.

The improvements offered by A-RED with respect to electrolysis can be better observed looking at Fig. 7-7, where the final removals of TOC obtained at 0, 1, 1.5 and 2.0 V and different SR are reported. It can be observed that RED process gives very high removal of TOC in the absence of external supply of energy only with the highest adopted SR; conversely, the standalone electrolysis gives good abatements only at 2.0 V. On the other hand, A-RED gives good abatements also coupling intermediates value of both SR and external cell potential.

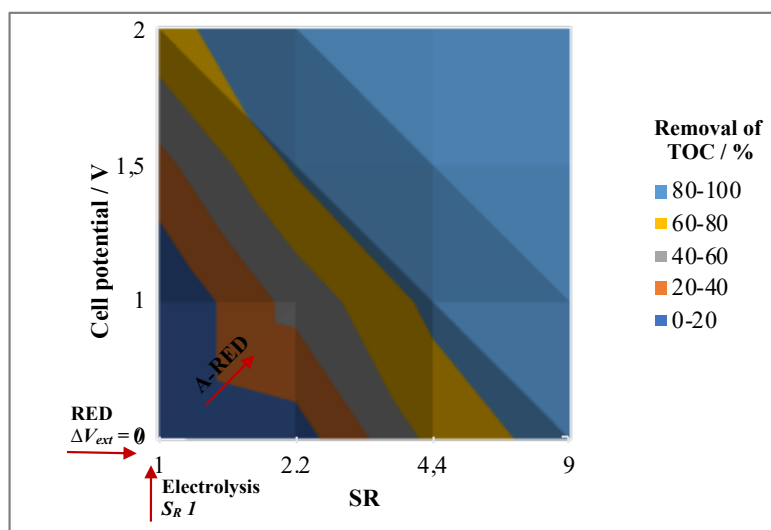


Fig. 7-7 The removal of TOC in the anodic compartment achieved by A-RED, RED and electrolysis (data of Fig. 7-2 ~ 6).

The same data were plotted again in Fig. 7-8, for fixed SR, at different cell potentials applied by the potentiostat. It can be seen that for all the employed salinity gradients, the removal of TOC increased applying an external supply of energy. In particular, for low SR (Fig. 7-8A), the external supply of energy is necessary to achieve final good abatements, while, for high SR (Fig. 7-8B), the supply of external energy is useful mainly to accelerate the mineralization process; Indeed at SR = 9, similar removals were obtained after 3 h with RED and with 1 h with A-RED at 1.5 V (Fig. 7-8B).

Hence, on overall the results reported above, demonstrates for the first time that A-RED can be used for the treatment of wastewater contaminated by organics using small salinity gradients and small stacks, allowing to obtain a fast and high removal of TOC and to save electric energy with respect to conventional electrolysis.

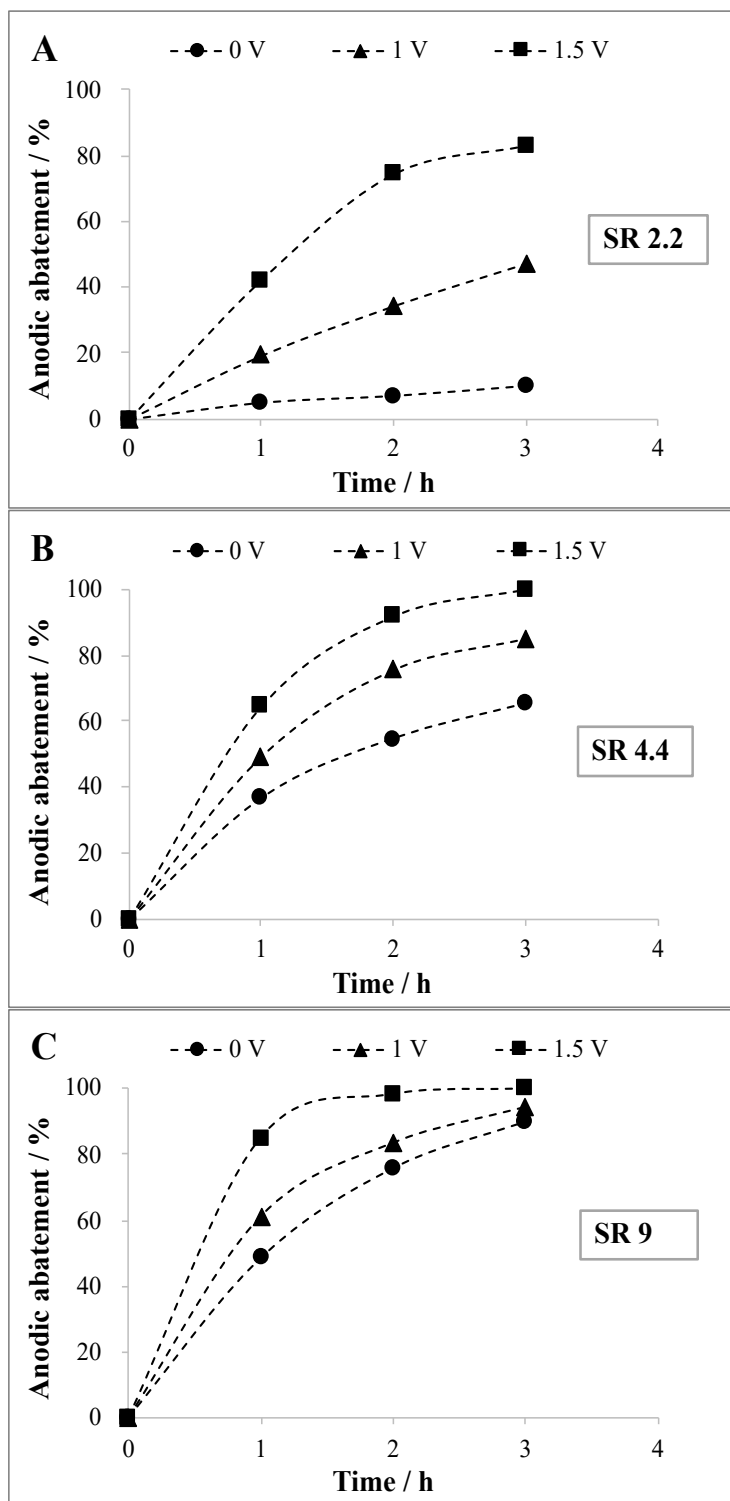


Fig. 7-8. A, B and C reports the removal of TOC achieved by A-RED at SR = 2.2, 4.4 and 9, respectively.

### 7.3.2 Cathodic conversion of carbon dioxide to formic acid

The electrochemical conversion of CO<sub>2</sub> in water to various products, including formic acid and CO, seems particularly promising. In particular, it has been reported that the utilization of tin cathodes allows the production of formic acid with good faradic efficiencies [8-12], particularly in acidic conditions. Agarwal et al. [13] have shown that this process could be interesting from an economic point of view, even if further work is necessary to enhance the overall economic attractiveness of the process, as an example by lowering the energetic consumptions. In particular, the reduction of CO<sub>2</sub> at tin cathodes requires a working potential between -1.8 and -2.0 V vs. SCE. Hence, if the cathodic process is coupled with the anodic oxygen evolution reaction or with the treatment of wastewater by electrogenerated active chlorine, as recently proposed to improve the economic figures of the process, a large cell potential is required, often higher than 3.3-3.5 V. Hence, the electrolysis requires high energetic consumptions. Hence, the utilization of RED or A-RED could be particularly interesting in order to reduce the energetic costs.

RED experiments were carried out using a concentration of NaCl of 150 g L<sup>-1</sup> (2.6 M) in HC and of 50 or 500 mg L<sup>-1</sup> in LC, for an initial SR of 3000 and 300, respectively. Fig. 7-10A reports the production of formic acid vs. time achieved with the two adopted initial SR and without salinity gradient. In the absence of salinity gradient, no formic acid was obtained, confirming that the activation of cathodic reduction is necessary to convert CO<sub>2</sub> to formic acid, while in the presence of salinity gradient, formic acid was obtained. It is worth to mention that it is, up to our knowledge, the first time that carbon dioxide is converted to formic acid by RED process, thus showing that salinity gradients can be used for this relevant scope. According to data reported in Fig. 7-10, both adopted SR were able to sustain the electrolytic process (Fig. 7-10C) and the production of formic acid (Fig. 7-10A), but the experiment performed with higher salinity gradient resulted in higher productions of formic acid due to the higher generation of current density (Fig. 7-10B).

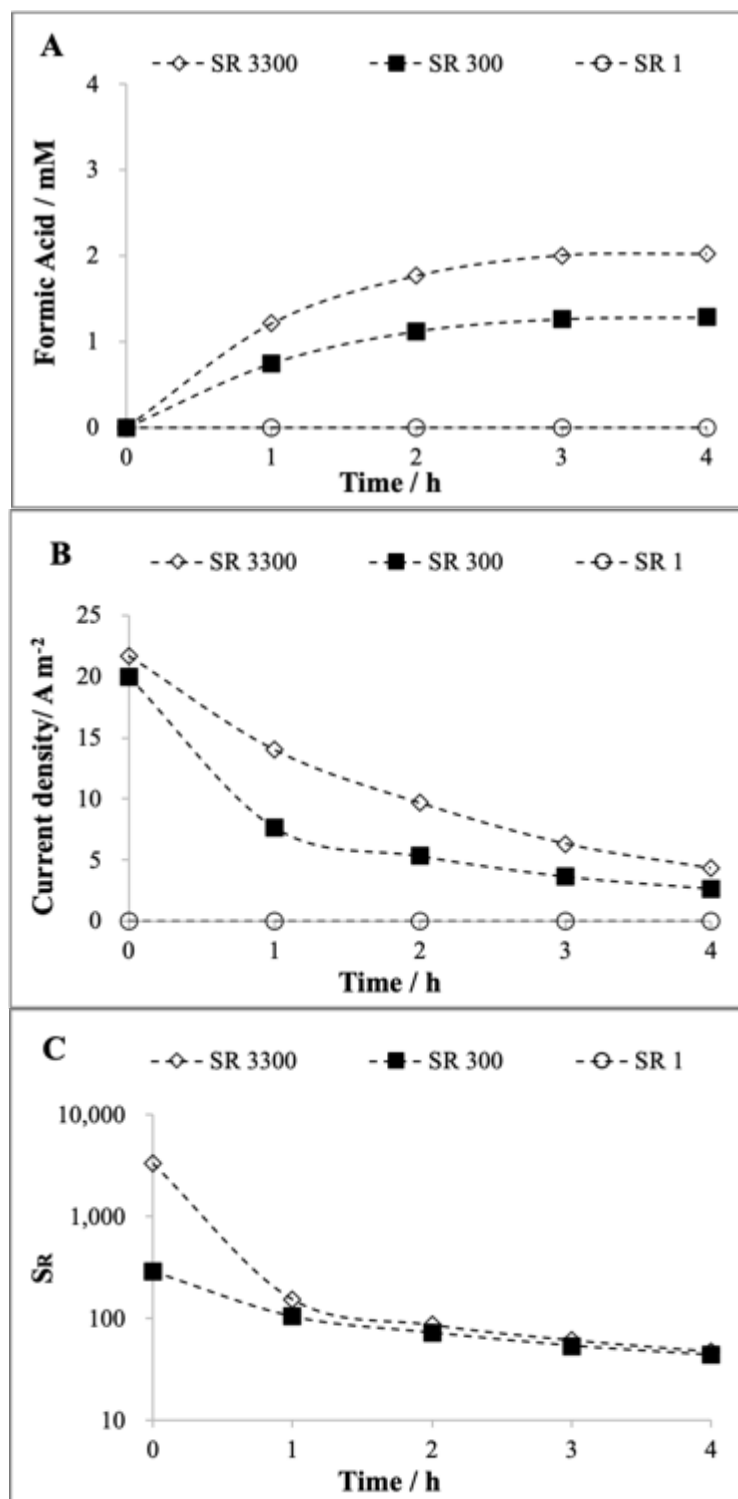


Fig. 7-10 The production of formic acid (A), generation of current density (B), salinity ratio (C) vs. time in the cathodic compartment achieved by RED performed with HC (NaCl concentration  $150 \text{ g L}^{-1}$ ) and LC (NaCl concentration  $50 \text{ mg L}^{-1}$  or  $500 \text{ g L}^{-1}$ , corresponding to  $\text{SR} = 3000$  and  $300$ , respectively).

However, the production of formic acid was quite limited, and its concentration reached a plateau value after 3 h (Fig. 7-10A), due to the strong decrease of the current density with the time passed (Fig. 7-10B). The decrease of the current density is due to the passage of ions from HC to LC, thus concentrating the diluted solution and reducing the salinity ratio (Fig. 7-10C) that becomes after 3 h not sufficient to sustain effectively the cathodic conversion of carbon dioxide.

Hence, the adoption of A-RED seems particularly important to sustain the electrolytic process. A series of A-RED experiments was carried out using an initial SR = 3000 and an external applied cell potential of 0.5, 0.65 and 0.8 V by the potentiostat. Fig. 7-11 reports the results achieved by A-RED, performing a series of experiments with different salinity gradients (2.2, 4.4 and 9) and external cell potentials supplied by the potentiostat. Hence, in this case, an external current is applied in the direction of the diffusional transport of ions which follows chemical potential gradients, thus allowing to couple the external electric energy and the energy coming from salinity gradient. Fig. 7-11A shows that the supply of a small external cell potential helps significantly the process; at 0.5 V the production of formic acid after 4 h was doubled with respect to RED (Fig. 7-11A) and the current density decreased in a quite limited way (Fig. 7-12B; 12% of reduction in 4 h). An increase of the external cell potential allowed to enhance the production of formic acid: at 0.8 V (which is lower than one fourth of the cell potential necessary for the electrolysis) a final concentration of formic acid of about 6.3 mM was achieved vs. the 2.0 mM obtained by RED and the 4.0 mM obtained by A-RED at 0.5 V.

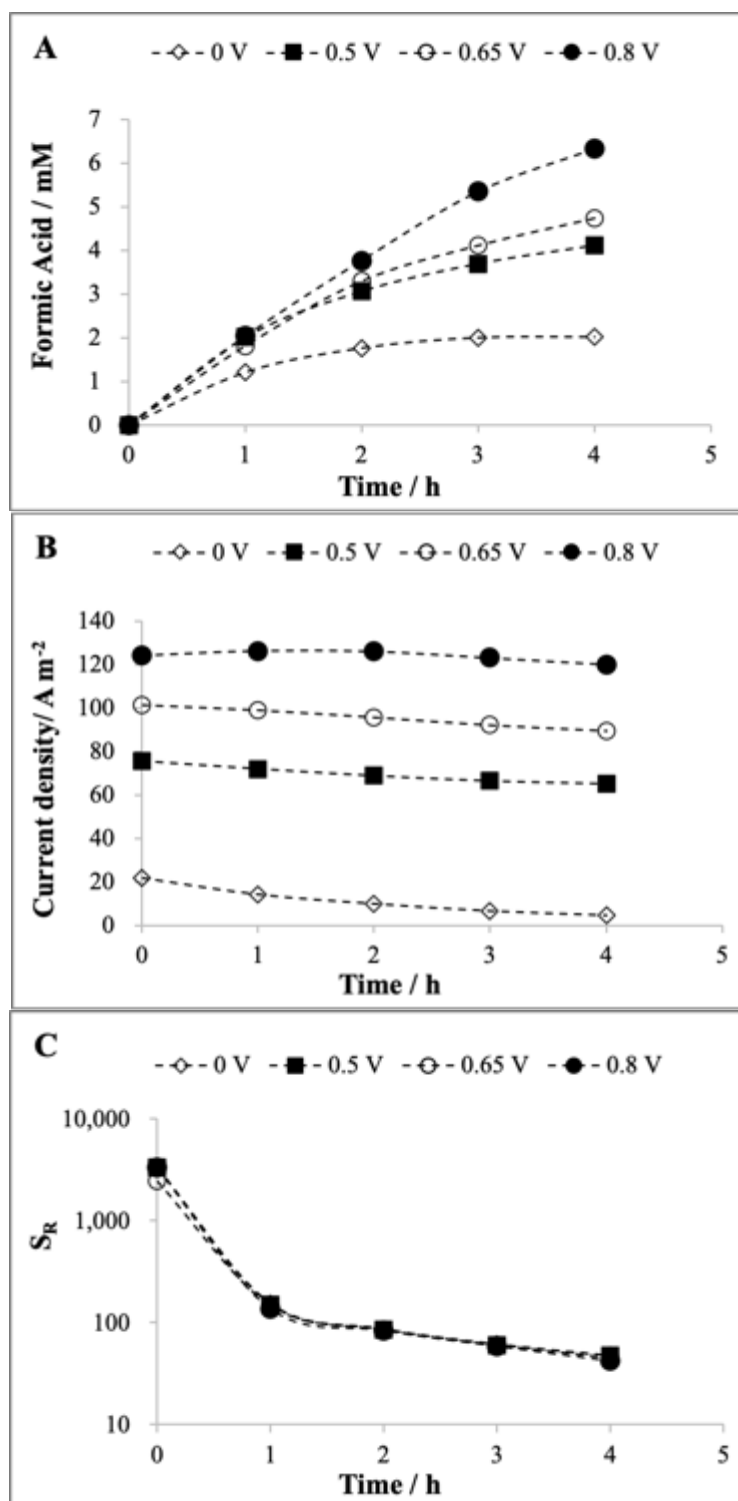


Fig. 7-11. The production of formic acid (A), current density(B) and SR (C) vs. time with SR= 3000. Conversion of CO<sub>2</sub> to formic acid in the cathodic compartment achieved by A-RED with different external cell potentials (0, 0.5, 0.65 and 0.8 V) performed with HC (NaCl concentration 150 g L<sup>-1</sup>) and LC (NaCl concentration 50 mg L<sup>-1</sup>, corresponding to SR = 3000).

Indeed, as shown in Fig. 7-11B, the increase of the external cell potential allowed both to enhance and to maintain more constant the current density during the experiment; at 0.8 V current density decreased of only 3% in 4 h while for RED process the decrease of the current density was of 80%, in spite of the fact that all these processes gave a very similar trend of SR with the time (Fig. 7-11C). Indeed, at RED the decrease of the salinity gradient occurred during the experiment for the passage of ions from HC to LC does not allow to sustain the redox processes after 2 h, while in A-RED, the assistance of the external energy supply allows the redox processes to work also with a reduced SR.

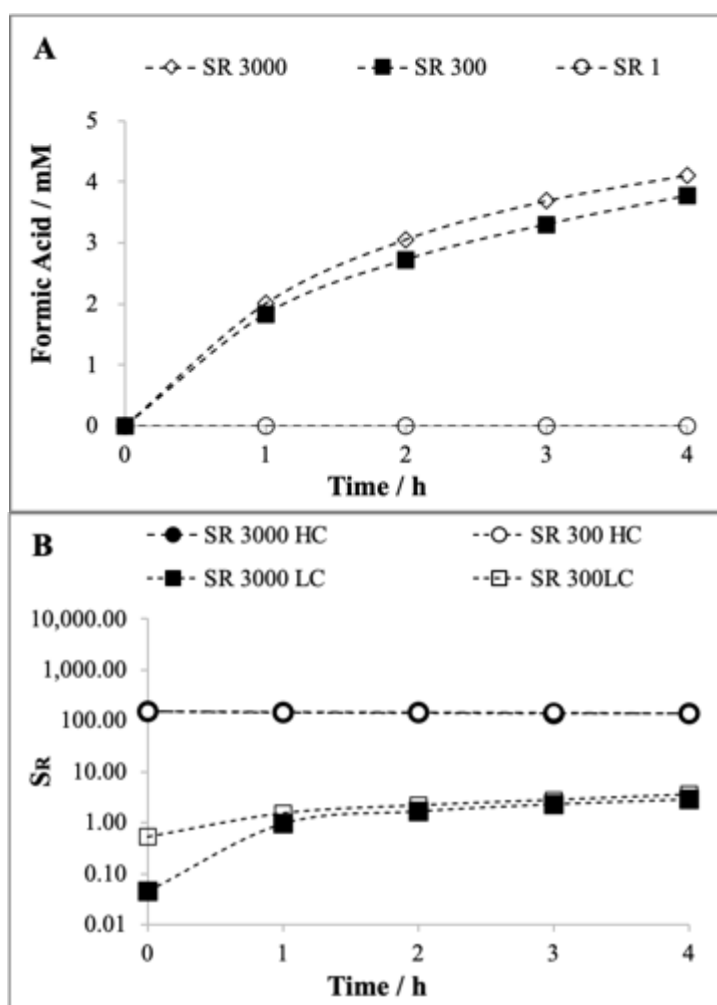


Fig. 7-12 The production of formic acid (A) and the concentration of NaCl in HC and LC (B) vs. time for an applied cell potential of 0.5 V for different initial SR. Conversion of CO<sub>2</sub> to formic acid in the cathodic compartment achieved by A-RED with different external cell potentials (0, 0.5, 0.65 and 0.8 V) performed with HC (NaCl concentration 150 g L<sup>-1</sup>) and LC (NaCl concentration 50 mg L<sup>-1</sup> or 500 g L<sup>-1</sup>, corresponding to SR = 3000 and 300, respectively).



To better evaluate this aspect, some A-RED experiments were repeated at 0.5 V reducing the initial SR to 300. As shown in Fig. 7-12A, the reduction of SR lead only to a small decrease of the formic acid production. Indeed, in HC the two solutions had the same initial concentration of NaCl while, for LC, the concentration of NaCl was 50 and 500 mg L<sup>-1</sup> in the two cases. However, as shown in Fig. 7-12B, the very low initial concentration of NaCl of 50 mg L<sup>-1</sup> rapidly increased, so that a similar SR was reached for the two cases after 1 h. Hence, on overall the results reported in this paragraph demonstrates for the first time that A-RED can be used in order to convert carbon dioxide to formic acid at very small cell potentials applied by the potentiostat, using different salinity gradients and small stacks, and allowing to reduce drastically the energetic consumptions with respect to conventional electrolysis.

#### 7.4 Summary

Assisted reverse electrodialysis (A-RED) is here proposed for the first time for two different model redox processes, the cathodic conversion of carbon dioxide to formic acid and the anodic treatment of water contaminated by organics, and compared with both electrolysis and RED. The main conclusions of the work for the reduction of carbon dioxide to formic acid are:

- 1) It was shown, for the first-time, that the cathodic conversion of CO<sub>2</sub> to formic acid can be performed by both RED and A-RED, saving electric energy with respect to electrolysis processes;
- 2) The adoption of A-RED increases significantly the production of formic acid and gives rise to a more stable current with respect to RED using a small external cell potential of 0.5-0.8 V; as an example, with an applied cell potential of 0.8 V, a final concentration of formic acid of about 6.3 mM was achieved vs. the 2.0 mM obtained by RED.

The main conclusions of the work for the anodic removal of TOC for a synthetic wastewater are:

- 1) RED was used for the first time for the anodic treatment of a synthetic wastewater contaminated by organics; in particular, A-RED gives higher abatement of TOC with respect to RED and requires lower applied cell potentials with respect to electrolysis; as an example, after 2 h with a SR = 4.4, an abatement of the TOC of about 55 and 92% were obtained, respectively, by RED and A-RED (with an applied cell potential of 1.5 V), while at 1.5 V an abatement lower than 30% was obtained by electrolysis;
- 2) The removal of TOC increased by means of an enhancement of salinity gradient and/or of the applied cell potential;
- 3) The adoption of A-RED allowed to obtain a partial removal of the TOC also using a low salinity gradient of 2.2, which is not sufficient for RED process, strongly reducing the energetic requirements with respect to electrolysis.

## 7.5 References

- [1] Xu S, Xu Z, Wu X, et al. Study on the mechanism of organic wastewater oxidation degradation with reverse electrodialysis powered by concentration gradient energy of solutions. *Acta Scientiae Circumstantiae*, 2018, 38: 4642–4651.
- [2] Higa M, Watanabe T, Yasukawa M, et al. Sustainable hydrogen production from seawater and sewage treated water using reverse electrodialysis technology. *Water Practice Technology*, 2019, 14: 645–651.
- [3] Hatzell M C, Ivanov I, Cusick R D, et al. Comparison of hydrogen production and electrical power generation for energy capture in closed-loop ammonium bicarbonate reverse electrodialysis systems. *Physical Chemistry Chemical Physics*, 2014, 16: 1632–1638.
- [4] Tufa R A, Rugiero E, Chanda D, et al. Salinity gradient power-reverse electrodialysis and alkaline polymer electrolyte water electrolysis for hydrogen production. *Journal of Membrane Science*, 2016, 514: 155–164.

- 
- [5] Krakhella K W, Bock R, Burheim O S, et al. Heat to H<sub>2</sub>: using waste heat for hydrogen production through reverse electrodialysis. *Energies*, 2019, 12 : 3428.
- [6] Nazemi M, Zhang J, Hatzell M C. Harvesting natural salinity gradient energy for hydrogen production through reverse electrodialysis power generation. *Journal of Electrochemical Energy Conversion Storage*, 2017, 14: 020702.
- [7] Vanoppen M, Criel E, Walpot G, et al. Assisted reverse electrodialysis-principles, mechanisms, and potential. *NPJ Clean Water*, 2018, 1: 1–5.
- [8] Scialdone O, Galia A, Lo Nero G, et al. Electro-chemical reduction of carbon dioxide to formic acid at a tin cathode in divided and undivided cells: effect of carbon dioxide pressure and other operating parameters, *Electrochimica Acta*, 2016: 199: 332–34 .
- [9] Sabatino S, Galia A, Saracco G, et al. Development of an electrochem- ical process for the simultaneous treatment of wastewater and the conversion of carbon dioxide to higher value products. *ChemElectroChem*, 2017, 4: 150–159.
- [10] Proietto F, Schiavo B, Galia A, et al. Electrochemical conversion of CO<sub>2</sub> to HCOOH at tin cathode in a pressurized undivided filter-press cell. *Electrochimica Acta*, 2018, 277: 30–40.
- [11] Proietto F, Galia A, Scialdone O. Electrochemical conversion of CO<sub>2</sub> to HCOOH at tin cathode: development of a theoretical model and comparison with experimental results. *ChemElectroChem*, 2019, 6:162–172.
- [12] Zhang F, Chen C, Tang Y, et al. CO<sub>2</sub> reduction in a microchannel electrochemical reactor with gas-liquid segmented flow. *Chemical Engineering Journal*, 2020, 392: 124798.
- [13] Agarwal A S, Zhai Y, Hill D, et al. The Electrochemical reduction of carbon dioxide to formate/formic acid: engineering and economic feasibility. *ChemSusChem*, 2011, 4: 1301–1310 .



## Chapter 8. Conclusions and innovations

The work carried out during the PhD thesis aimed to find innovative routes to face some problems involved in the electrochemical treatment of wastewaters contaminated by organics. The main findings of the studies performed during the thesis are reported below.

- 1) Electro-Fenton process can be improved by enhancing the conversion of oxygen to hydrogen peroxide in undivided cells equipped with cheap cathodes selecting proper operating conditions. The amount of hydrogen peroxide accumulated in the solution during electrolysis does not depend only on the amount produced on the surface of the cathode but also on its decomposition reaction on the surface of the anode. When the ratio of the surface area of the cathode to the anode increases from 1 to 4, the smaller anode area reduces the decomposition reaction of  $\text{H}_2\text{O}_2$  at the anode, and the accumulation of  $\text{H}_2\text{O}_2$  increases 3-4 times. When the current density is adjusted and the working voltage is  $-0.9 \text{ V vs. SCE}$ , the maximum  $\text{H}_2\text{O}_2$  accumulation concentration can be obtained in the solution. Furthermore,  $\text{Ti}/\text{IrO}_2\text{-Ta}_2\text{O}_5$  anode facilitates the accumulation of  $\text{H}_2\text{O}_2$ , inhibiting the decomposition of  $\text{H}_2\text{O}_2$  on the anode surface. With respect to previous papers devoted mainly to the cathode function, the thesis provided a new approach and avoided the high cost of complex electrolysis equipment and of electrode material modification.
- 2) For direct electrochemical oxidation of organics, the performances of the process depend dramatically on the content of  $\text{NaCl}$  and of other supporting electrolytes. Furthermore, different anodes could be selected depending on these parameters. Focusing on real wastewater with low conductivity, the study proposed to replace the traditional electrochemical reactor with a microfluidic reactor, and establishes a low energy consumption process.
- 3) It was demonstrated for the first time that it could be possible to avoid the supply of electric energy for the electrochemical treatment of wastewater by using a

reverse electrodialysis stack and the salinity gradient of synthetic wastewaters. Furthermore, if no high salinity gradients are available or if very high cell potentials are needed, a relevant saving of electric energy can be achieved using an assisted reverse electrodialysis approach as demonstrated in the thesis for the first time.

## Acknowledgements

I would like to express my sincere gratitude to my tutor Prof. Onofrio Scialdone, as well as to my co-tutor Prof. Alessandro Galia, for their continuous support during my PhD and with related research. Thanks for their patience, motivation, and immense knowledge. I am very grateful for their scientific advices and many insightful discussions on my PhD work.

Special thanks go to my laboratory colleagues and friends Claudia Prestigiacomio, Simona Sabatino, Federica Proietto, Adriana D'Angelo, Fabrizio Vicari... ..

Finally, thanks to my mother. Thank you for supporting me for everything in my life!

## Publications and Meetings

### Publications:

- [1] **Pengfei Ma**, Hongrui Ma, Simona Sabatino, Alessandro Galia, Onofrio Scialdone. Electrochemical treatment of real wastewater. Part 1: Effluents with low conductivity. *Chemical Engineering Journal*, 336 (2018) 133–140.
- [2] **Pengfei Ma**, Hongrui Ma, Alessandro Galia, Simona Sabatino, Onofrio Scialdone. Reduction of oxygen to H<sub>2</sub>O<sub>2</sub> at carbon felt cathode in undivided cells. Effect of the ratio between the anode and the cathode surfaces and of other operative parameters. *Separation and Purification Technology*, 208 (2019) 116–122.
- [3] **Pengfei Ma**, Xiaogang Hao, Alessandro Galia, Onofrio Scialdone. Development of a process for the treatment of synthetic wastewater without energy inputs using the salinity gradient of wastewaters and a reverse electrodialysis stack. *Chemosphere*, 248 (2020) 125994.
- [4] **Pengfei Ma**, Xiaogang Hao, Federica Proietto, Alessandro Galia, Onofrio Scialdone. Assisted reverse electrodialysis for CO<sub>2</sub> electrochemical conversion and treatment of wastewater: A new approach towards more eco-friendly processes using salinity gradients. *Electrochimica Acta*, 354 (2020) 136733.

### Meetings:

XXXIX GE-RSEQ Meeting. 2-5 July 2018, Madrid, Spain.

- Electrochemical Treatment of Real Wastewater - Effluents with Low Conductivity(oral)
- Reduction of Oxygen to H<sub>2</sub>O<sub>2</sub> at Carbon Felt Cathode in Undivided Cells - Effect of the Ratio Between the Anode and the Cathode Surfaces(poster)

69th Annual Meeting of the International Society of Electrochemistry. 2-7 September 2018, Bologna, Italy.

- Electrochemical Treatment of Real Wastewater with Low Conductivity(poster)
- Reduction of Oxygen to H<sub>2</sub>O<sub>2</sub> at Carbon Felt Cathode in Undivided Cells. Effect of Various Operative Parameters(poster)



"Green Energy, Green Manufacturing, Green Development" National Academic Forum.  
14-16 October, Taiyuan, China.

- Electrochemical Treatment of Wastewater with very Different Conductivity using Reverse Electrodialysis (oral)

**Appendix A: The activity coefficient of the NaCl solution**

---

NaCl concentration /(mol kg <sup>-1</sup> )	activity coefficient
0	1
0.01	0.902
0.02	0.87
0.05	0.82
0.1	0.778
0.2	0.735
0.4	0.693
0.6	0.673
0.8	0.662
1	0.657
1.2	0.654
1.4	0.655
1.6	0.657
1.8	0.662
2	0.668
2.5	0.688
3	0.714
3.5	0.746
4	0.783
4.5	0.826
5	0.874

---

**Appendix B: conductivity of different NaCl concentration solution**

<b>NaCl (g L<sup>-1</sup>)</b>	<b>Conductivity (ms cm<sup>-1</sup>)</b>
0	0
0.05	0.1
0.2	0.48
0.5	1.3
1	3.33
5	11.51
20	54.8
100	234
150	343